TAMPERE UNIVERSITY OF TECHNOLOGY

TOMMI SEPPÄ

THE EFFECT OF DIFFERENT NANOFILLERS ON PROPERTIES AND MIXING OF ETHYLENE PROPYLENE DIENE RUBBER.

Master of Science Thesis

Examiner: Professor Jyrki Vuorinen

Examiner and topic approved in the Automation, Mechanical and Materials Engineering Department Council meeting on 12th of December 2010

TIIVISTELMÄ

TAMPEREEN TEKNILLINEN YLIOPISTO
Materiaalitekniikan koulutusohjelma
SEPPÄ, TOMMI: Nanotäyteaineiden vaikutus eteeni propeeni dieeni kumin ominaisuuksiin ja sekoittamiseen
Diplomityö, 83 sivua, 0 liitesivua
Heinäkuu 2010
Pääaine: Muovitekniikka / Polymeerimateriaalit
Tarkastaja: Professori Jyrki Vuorinen
Avainsanat: Nanomateriaalit, nanofillerit, täyteaineet, elastomeerit, kumit, kumi komposiitit, sekoitus, ominaisuudet

Polymeerisiä nanokomposiitteja on tutkittu viime vuosina intensiivisesti. Syynä ovat niillä saavutettavissa olevat ylivoimaiset ominaisuudet verrattuna perinteisiin komposiitteihin. Käytännössä näitä ominaisuuksia ei ole vielä saatu riittävän hyvin esille. Varsin ongelmallisiksi ovat osoittautuneet riittävän hyvän dispersion sekä täyteaineen ja matriisipolymeerin välisten vuorovaikutusten aikaan saaminen.

Muovikomposiitteihin verrattuna kuminanokomposiittien tutkimus ei ole ollut yhtä kattavaa ja vapaasti saatavilla olevien julkaisujen määrä on rajallinen. Kumeilla on saatu saman kaltaisia tuloksia kuin muovinanokomposiiteillakin ja huomattava ominaisuuksien paraneminen on saavutettavissa. Ongelmat ovat myös samankaltaisia ja kumeilla varsinkin vaikeasti kontroloitavissa oleva eikä vielä täysin tunnettu sekoitusprosessi vaikeuttaa nanotäyteaineiden käyttöä.

Tutkimuksessa vertaillaan erilaisten nanomateriaalien vaikutusta eteeni propeeni dieeni kumin (EPDM) ominaisuuksiin ja sekoittamiseen. Lujittamiseen käytettiin pääasiassa savipohjaisia materiaaleja, mutta myös moniseinämäisiä hiilinanoputkia ja nanoliitujauhetta kokeiltiin.

Kirjallisuusselvitys keskittyy nanotäyteaineiden ominaisuuksiin ja niiden sekoittamiseen elastomeerien näkökulmasta. Alkuosassa käsitellään peruskumin ominaisuuksia sekä täyteaineiden vaikutusta elastomeerimateriaalin käyttäytymiseen. Loppuosassa käsitellään nanotäyteaineiden ominaisuuksia ja käytettyjä modifiointimenetelmiä sekä tarkastellaan täytetyn kumin sekoitusprosessia.

Käytännön osuudessa testattiin kuuden erilaisen nanotäyteaineen vaikutusta EPDM kumin ominaisuuksiin ja sekoittamiseen. Nanomateriaaleina käytettiin kahta modifioitua montmorilloniittisavea, aktivoitua montmorilloniittia, halloysiitti saviputkia, moniseinämäisiä hiilinanoputkia ja nanoliitua. Lisäksi halloysiitti nanoputkia modifioitiin silaanilla ja sen vaikutusta ominaisuuksiin tutkittiin.

Mallina sekoituksille käytettiin teollisessa käytössä olevaa EPDM reseptiä. Reseptissä osa noesta korvattiin nanotäyteaineilla, jolloin täyteaineiden määrä pysyi vakiona.

Sekoittamiseen käytettiin sisäsekoittajaa, joka oli varustettu intermeshing tyyppisillä roottoreilla. Valmis sekoitus rikitettiin ja levytettiin 2-tela valssilla.

Kompaundeista testattiin vetolujuus, repimislujuus, kovuus, jäännöspuristuma ja sitoutuneen kumin määrä, lisäksi niiden reologista ja vulkanointi käyttäytymistä tutkittiin. Kompaundeille tehtiin myös suppea elektronimikroskooppi tarkastelu.

Mekaanisissa ominaisuuksissa ei havaittu suuria parannuksia nanotäyteaineilla. Erilaisten nanotäyteaineiden voitiin nähdä vaikuttavan ominaisuuksiin erilailla, varsinkin hiilinanoputkien muista poikkeava käyttäytyminen oli silmiinpistävää. Lisäksi matalilla täyteainepitoisuuksilla materiaalien todettiin käyttäytyvän eri tavalla kuin korkeilla pitoisuuksilla.

Vulkanointikäyttäytymiseen sekä reologisiin ominaisuuksiin nanotäyteaineet vaikuttivat hyvinkin voimakkaasti. Moniseinämäisillä hiilinanoputkilla havaittiin muista materiaaleista poikkeavasti nopeampi vulkanoituminen, korkeampi viskositeetti ja suurempi vääntömomentin kasvu vulkanoinnin aikana. Tämä johtui paremmasta yhteen sopivuudesta kumin kanssa sekä niiden korkeammasta pinta–alasta, joka lisää aktiivisen lujitteen osuutta tilavuudesta. Savimateriaaleilla vulkanoitumisaika kasvoi verrattuna nokitäytteiseen kumiin. Tämän oletetaan johtuvan aktivaattorien ja kiihdyttimien adsorboitumisesta kemiallisesti samankaltaisen nanotäyteaineen pinnalle, sen sijaan että ne olisivat reagoineet poolittoman polymeerin kanssa. Amiinimodifioidulla nanosavella havaittiin vulkanoitumisen hieman nopeutuvan amiinin vaikutuksesta.

Nanosavien lisäys aiheutti vulkanointikäyttäytymiseen marssivan modulin muodostumisen. Modulin ansiosta momentti ei saavuta vakioarvoa vulkanoitumisen aikana, vaan kasvaa ajan funktiona. Tämä aiheuttaa virhettä ominaisuuksien vertailemisessa, sillä vulkanointiajan määrittäminen tarkasti ei onnistu.

Moniseinämäisillä hiilinanoputkilla, halloysiitti nanoputkilla ja nanosavella tutkittiin nanotäyteainepitoisuuden vaikutusta ominaisuuksiin. Näissä tutkimuksissa havaittiin hyvin matalilla nanotäyteainepitoisuuksilla ominaisuuksissa suuriakin muutoksia ja korkeammilla pitoisuuksilla ominaisuudet omaksuivat tietynlaisen käyttäytymismallin. Käyttäytymisen oletetaan johtuvan täyteaineen nanoefektistä, joka menetetään suuremmilla pitoisuuksilla, joko agglomeroitumisen tai kumin ja täyteaineen välillä olevien riittämättömien vuorovaikutusten vuoksi.

Halloysiitti nanoputkien ominaisuuksia pyrittiin parantaa piidioksidin kanssa käytetyllä silaani modifioinnilla. Tämän mahdollisti piioksidissa ja halloysiitissä olevat samankaltaiset aktiiviset rymät. Ominaisuuksia ei kuitenkaan onnistuttu parantaan modifioinnilla ja eroavaisuudet materiaalien ominaisuuksien välillä olivat hyvin pienet. Ainoa selvä muutos oli marssivan modulin muodostuminen jo pienemmillä nanotäyteaine pitoisuuksilla.

Kokeesta saadut tulokset olivat kohtalaiset suhteessa odotuksiin. Nanotäyteaineilla odotettiin saatavaksi aikaan parannuksia ominaisuuksissa, toisaalta nanotäyteaineiden sekoittaminen kemialliselta luonteeltaan erilaiseen kumiin on todella haastavaa. Pienoinen yllätys oli ehkä savimateriaaleilla saavutetut huonohkot ominaisuudet. Modifioiduilla materiaaleilla olisi voinut odottaa olevan selvästi paremmat ominaisuudet verrattuna modifioimattomiin materiaaleihin. Tutkimuksesta saadut tulokset herättivät paljon uusia kysymyksiä ja saatuja tuloksia voidaan käyttää hyödyksi jatkotutkimuksissa.

ABSTRACT

TAMPERE UNIVERSITY OF TECHNOLOGY
Master's Degree Programme in Material Science
SEPPÄ, TOMMI: The Effect of Different Nanofillers on Properties and Mixing of Ethylene Propylene Diene Rubber
Master of Science Thesis, 83 pages, 0 Appendix pages
July 2010
Major: Polymeric materials
Examiner: Professor Jyrki Vuorinen
Keywords: Nanomaterials, nanofillers, nanotechnology, nanocomposite, rubber, elastomer, rubber composites, mixing, properties

Polymer nanocomposites have intensively been studied in the recent years. The reason for this are the superior properties that can be obtained by the use of nanofillers compared to traditional ones in certain materials such as thermoplastics. However, the improvement in properties of rubber by using nanofillers has been difficult to demonstrate. The main problems which were experience in this study were the dispersion or agglomeration of the filler and the poor interaction between the matrix and the nanofiller.

This study compares processing and properties of different kinds of commercial nanofillers with ethylene propylene diene rubber (EPDM). The fillers used are mainly clay based, but carbon nanotubes and calcium carbonate are also evaluated.

The literature review focuses on the elastomer and the fillers used in this study, and the improvements in properties achieved so far. Properties of the rubber, of the nanofillers as well as modifications of the fillers are addressed. In the final part, the mixing process and different mixing techniques of filled rubber are discussed.

In the practical part, six different nanofillers were tested in an EPDM matrix. Of these, the most interesting fillers were selected and tested in concentrations from 0,5 to 7,5 phr. Finally, one filler was selected for modification in order to investigate if the properties could be further enhanced.

Testing of the materials included tensile properties, tear strength, hardness, compression set and bound rubber. In addition, curing behaviour and Mooney viscosity were analyzed. Scanning electron microspore was used to investigate the microstructure of the composites.

Within this study, a significant improvement of the property profile of the materials by the addition of nanofillers was not observed. The most probable reason for this is an insufficient dispersion of the fillers, with the consequence that the material lacks the filler–filler and filler–polymer network necessary for a good reinforcing effect. The filler–polymer interactions are poor, despite the modifications used in some materials, which also negatively influences the properties.

PREFACE

This master thesis was made at Tampere University of Technology between October – May 2010. My thesis was a part of the WILMIX–project and was done in co–operation with TEKES, Tampere University of Technology and industrial partners. The goal of the Wilmix project is to develop new efficient and environmentally–friendly elastomer based materials and their mixing technologies.

I would like to thank my examiner Prof. Jyrki Vuorinen and supervisor Wilma Dierkes for the opportunity to work on such an interesting subject and for evaluating my thesis. I also want to thank Teknikum Oy for their scientific and practical support, and access to their equipment for my study.

I would also like to thank DI Minna Poikelispää for her advice and insights, and the laboratory engineer Tommi Lehtinen and Sinikka Pohjonen for their input and help during the practical part of my thesis. I also want to thank everyone at the Plastics and Elastomer Laboratory.

Finally, I want to thank my parents for their encouragement and special thanks to my loving wife for her support during my MSc. thesis work.

Tampere 31.05.2010

Tommi Seppä

TABLE OF CONTENTS

TERMS AND THEIR DEFINITIONS

AMIC	1–allyl–3–methyl imidazolium chloride.
APA	Advanced polymer analyzer (Determination of the vulcanization behavior of rubber).
APTES	γ–aminopropyltriethoxysilane.
Baytubes	Multiwalled carbon nanotubes
BR	Butyl rubber.
CB	Carbon black.
CBS	N–cyclohexylbenzothiatsole–2–sulfenamide (Vulcanisation accelerator
CNT	Carbon nanotube.
Complex modulus	The overall resistance to deformation of a material, regardless of whether is it elastic or viscous.
CRI	Cure rate index.
DPG	Diphenyl guanidine (Vulcanisation accelerator).
DTDM	Dithimorpholine (Vulcanisation accelerator).
EPDM	Propylene ethylene diene rubber.
HNT	Halloysite nanotube.
Loss modulus	Presents the energy dissipated from the viscoelastic material as heat. The viscous component of the material.
MBT	2–mercaptobenzothiatsole (Vulcanisation accelerator).
MBTS	2, 2–dithiobenzothiatsole (Vulcanisation accelerator).
MMA	Maleic anhydride.
Mullins effect	Under cyclic stress, cycles following the first require less force to achieve same strain.
Multifex	Nano–size calcium carbonate.
MWCNT	Multiwalled carbon nanotubes.
N116	Na+ activated clay (Nanofil 116).
Nanofil 116	Na+ activated nanoclay.
Nanofil 5	Unpolar treated nanoclay.
Nanomer	Amine treated nanoclay.
NBR	Nitrile rubber.
$nCaCO_3$	Nano–sized calcium carbonate.
NOC	Organically modified nano–sized clay.
NR	Natural rubber.
Payne effect	Dependence of the viscoelastic storage modulus on the applied strain. When a critical amplitude is reached, the filler network is broken and the modulus decreases rapidly.
phr	Parts per hundreds of rubber. Unit used in rubber compound recipes.
SA	Sorbic acid.

SBR	Stryrene butadiene rubber.
Si–69	Silane based modification agent.
Storage modulus	Presents the elastic energy stored in the viscoelastic material. The elastic component of the material.
SWCNT	Single walled carbon nanotube.
T1	Time when torque is 1 % of the maximum value during vulcanization.
T2	Scorch time. Time at 2 % of maximum torque. Describes the time available before the vulcanization starts.
T90	Vulcanisation time. Time when 90 % of the maximum torque is achieved.
Tan Δ	Phase difference between the elastic and viscous components of the material.
TBBS	N–butylbenzothiazole–2–sulfenamide (Vulcanisation accelerator).
T_g	Glass transition temperature.
TMTD	Tetramethylthiuram disulfide (Vulcanisation accelerator).
wt–%	Weight percentage.
ZDBC	Zinc dibenzyldithiocarbamate (Vulcanisation accelerator).
ZDMC	Zinc dimethyldithiocarbamate (Vulcanisation accelerator).
Δ torque	Difference of the highest and lowest torque values. It is the relative increase in torque.

1. INTRODUCTION

Polymer nanocomposites have been under intense study since their development. Nanofillers offer superior properties compared to traditional fillers. Large improvements can be obtained even with small filler loadings. However, the new nanofillers are more difficult to process than conventional fillers, although some of them (carbon black) are in nano–scale. The agglomeration of filler particles, dispersion and interactions between filler and polymer matrix, have turned out to be difficult to control. Many different methods have been utilized to overcome these problems including surface modification, grafting and different kinds of compatibilizing systems.

Not much attention was paid to the use of the newly developed nanofillers with elastomers in spite of the fact that 'nanofillers' have been used by the rubber industry for decades in the form of carbon black and silica. Recently, tyre manufacturers turned their interest towards nanofillers as a reaction on increased requirements for tyres, especially a lower rolling resistance with at the same time good traction and abrasion resistance. For rubber, the problems related to the utilisation of nanofillers are the same as encountered for other polymers. In addition, the mixing process of rubber is rather complicated and difficult to control. Altogether, this makes the dispersion and distribution control more difficult than for other polymers. It is possible though, that the high viscosity of rubbers compared to thermoplastics during processing, can be used as an advantage for the dispersion of nanofillers by imposing higher shear forces to disperse the filler.

In this study, different types of nanofillers are used to reinforce ethylene propylene diene rubber (EPDM). The aim is to get improved mechanical properties by adding small quantities of nanofillers in a blend with conventional fillers: the nanofillers replace a part of the carbon black in an industrially used EPDM compound. After a screening study of different nanofillers, the influence of filler loading is studied on a choice of the most interesting fillers. One of these fillers is then modified with silane in order to increase the compatibility of the filler with EPDM.

The rubber is compounded with the nanofillers and other additives using an internal mixer with intermeshing rotors. The addition of the curing additives is done on a two roll mill. The rheological properties are determined, as are the mechanical properties including tensile, tear, hardness, abrasion and compression set. In addition, the bound rubber content is determined as a measurement of the filler–polymer interaction, and the structure is evaluated by transmission electron microscopy.

2. THEORETICAL BACKGROUND

2.1. Ethylene propylene diene rubber

2.1.1. Chemistry

The main constituents of Ethylene propylene rubber (EPDM) are ethylene, propylene and a diene. EPDM has a saturated backbone, the unsaturation is in the diene–side chain. It is also a very non–polar polymer compared to other elastomers. Different dienes are used in order to obtain specific vulcanization behaviour. The structure of EPDM with ethylidene norbomene as diene is shown in Figure 2.1.1–1. Other common dienes are dicyclopentadiene and 1, 4–hexadiene. [1] EPDM can be manufactured with different ethylene to propylene ratios. An increasing ethylene content improves the mixing behaviour, but unfortunately also decreases the low temperature properties. [2] Commercial grades normally have 50–70 % of ethylene. [1]

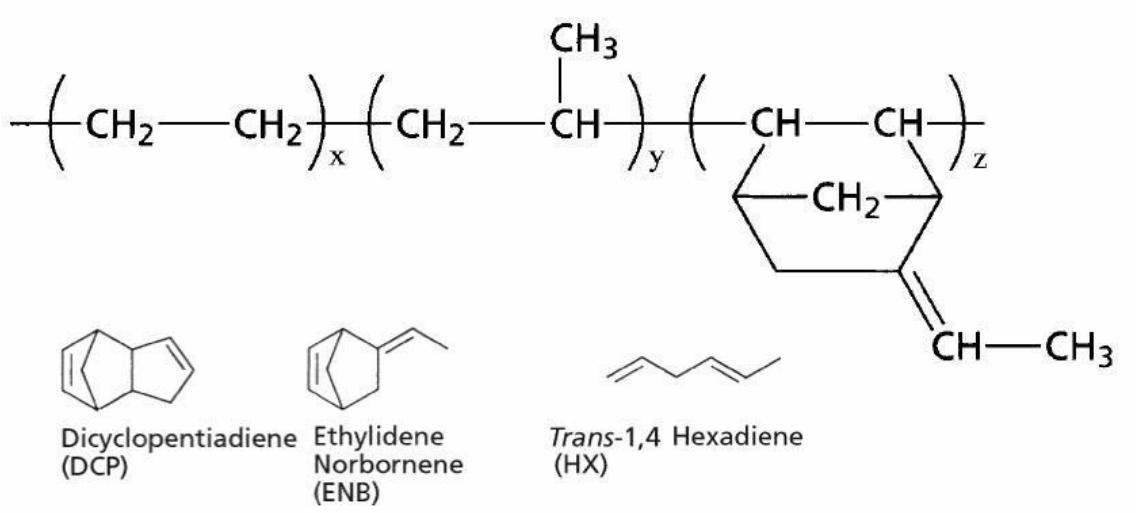

Figure 2.1.1–1 *Structure of EPDM rubber with ethylidene norbomene as diene, and dienes used in EPDM.* [2]

Polymerisation of EPDM is mainly done by addition polymerisation using the coordination method [1]. In coordination polymerisation, the initiator, a metal complex, attaches to the polymer chain. New polymer units attach to this complex, until termination occurs. Most common initiators are Ziegler–Natta catalysts. As the polymerisation can sterically and geometrically be controlled, regular structures can be obtained. [3]

2.1.2. Vulcanization

During vulcanization, the rubber mixture is turned from a viscoelastic material into an incompressible elastic one. In vulcanization, permanent crosslinks are created between elastomer chains and a three–dimensional network is formed. Crosslinks can be sulphur chains, single sulphur atoms, or direct carbon–carbon linkages. The shorter the linkages are the more rigid they become and better mechanical properties are achieved. The most commonly used vulcanization agent is sulphur. For sulphur vulcanization, the additives include the actual vulcanization agent, accelerators and activators, retardation agents might also be used to avoid scorch during processing. Many different kinds of chemicals act as accelerators in sulphur vulcanization of rubber, as listed in Table 2.1.2–1.

Table 2.1.2–1 *Different accelerators used with EPDM* [3, 4]

Primary curing agents	**Secondary curing agents**
Sulfenamides/-imides	**Dithicarbamates**
N-cyclohexylbenzothiatsole-2-sulfenamide CBS	Zinc dimethyldithiocarbamate ZDMC
N-butylbenzothiazole-2-sulfenamide TBBS	Zinc diethyldithiocarbamate ZDEC
2-morpholimothiobenzothiazole MBS	Zinc dibenzyldithiocarbamate ZDBC
N-dicyclohexylbenzothiazole-2-2sulfenamide DCBS	Zinc dibutyldithiocarbamate ZDBEC
Thiazoles	**Thiurams**
2-mercaptobenzothiatsole MBT	Tetramethylthiuram monosulfide TMTM
2,2-dithiobenzothiazole MBTS	Tetramethylthiuram disulfide TMTD
	Tetraethylthiuram disulfide TETD
	Tetrabenzylthiuram-disulfide TBzTD
	Guanidines
	Diphenyl guanidine DPG
	Di-o-tolylguanidine DOTG
	Dithiophosphates
	Sulphur donors
	Tetramethylthiuram disulfide TMTD
	4,4-dithiodimorpholine DTDM
	2-morpholino-dithio-benzothiazole MBSS
	Caprolactam disulfide

Accelerators can be divided into two categories: primary and secondary accelerators. Primary accelerators are fairly efficient and offer good processing safety with moderate curing rates and long scorch times. Examples of primary accelerators are thiazoles, sulfenamides and imides; they are used in quantities of about 1 phr (parts per hundred kilos of rubber). [5]

To obtain the desired curing properties, different accelerators are combined. Secondary accelerators are used to modify the curing behaviour of primary accelerators. Substances used for this purpose are guanidines and thiurams; they have short scorch times and fast cure rates. Usually they are utilized in quantities below 0,5 phr. As can be seen in Figure 2.1.2–1, the secondary accelerators TMTD and ZDMC have much faster curing rates and shorter scorch times than the primary accelerators TBBS or MBTS. A higher crosslink density is usually obtained with secondary accelerators, which is

indicated with the increased maximum torque. Different accelerators can work synergistically and faster cure is achieved when primary and secondary accelerators are used together. The same effect can be achieved when multiple accelerators from the same group are used. [5]

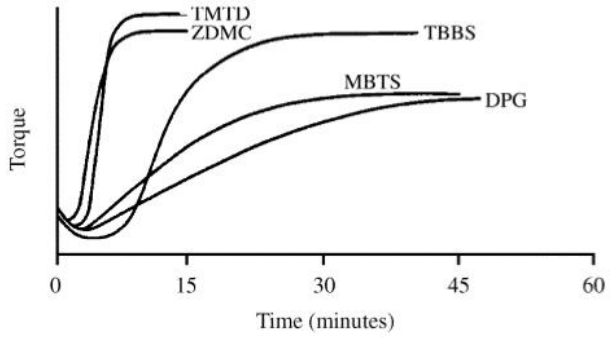

Figure 2.1.2–1 *Curing curves for different kinds of accelerators.* [5]

EPDM has a rather low concentration of double bonds, which are located in the side chains, making vulcanization challenging: due to the low amount of double bonds, the curing rate is low compared to more unsaturated elastomers. This is why EPDM needs a high ratio of accelerators to sulphur.[6] The curing rate of EPDM is also decreased by the low polarity: The accelerators are rather polar and they have a low affinity for the non–polar polymer [5]; therefore their solubility in EPDM is low. To overcome these limitations, a multitude of different vulcanization systems has been evaluated. Four different vulcanization systems for EPDM are presented in Table 2.1.2–2. [4] System 1 is one of the first systems developed for EPDM, offering low cost and medium cure rates. However, it has great tendency to bloom. System 2 uses thiurams, dicarbamates and thiazoles to create a system that gives a good compression set and heat ageing resistance. High amounts of sulphur donors result in monosulfidic crosslinks, which lead to good temperature stability [5]. However, this system is costly and also suffers from blooming. System 3 is a good general purpose system. It does not bloom and has a good performance, but the cure rate is relatively slow and compression set is higher compared to the other systems mentioned before. The last system is statistically designed for balanced fast cure and good physical properties. [5, 6]

Table 2.1.2–2 *Examples of cure systems used with EPDM.* [5, 6]

System 1	System 2	System 3	System 4
Sulphur 1,5	Sulphur 0,5	Sulphur 2,0	Sulphur 1,0
TMTD 1,5	ZDBC 3,0	MBTS 1,5	ZBPD 2,0
MBT 0,5	ZDMC 3,0	ZDBC 2,5	TMTD 1,0
	DTDM 2,0	TMTD 0,8	TBBS 2,0
	TMTD 3,0		

Peroxides can also be used for rubber vulcanization. When peroxides are used, polymeric double bonds are not needed. Peroxides produce active sites on polymer chains by removing hydrogen. These active sites react with each other forming direct

carbon–carbon bonds. These bonds are much stronger and more thermally stable than sulphur–carbon crosslinks. There is no need for accelerators in peroxide vulcanization, but coagents can be used to improve the degree of vulcanization. Peroxide crosslinking improves heat ageing, compression set, but decreases mechanical strength and fatigue life. [2]

EPDM has a certain concentration of allylic hydrogens due to its unsaturated side chain, and allylic hydrogens are readily and efficiently turned in to crosslinks. Therefore it is easy to crosslink with peroxides. Vulcanization of EPDM can be done with peroxides like 2, 3–dimethyl–2, 5–di(t–butylperoxy)hexane. Two peroxides used with rubber shown in Figure 2.1.2–2. Coagents like triaryl isocyanurate and sulphur are commonly utilised to enhance curing. Examples of recipes for peroxide curing of EPDM are shown in Table 2.1.2–3. [5]

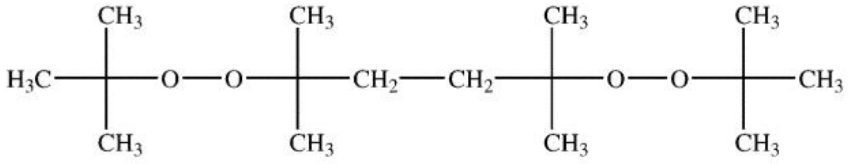

2,5-Bis(tert-butylperoxy)-2,5 dimethyl hexane

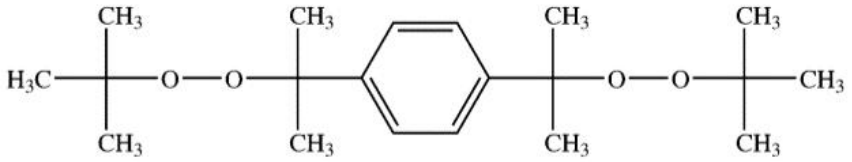

1,4-Bis(tert-butylperoxy isopropyl) benzene

Figure 2.1.2–2 *Two peroxides used in vulcanization of rubber [5].*

Table 2.1.2–3 *Recipes of EPDM compounds with peroxide vulcanisation system.* [5]

Materials	Formulation 1 (phr)	Formulation 2 (phr)
EPDM	100	100
Carbon black	50	50
ZnO	5	5
Dicumyl peroxide	6,6	-
(Phenylene di-isopropylidene) bis (tert-butyl peroxide)	-	4,1
Antioxidant	0,5	0,5

2.1.3. Properties

EPDM has outstanding weather, ozone and oxygen resistance, which derives from its unsaturated backbone. For the same reason, heat and ageing resistance is much better than for natural and styrene butadiene rubber. Chain scission does not occur in the main chain and the deterioration of the properties is much slower compared to polymers with unsaturation in the backbone. [7] During oxidation, EPDM can react with peroxides and undergoes cyclization or crosslinking. This results in increased hardness and modulus

with increasing crosslinking. At the same time, ultimate elongation decreases. [7, 8]. Some property ranges of EDPM are given in Table 2.1.3–1. [3]

Table 2.1.3–1 *Properties of EPDM rubber. [4]*

Property	Value
Hardness, Shore A	30 – 90
Tensile strength, MPa	up to 18
Elongation at break, %	up to 600
Max. service temperature, °C	130
Min. service temperature, °C	-60

EPDM rubber has a decent chemical resistance. It has an excellent resistance to inorganic and highly polar fluids, like diluted acids, alkalis and alcohol. However, it has a very poor resistance against aliphatic, aromatic, and chlorinated hydrocarbons. [3]

Pure EPDM has extraordinary electrical insulation and dielectric properties, but the final properties of a compound depend on the other ingredients, mainly fillers [3,4].

2.1.4. Applications of EPDM

EPDM rubber is mainly used in the automotive industry, in building and construction applications and in cable insulation and jacketing. [3] In the automotive industry, it is used as profiles, hoses and seals, because of the good temperature resistance and excellent weathering resistance. Examples are radiator and heater tubes and weather strips. In building and construction it is used in profiles like window channels, roofing membranes and seals.[2, 3] Due to the extraordinary electrical properties, EPDM is a good material for cable insulation and jacketing [3].

2.2. Fillers

2.2.1. Filler categories

Fillers are divided into three categories depending on their reinforcing effect. The different filler classes are:

- Reinforcing,
- Semi–reinforcing and
- Non–reinforcing fillers.

With reinforcing fillers, significant increase in different properties is gained. Especially tensile, tear and abrasion properties improve. A good example of a reinforcing filler is carbon black. Carbon black has high surface area due to its porous agglomerate structure and a small particle size. This combination enhances the interaction with the

matrix. Another reinforcing filler for rubber is silica. The difference in properties between reinforcing and non–reinforcing fillers is shown in Figure 2.2.1–1. [4, 9]

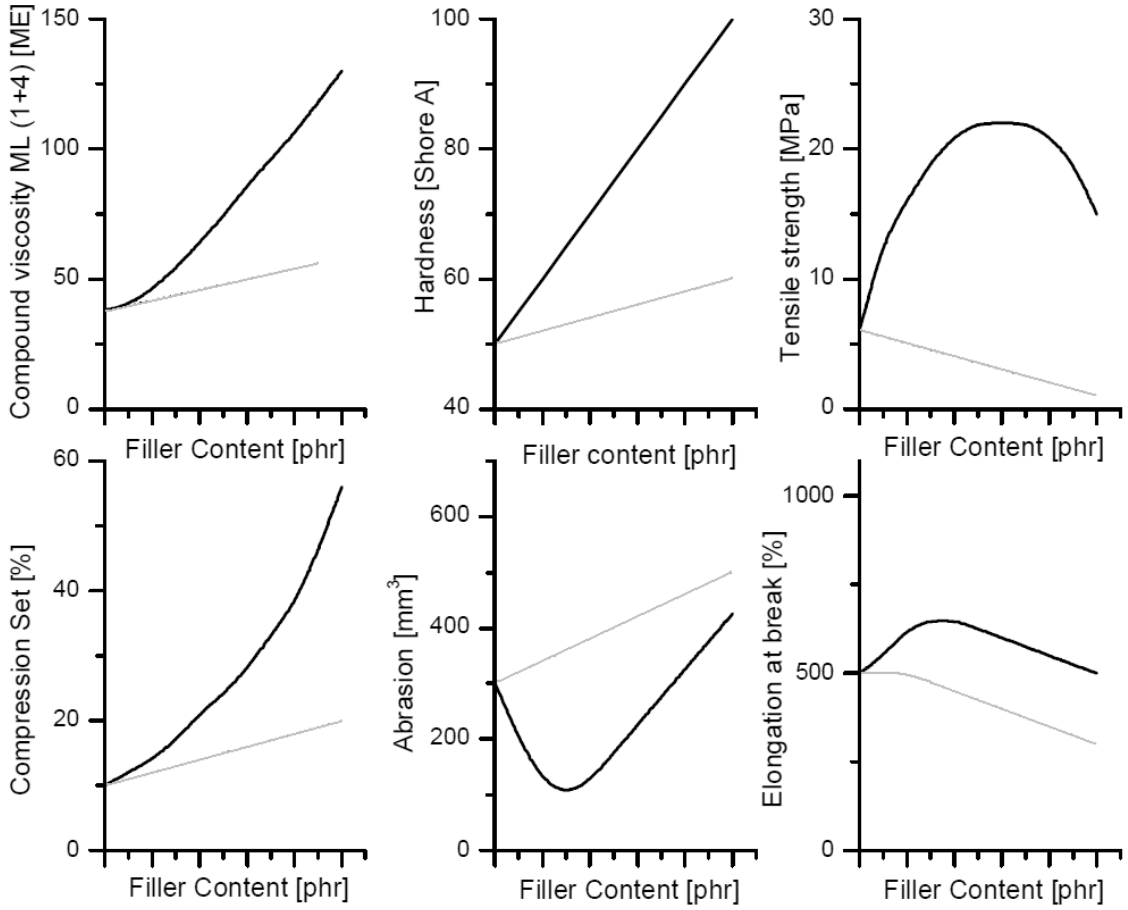

Figure 2.2.1–1 *Difference in properties of rubber filled with reinforcing and non–reinforcing fillers.* [10]

With semi–reinforcing fillers some increase in properties is achieved. Clay fillers are a good example of semi–reinforcing fillers. They have a larger particle size than carbon black and form layered structures that are difficult to disperse. Clays are also hydrophilic unlike polymers. [4, 9, 10]

Non–reinforcing fillers do not provide increased properties and act only as filling material to lower cost of the compound. Examples of non–reinforcing fillers are talc, $CaCO_3$, and sawdust [4, 9]

2.2.2. Behaviour of filled rubber

The influence of the filler on the material properties is controlled by the particle size of the filler, shape and complexity of the filler particles and surface properties. These factors are determining the filler–filler and filler–polymer interactions [12].

Just by adding particles to a fluid, the viscosity increases. It is called hydrodynamic effect. This effect also occurs with viscous fluids like polymers. [9, 11]

Particle size has the most significant effect on reinforcing: Smaller particles have a higher surface area for the rubber to interact with. This leads to enhanced interactions between the filler and the polymer. To fully exploit the better interactions gained from smaller particle size, sufficient dispersion needs to be achieved. [9]

The shape of fillers is also affecting the properties of the compound. Fillers with a large aspect ratio are more reinforcing than fillers with small aspect ratio. Especially the strength of the compound in the axial direction of the filler is higher: By orientation of the fillers, strength can be increased in a specific direction. This leads to anisotropic material. With platelet type fillers, barrier properties can be significantly improved. Platelet shape makes the diffusion path through the material longer. [13]

The structure of fillers describes the complexity of the filler agglomerates and the void volume in the structure. Fillers having a large structure are highly porous. For carbon black, higher structure increases tensile strength and abrasion resistance. A higher structure can also increase the modulus significantly by promoting bound rubber formation. The effect of different filler parameters on the properties of a filled rubber material is shown in Table. 2.2.2–1. [9]

Table 2.2.2–1 *The effect of different filler parameters on the properties of the material [9].*

Property	Particle size decrease	Structure increase	Dispersion increase	Interaction increase
300% Modulus	+	++	little	++
Tensile strength	++	little	+	+
Hardness	++	++	-	+
Elongation at break	-	-	++	-
Tear resistance	++	little	little	little
Hysteresis	++	+	-	-
Abrasion resistance	++	+	++	++

Reinforcement is significantly affected by the interactions between the filler and the polymer. Good interaction notably increases the strength of the material. One form of interactions is the occlusion of polymer chains in the filler structure. Bonding between the filler and polymer can be physical or chemical in nature. In some cases, surface modifications of fillers are used to enhance bonding, e.g. silica is modified with silanes. Mechanical bonding occurs, when polymer chains are locked to filler particles by entanglement and formation of crosslinks. The polymer, that is mechanically or chemically bond to the filler, is called bound rubber. [9] The bound rubber acts more

like filler, and does not contribute to the elastic behaviour of the rubber. Bound rubber increases the effective volume of the filler and enhances the effect of the filler. It causes a significant increase in modulus by immobilizing polymer chains. The modulus increase is strain independent. [11, 13]

Interactions between fillers are caused by van der Waals and electrostatic forces amongst others. These interactions create a strain amplitude dependent change in the complex shear modulus as can be seen in Figure 2.2.2–1. This effect is called Payne effect. When the strain amplitude is increased above a critical value, there is a dramatic decrease in the complex shear modulus. This is caused by the breakage of the bonds between the fillers. This phenomenon is largely reversible and the bonds can be reformed when the strain is removed. The magnitude of the Payne effect is controlled by the type of the filler, through the strength of filler–filler bonding, but also by the filler–polymer interactions. [11]

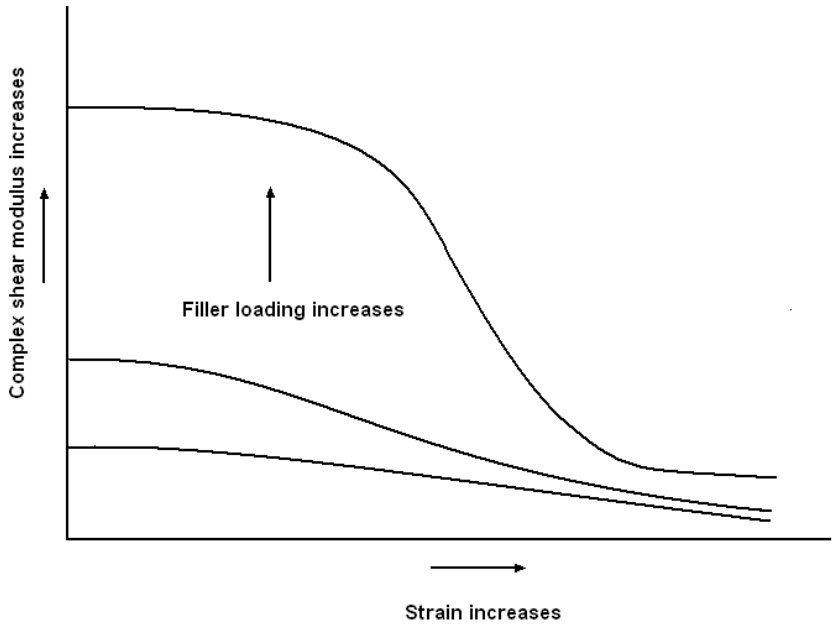

Figure 2.2.2–1 *Payne effect of filled rubber.*

Filled rubbers undergo pronounced stress softening called the Mullins effect. When filled rubber is stretched and allowed to retract, the next stretch requires less force to reach same elongation. This effect reaches steady state after a few stretches and is more pronounced at the start. It is attributed to debonding of filler–filler and filler–polymer interactions. The Mullins effect is shown in Fig. 2.2.2–2. [12]

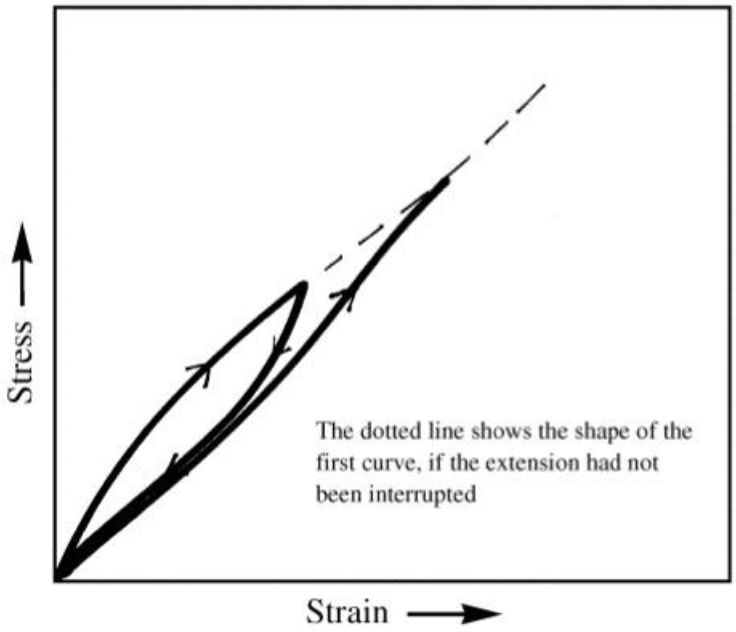

Figure 2.2.2–2 *Stress softening of filled rubber also known as the Mullins effect [9].*

2.2.3. Nanofillers

2.2.3.1 Carbon nanotubes

Structure

The structure of carbon nanotubes (CNT) is comparable to rolled graphene sheets. The carbon atoms form planar hexagonals, which are connected by carbon–carbon single and double bonds, like in graphene. [15] Because of this very stable structure, the modulus is nearly 1 TPa, and the tensile strength of 200 GPa rivals those of a diamond. [16] The length of a CNT can be many micrometers, up to even centimetres in special cases. Single walled carbon nanotubes (SWCNT) consist of one rolled graphene sheet. The diameter of the tubes can be from under 1 nm to close to 50 nm. The multiwalled carbon nanotubes (MWCNT) consist of two or more coaxial nanotubes. These layers are separated by approximately the interlayer spacing of graphite. The outer diameter of a MWCNT can vary between 2 and 50 nm; the inner hollow core is usually approximately half the size of the outer diameter. Fig. 2.2.3.1–1 shows different carbon nanotube types. [15] The high specific surface energy of CNTs induces entanglement and agglomeration, which limits homogenous distribution and makes their dispersion challenging [17].

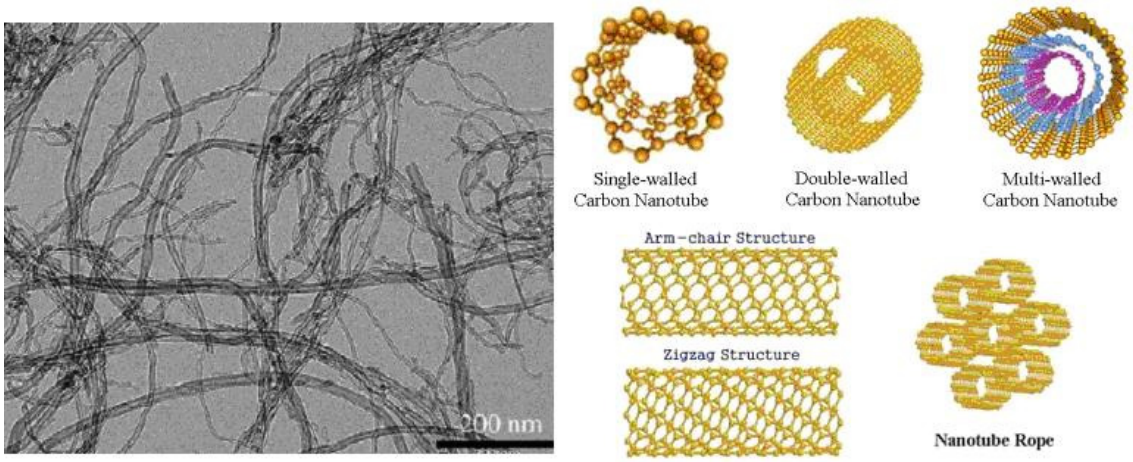

Figure 2.2.3.1–1 *Left: TEM image of multiwalled nanotubes [18]. Right: Different carbon nanotube structures [19].*

Curing behaviour

No specific work is reported concerning reinforcement of EPDM with MWCNTs. Therefore, the influence of this material on various elastomers is described. Nanomaterials have been noted to affect the curing times of elastomers. Incorporation of MWCNTs or SWCNTs into rubber (SBR, NBR and NR) is reported to increase the curing time, as CNTs aren't able to promote the curing activity of sulphur, like carbon black does. [17, 20, 21] This is due to the inert graphite–like structure [20]. An increase in curing time may also be attributed to adsorption of curing agents on the tube surface, especially with more unpolar rubbers like EPDM [21]. Both reduction and increase have been observed with the CNTs for scorch time [17, 20]. The effect on curing characteristics is expected to depend strongly on the cure system and modification of CNTs.

The MWCNTs are reported to decrease the penetration of solvents into the structure with increasing nanofiller loading. This is attributed to increased crosslinking of the composite. [17, 21, 22]

Mechanical properties

Adding MWCNT to elastomers (SBR, NBR or NR) increases elastic modulus, tensile strength and strain at break compared to pristine rubber. Stress strain behaviour and modulus of certain MWCNT / EPDM composites is shown in Figure 2.2.3.1–2. Improvements are caused by the high aspect ratio of the tubes, high surface area and occluded / bound rubber. The occluded rubber is shielded from deformation and the effective volume of the filler is increased. [16, 17, 23–26]. For the addition of 10 phr MWCNT to pure SBR, a 470 % increase in modulus, a 670 % increase in stress and a 47 % increase in strain at break, has been reported. These values are higher than those obtained with CB with the same filler loading. Modulus at 200 % and 300 % elongation increases as the MWCNT loading is increased due to the filler effect of occluded rubber

[26]. Elongation at break decreases with increasing MWCNT filler loading. [16, 17, 23–26], although some reports show a small increase with low filler loadings [16, 22].

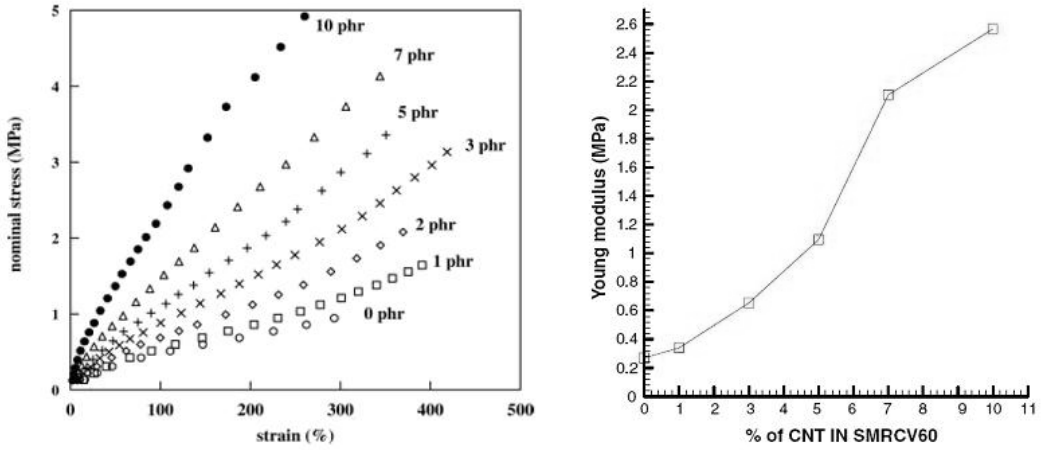

Figure 2.2.3.1–2 *Stress strain behaviour of SBR reinforced with MWCNT [22] and modulus for NR reinforced with MWCNT [16].*

A typical stress softening hysteresis, the Mullins effect, was achieved with consecutive stretches of MWCNT filled SBR. This indicates a breakdown of certain bonds between the MWCNT and the polymer: when the rubber is stretched consecutively, the force needed to reach the same strain becomes lower. Bokobza et al. reported stress softening of MWCNT filled SBR to be of the same magnitude as SBR with 50 phr of CB. [22]

MWCNTs have synergistic effects on properties with CB, which is evident from Fig. 2.2.3.1–3 [17, 23]. Specimens with a blend of the two fillers showed higher tensile strength, modulus and elongation at break than any single filler did. Stress softening was also increased by use of a filler blend containing both, CB and MWCNTs. [17, 23] Tear strength is reported to increase, when a blend of both fillers is used. Yan et al. reported an increase of approximately 40 % with silane–modified MWCNT for a MWCNT/CB/rubber ratio of 5/20/100 in phr compared to a composite with only 25 phr of CB [17].

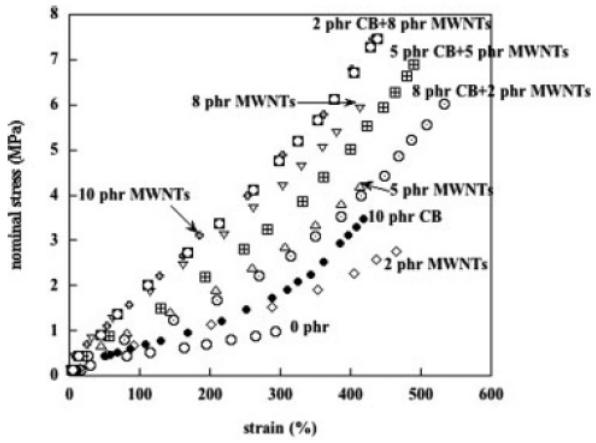

Figure 2.2.3.1–3 *Synergistic reinforcement of CB and MWCNT [23].*

Dynamical properties

MWCNT reduce the maximum tan δ value of rubbers (NBR, SBR and NR) and increase the loss and storage moduli at room temperature as can be seen in Fig. 2.2.3.1–4. The tan δ value or loss factor is the ratio of energy lost to the energy stored. The higher the tan δ value, the less elastic the rubber is and energy is turned into heat; with lower tan δ values, the rubber is more elastic. MWCNT are reported to shift the glass transition temperature (T_g) of rubbers to higher temperatures, which is due to its ability to hinder chain movement. These effects are more pronounced when CB and MWCNT are used together [17, 21 , 25]

While the dynamic properties of unfilled rubber depend on only temperature and frequency, the properties of filled rubbers are also amplitude dependent. Above a certain critical amplitude a drastic decrease in the storage modulus is observed. This behaviour is known as Payne effect. Rubber composites containing less than 3,8 wt–% MWCNT are reported to not show a Payne effect, as the filler–filler interaction is very low. [22]

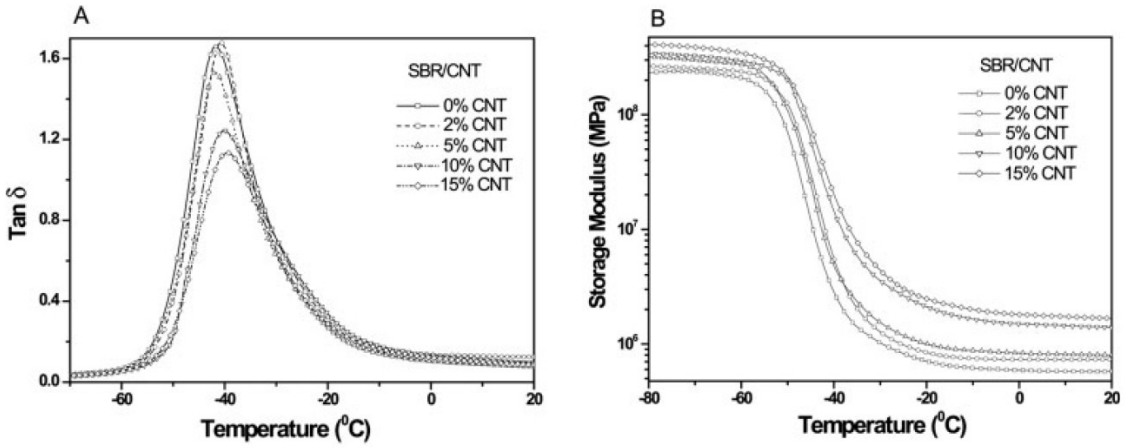

Figure 2.2.3.1–4 *Dynamic properties of SBR / acid treated MWCNT [21].*

Other properties

MWCNTs are expected to increase the thermal stability of the material by facilitating heat dissipation due to the good thermal conductivity [23]. It can absorb active degradation products, thus increasing thermal stability. Adding MWCNT increases the stability of SBR and NBR by increasing the onset of degradation. [21]. Thermal stability is assumed to depend on the interfacial bonding between the polymer and the filler: if the interfacial interactions are weak, the heat dissipation between filler particles and elastomer is limited and the heat distribution remains heterogenous [23].

MWCNT form interconnecting semi–conductive filler networks with elastomeric materials, when the loading is between 2 and 6 phr. [21, 22–24, 26, 27] At this percolation threshold, electrical resistivity drops several orders of magnitude. Formation of this semi–conductive network has been reported to be enhanced when both, CB and

CNT, are present [18, 23, 26]. The synergistic effect of CB and MWCNT can be seen in Fig. 2.2.3.1–5. In the case of filler blends, lower loadings of MWCNTs are needed to achieve the same decrease in resistivity as with the nanotubes alone. Resistivity decreases when the MWCNT filled specimen is stretched and is not fully recovered after unloading. Increase in resistivity results from the breakage of the conductive network, which do not reform. [18, 23]

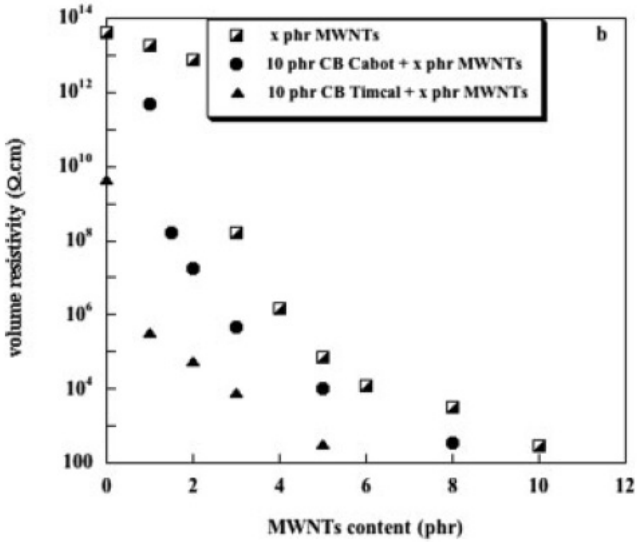

Figure 2.2.3.1–5 *Synergistic effect of CB and MWCNTs on resistivity of SBR. Cabot is a normal CB and Timcal is a conductive CB grade* [23].

2.2.3.2 Halloysite nanotubes

Structure

Halloysite nanotubes (HNT) are natural aluminosilicates. Halloysites have two layered crystalline tube structures, as can be seen in Fig. 2.2.3.2–1. The outer layer has a tetrahedral sheet structure and the surface resembles SiO_2, forming Si–O groups on the surface. The inner layer has an octahedral structure and the surface properties resemble Al_2O_3, with Al–OH groups inside the tube. Like in other clays, the OH–groups make dispersion very difficult due to their inter–particle affinity. The length of halloysite nanotubes varies between 1 to 15 μm and the inner diameter from 10 to 150 nm, depending on the deposit it is originated from. Unlike layered silicates and carbon nanotubes, halloysite nanotubes do not form tightly entangled structure, due to lower filler–filler interactions and there is no need for exfoliation. [28, 29] HNTs have potential to be well dispersible, because of the tubular morphology, a low hydroxyl density on the particle surface, favourable charge distribution and a unique crystal structure. [30, 31]

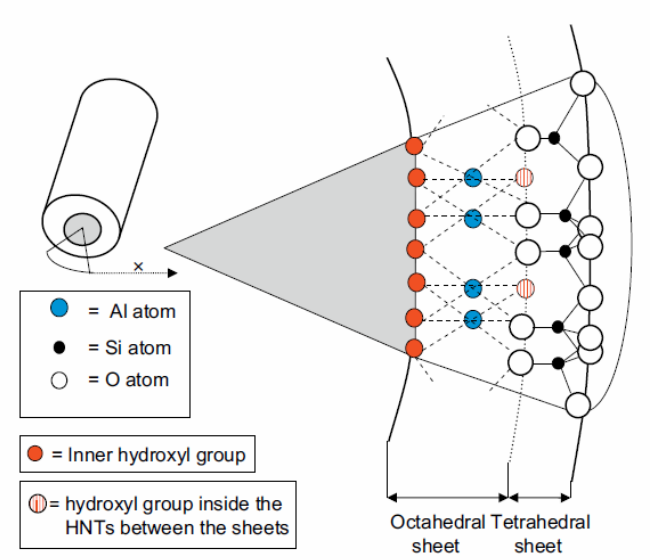

Figure 2.2.3.2–1 *Structure of HNTs [31].*

Curing behaviour

Pasbakhsh et al. partially replaced fillers by HNTs in two different EPDM compounds. The reference compounds contained silica or $CaCO_3$ as a co–filler with HNTs. As a result, curing time decreased and curing rate increased with increasing HNT fraction for both compounds. Cure time decreased, because HNTs do not adsorb accelerators so easily as silica and $CaCO_3$. They can also affect the pH differently, which facilitates different curing behaviour. HNTs have also much larger surface area than the traditional fillers. This leads also to faster curing due to decreased free volume. [31]

With silica / HNT compound, cure time decreased from ~29 to ~17 min and cure rate index increased from ~4 to ~7 min^{-1}, when HNT content increases from 0 to 30 phr. Cure rate index (CRI) is the time interval between 1 % and 90 % vulcanisation. The higher the index is, the faster the cure rate becomes. Replacing part of the silica with HNTs did not affect the scorch time. The minimum torque decreased with increasing HNT loading, which might make the processing of the compound easier. The delta torque decreased, when the amount of HNTs was increased, indicating a decrease in crosslink density. Delta torque is the difference of highest and lowest torque values during curing, and the increased delta torque values indicate higher crosslink density. [31]

With $CaCO_3$, the cure time decreased from ~22 to ~14 min, and the CRI peaked, when the ratio of the $CaCO_3$ and HNTs was 1:1. Replacing $CaCO_3$ with HNTs decreased the scorch time of the compound from ~7 to ~1 min, when HNT content increased from 0 to 30 phrs. HNTs decrease the damping properties of the compound, but enhance its resilience. The delta torque was slightly increased with replacement of $CaCO_3$ with HNTs, indicating better crosslink density. [31] Rooj et al. reported small increase in

curing and scorch time when 10 phr of HNT was used with NR. Curing rate also showed a decrease when HNTs were added [29].

Mechanical properties

Halloysite nanotubes enhance the mechanical properties of EPDM rubber. Tensile strength, elongation at break and modulus at 100 % elongation are improved greatly, especially for higher loadings, as can be seen from Fig. 2.2.3.2–2. The improvements stem from a good dispersion of HNTs, penetration of the elastomer into the tube lumen and the edge–to–face and edge–to–edge interactions of HNTs. Edge–to–edge and edge–to–face interactions are caused by the charge distribution of the HNTs, unusual crystal structure and low polarity of EPDM. Interactions between HNTs also cause formation of zig–zag –structures and a three dimensional orientation, which affect the properties of the composite. These structures can be seen in Fig. 2.2.3.2–3. The rubber occluded in the tube structure is shielded from deformation and reinforces the composite more efficiently than unoccluded rubber. [30]

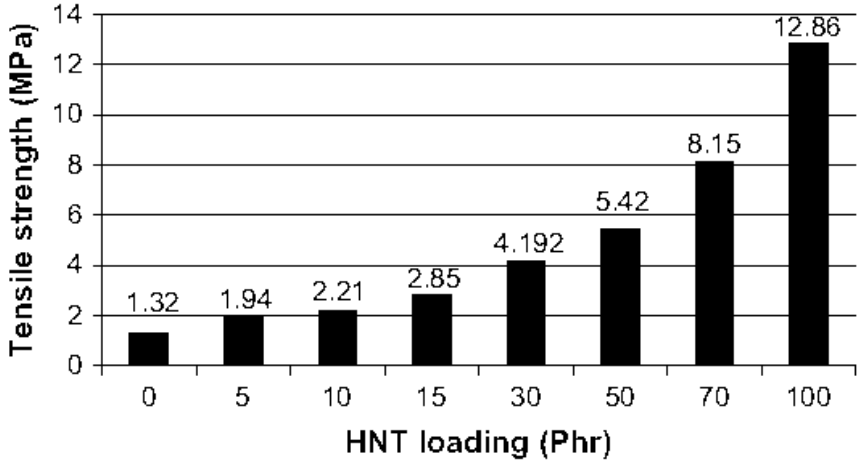

Figure 2.2.3.2–2 *Tensile strength of EPDM filled with HNTs at different loadings* [30].

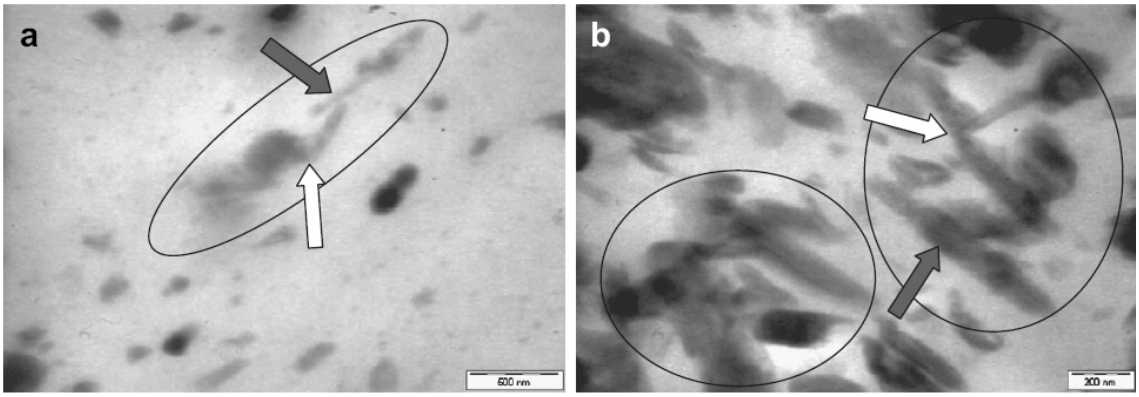

Figure 2.2.3.2–3 *Zig–zag -structures formed by HNTs in an EPDM matrix* [30].

Pasbakhsh Pooria et al. replaced $CaCO_3$ and silica by HNTs. They found, that tensile strength and elongation at break were improved as the HNT loading was increased.

Modulus at 100 % and 300 % elongation increased with an increasing amount of HNTs. [31]

In a silica compound, the tensile strength and elongation at break were enhanced for 5 phr loading of HNTs, but decreased drastically when further increasing the amount of HNTs. With silica, the modulus at 100 % elongation did not experience change, but modulus at 300 % elongation was increased. With HNT loading the quantity of the crosslinked polymer chains was increased compared to a pure silica compound, enhancing the modulus at higher strains [31]

With $CaCO_3$, the crosslink density was higher than with silica. This gave better properties, but also a low strain level. Improved mechanical properties were a consequence of the HNT's tubular shape, a higher surface area and a better dispersion in the EPDM matrix than with common fillers.
[31]

Dynamic and thermal properties

The dynamic properties are affected by the presence and the loading of HNTs. The effect also depends on the amount and type of other fillers in the blend. Pasbakhsh P. et al. demonstrated that tan δ, loss and storage modulus show the highest values, when the amount of common fillers is 25 phr and the HNT loading is 5 phr. This is the result of a smaller particle size, a larger specific surface area and the specific structure of the HNTs. It is also stated that this could be caused by synergistic structures created by the two different kinds of fillers. The new structure would resist periodic stress better than the normal structure with just single filler. [31]

In addition, enhancement in fire retardation and heat resistance has been detected with HNT fillers. Fire retardation and heat resistance are enhanced because of the larger char formation and occlusion of degradation products in the filler structure.

2.2.3.3 Nano–sized calcium carbonate

Structure

Calcium carbonate can be found naturally in several minerals. Calcium carbonate has many crystal forms; the mostly used one being trigonal rhombohedral, trigonal scalenohedral and orthorombic. Nano $CaCO_3$ ($nCaCO_3$) has an irregular globular shape and the mean particle size is between 20–400 nm. Crystal structure and composition depend on the base mineral. Nano $CaCO_3$ particles are hydrophilic and they form tight agglomerates, like clay particles. [13]

Vulcanization behaviour

Nano CaCO3 has been reported to increase the curing rate and curing time of the composite [32]. Swelling of $nCaCO_3$ filled SBR is reduced with increasing filler loading. Nano–sized, uniformly distributed and dispersed filler takes up more volume, forcing the polymer and curing agents in a smaller space making the reactions more probable and thus enhancing the crosslinking. [33–35]

Mechanical properties

In BR and SBR, the tensile strength increases up to 8–10 wt–% nano $CaCO_3$, after which it starts to decrease due to agglomeration. Nano $CaCO_3$ reinforced SBR has a higher tensile strength than with commercial $CaCO_3$ (size 20 μm), and an increase of 12 %, 42% and 92% in tensile strength is gained with the addition of 8 wt–% of nano $CaCO_3$ having particle sizes of 21, 15 and 9 nm respectively. Elongation at break increased with increasing filler loading with both rubbers. Elongation at break of filled SBR increased compared to the commercial $CaCO_3$ for all compositions as can be seen in Fig. 2.2.3.3–1. [33–36]

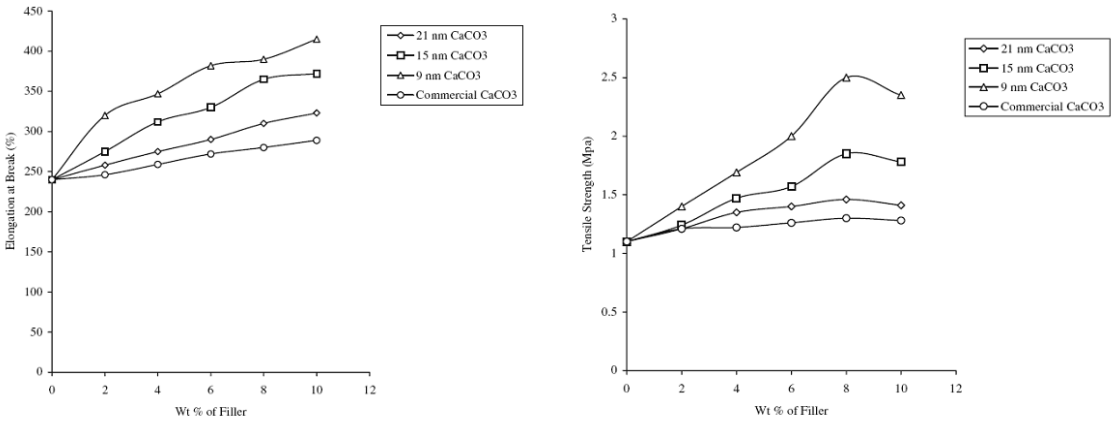

Figure 2.2.3.3–1 *Tensile strength and elongation at break for differently sized $CaCO_3$ [33].*

In SBR rubber, the modulus at 300 % elongation kept increasing with the loading of $nCaCO_3$ up to 8 wt–% of the filler, compared to commercial grade of $CaCO_3$. At loadings higher than 8 wt–%, modulus declined rapidly, due to the agglomeration of the nano filler. [34, 35]

When the filler loading increases in BR, the energy required for tearing gets higher. This was reported to happen up to a filler concentration of 15 wt–%, at even higher concentrations the tear energy starts to decline again. Increased tearing resistance is caused by the even dispersion and distribution of the filler and good interactions between the filler and matrix. Improvement in tear strength was also reported by Mishra et al. using $nCaCO_3$ filler. [36, 37]

Abrasion and hardness of SBR is reported to increase with $nCaCO_3$ compared to commercial grade $CaCO_3$ fillers or pure SBR. [35–37] The enhanced properties stem from the increased interactions between the nano–sized filler and the matrix due to an increased surface area [33–35, 36].

Dynamic and thermal properties

The glass transition temperature is reported to increase, when $CaCO_3$ particles are small enough, 9 nm in diameter in this case. The small particles hinder elastomer chain movement and shift the transition to glassy state to higher temperatures. [33]

Nano–sized calcium carbonate affects the thermal properties of rubber materials. Introducing $CaCO_3$ filler into a BR compound enhances the thermal stability by decreasing the initial decomposition temperature. [35, 37] SBR shows the same trend: the initial degradation temperature of the compound filled with nano–sized $CaCO_3$ increases compared to a conventional $CaCO_3$ filler [33, 34].

Also, the flame retardancy of SBR increases compared to commercial size $CaCO_3$ filler. Fig. 2.2.3.3–2 illustrates the effect of particle size of the filler on the fire retardancy [33, 34].

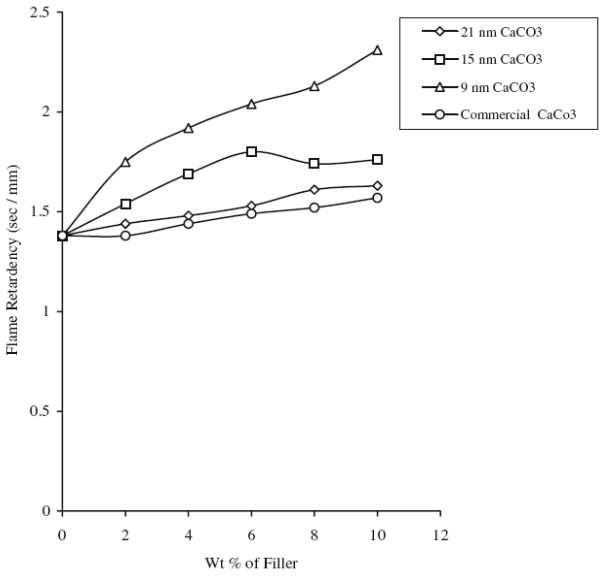

Figure 2.2.3.3–2 *Flame retardancy with differently sized $CaCO_3$ particles in SBR [33].*

Inorganic nano–scale fillers like $CaCO_3$ form a char layer on the surface of the burning material just like traditional fillers. The char layer acts like a thermal insulator and mass transfer barrier. The char shields the rubber from the heat and restricts volatile combustion products from escaping from the rubber. [33, 35]

2.2.3.4 Nano–sized clays

Structure

Usually, the layered silicates used as fillers are phyllosilicates like montmorillonite, hectorite and saponite. Phyllosilicates form platelet structures that consist of layers of silicate sheets. The sheets are s few nanometres thick, but width and length can be hundreds of nanometres depending on the type of silicate. The crystal structure of the layer is shown in Figure 2.2.3.4–1. [38, 39]

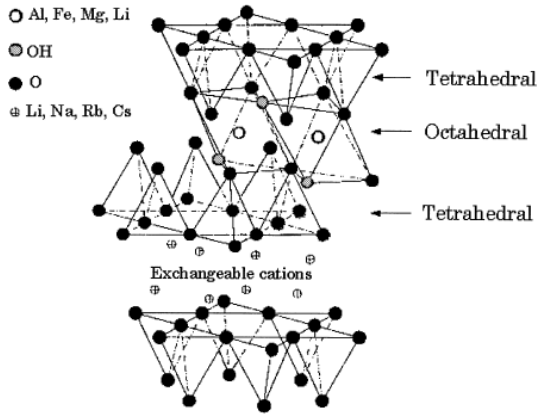

Figure 2.2.3.4–1 *Structure of layered silicate [39].*

These layers are stacked together forming a gap in–between; they are held together by van der Waals forces. This gap is called the interlayer or the gallery. The platelet structure can be expanded or even broken down to achieve thin platelets. In expanded fillers the polymer chains can penetrate into the galleries. Possible composite structures of clay nanoplatelets are shown in Fig. 2.2.3.4–2. The composite properties improve from left to right, so the exfoliated structure has the best properties. Silicates are very hydrophilic and are usually modified to better interact with hydrophobic polymers. These clays are usually termed organoclays. [38, 39]

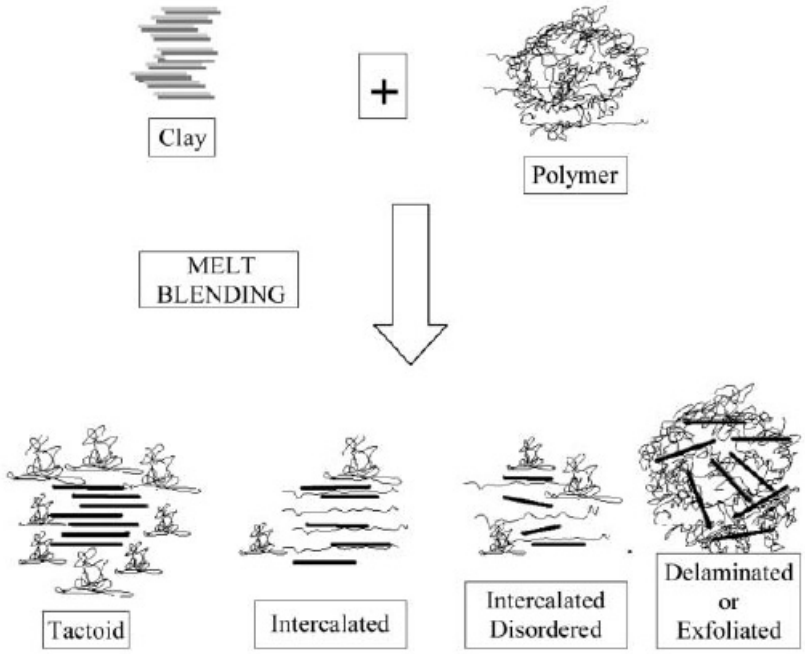

Figure 2.2.3.4–2 *Structures of nanoclay filled composites [38].*

Vulcanization behaviour

When nano–sized organoclay (NOC) filled EPDM is being vulcanized with sulphur, scorch and cure time can increase or decrease compared to the pristine EPDM depending on the modification of the clay. Cure and scorch time decrease rapidly with amine treated nanoclay, when small amounts, 2,5 phr, of filler is added, and start to level off when loading is further increased. The curing behaviour of octadecyltrimethylamine–modified clay as a function of filler loading is shown in Fig. 2.2.3.4–3. The acceleration effect of NOC is caused by the amine treatment that is commonly used with NOC to promote interactions between the filler and matrix. Amine modification eases the accelerator complex formation and thus speeds up the vulcanization. There is also a noticeable increase in the minimum and maximum torque during curing compared to pristine EPDM. The higher torque is related to the larger filler surface area and the effect of amine modification on the cure characteristics. [40, 41] In contrast to this, an increase in cure and scorch time was reported by Chang et al. and Tan et al. The reason for the increase in cure and scorch time in this case is the partial adsorption of curing agents on the filler surface or the interactions between the modification agent and the curatives. The increase in torque values and delta torque was lower than in with amine modified nanoclays. [40, 42]

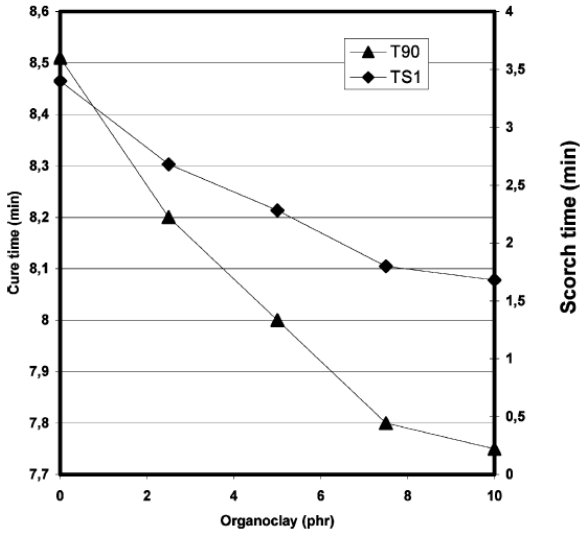

Figure 2.2.3.4–3 *Vulcanization behaviour of nanoclay reinforced EPDM modified with octadecyltrimethylamine and cured with sulphur [42].*

Mechanical properties

Addition of modified NOC to EPDM increases tensile strength and modulus compared to unfilled EPDM. Tensile strength and modulus increase with increasing filler loading. There are also reports that suggest properties to decrease or level of after certain loading is reached. Tensile properties of different types of nanoclay / EPDM composites are shown in Fig. 2.2.3.4–4. Elongation at break is reported to peak at certain filler loading. The properties are strongly affected by the specific modification used. Gatos et al. suggests that the decrease after peak is caused by the agglomeration of filler particles. [42–44] There are also reports of decreasing elongation at break as filler loading is increased. [42, 45] Enhancement in tensile properties is due to an intercalation of rubber into the galleries of clay and because of the strong interaction between the filler and the matrix. [42–44] Nanoclay can act synergistically with CB and increase properties of the hypridcomposite. [46]

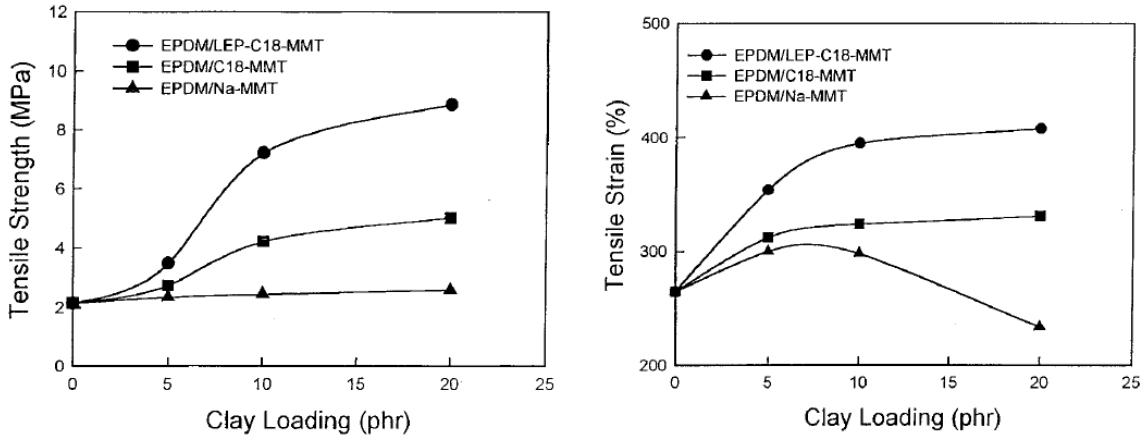

Figure 2.2.3.4–4 *Tensile strength and strain for unmodified, octadecylamine treated and amine modified montmorillonite with low molecular mass EPDM [42].*

Tear strength also undergoes improvement with increasing NOC loading compared to pristine EPDM, because of the quite uniform distribution and dispersion of fillers, which hinders crack propagation. [42, 43] Hardness has also been reported to increase with increasing loading. [40]

Dynamic properties

Addition of modified NOC filler to EPDM decreases the tan δ and increases the storage modulus compared to pristine EPDM, making the polymer more elastic. The presence of NOCs also shifts T_g towards higher temperatures. [40, 42–44] The changes in dynamic properties are explained by good interactions between the filler and the matrix. [42–44]

Other properties

Thermal stability of NOC filled EPDM is increased as can be seen from Fig. 2.2.3.4–5. The effect is more pronounced with higher NOC loadings. NOC fillers are preventing the diffusion of volatile decomposition products and are the reason for the improved thermal stability. [41, 43]

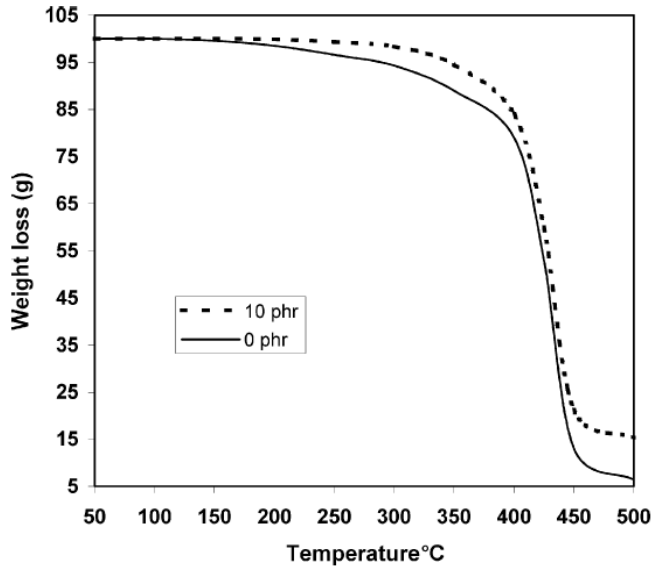

Figure 2.2.3.4–5 *Thermal stability of octadecyltrimethylamine treated montmorillonite clay / EPDM composite [41].*

Clay fillers decrease gas permeability: Increased barrier properties are derived from the even distribution of nanoparticles, their platelet shape and planar orientation. 60 % decrease in oxygen permeability has been reported by Chang et al., with 10 phr of amine modified NOC compared to pristine EPDM. [42]

2.2.4. Modification of nanofillers

2.2.4.1 Carbon nanotubes

CNTs do not have functional groups that are suitable for strong interactions with the elastomer matrix. [21] Due to weak interactions between carbon nanotubes and the elastomers, several different modification methods have been used to gain stronger interactions.

One method used to modify CNTs is ball–milling: CNTs are milled in the presence of a reactant, for example NH_3, H_2S, Cl_2 or CH_3SH gasses. Grinding in a ball mill breaks C–C bonds within the carbon nanotubes and reactions with the reactant induces active groups in the structure. Some active groups, which were introduced into the CNT structure with a gaseous reactant, are given in Table 2.2.4.1–1. These groups might enhance interactions with the matrix as such, or they can be used to further modify CNTs. Milling can improve properties also by opening the CNT structure for polymer occlusion and breaking of the entangled structure. At the same time, the CNTs aspect ratio decreases and flaws are introduced into the CNT structure. These can cause deterioration in the CNTs properties. [22, 47, 48].

Table 2.2.4.1–1 *Functional groups introduced into carbon nanotube structures [48].*

Reactant	Functional group
H_2S	-SH
NH_3	$-NH_2$, $-CONH_2$
Cl_2	-Cl
CO	>C=O
CH_3SH	$-SCH_3$
$COCl_2$	-COCl

Chemical modification methods are also studied extensively. Compared to ball milling, chemical modification is a more gentle process and the CNT structure is not broken during modification. Two approaches have been utilized: non–covalent and covalent surface modification. Non–covalent modifications do not alter the chemical structure of the CNT surface, but the enhancement in interactions towards the matrix can be less intensive than for the covalent approach. However, if interactions are good enough, better mechanical properties might be expected because of the pristine CNT structure. [49, 50] Non–covalent modification is achieved by wrapping polymers around the CNTs or by adsorption of the polymers to the surface. [50]

MWCNT have been treated with mixtures of oxidizing acids to promote the surface functionality. Sulphuric and nitric acid mixtures are mainly used. With this method, carboxylic acid groups have been introduced into the surface. [49, 51] This can also be achieved by UV / ozone treatment [52]. Formed carboxyl and hydroxyl groups can

promote interactions between the filler and matrix: For example, oxygenated or nitrogenated functional groups can interact with the unsaturated carbon bonds on the elastomer. [21] This carboxylation has also been used to link different polymer molecules to CNT structure [49, 51].

Silane coupling agents has also been used to modify CNTs, which have –OH groups on the surface. The silane functionalization process is illustrated in Fig. 2.2.4.1–1.

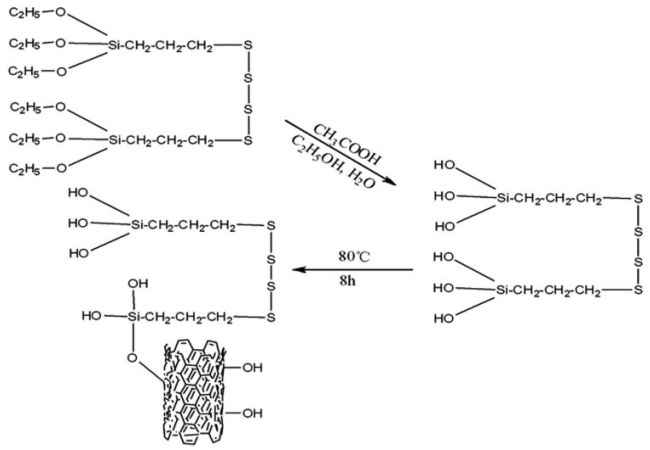

Figure 2.2.4.1–1 *Introducing silane to MWCNT structure [17].*

The silane modified CNTs are suggested to react with natural rubber matrix according the reaction illustrated in Fig 2.2.4.1–2. During vulcanization, the polysulfide groups are broken and form reactive mercapto groups, which can react with the polymer. [17]

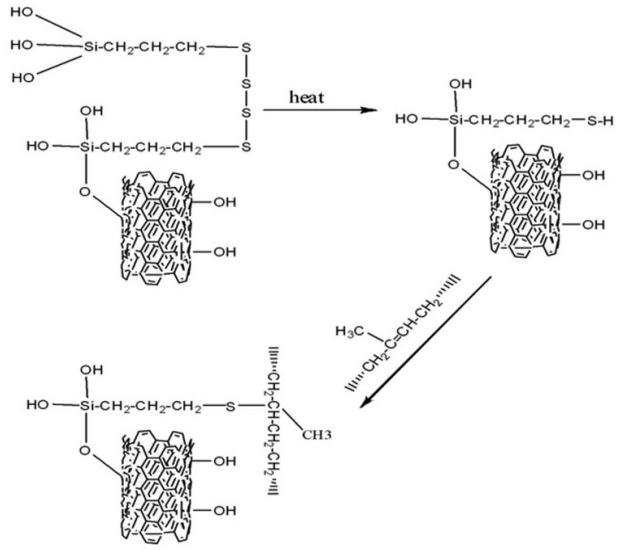

Figure 2.2.4.1–2 *Binding of functionalized MWCNTs to a polymer* [17].

CNT rubber compounds have also been modified with ionic liquids, 1–allyl–3–methyl imidazolium chloride (AMIC) shown in Figure 2.2.4.1–3. Mixing of CNTs and anionic liquids was done in ethanol in an ultrasound bath. The double bond on the tail of the AMIC's structure, is stated to form sulphur bridges with double bonds in the elastomers

structure during curing, thus enhancing the interactions of the filler–matrix system. Using ionic liquid modificated CNTs enhanced mechanical properties, especially elongation at break, which doubled compared to composites without modification. The ionic liquid modification decreased the resistivity of the composite from 10^{-6} to 10^{-4} S/cm. The T_g temperature shifted towards higher temperatures and tan δ decreased. [20]

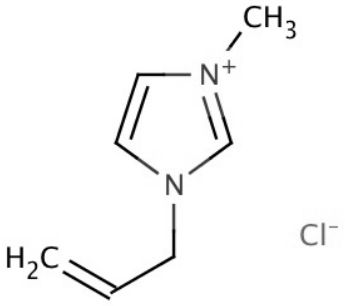

Figure 2.2.4.1–3 *1–allyl–3–methyl imidazolium chlorides structure [20].*

2.2.4.2 Halloysite nanotubes

Halloysites are normal hydrophilic clays. Unlike many clays, they do not have –OH groups on their outer surface. The OH–groups are inside the tube and the outer surface is composed of siloxane moieties. Attempts have been made to change these hydrophilic surface properties into a more hydrophobic character by surface modification. For rubbers not much research was done, but a few methods utilized are described below. [38, 39]

One modification method is a chemical modification with organosilanes. In this method, the amino group of the silane reacts with the OH–groups inside the tube. Yuan et al. utilized for this modification γ–aminopropyltriethoxysilane (APTES). The possible structure of the modified HNTs is shown in Fig. 2.2.4.2–1. It is suggested that APTES reacts directly with the –OH groups, but would also form bonds with oligomerized APTES and other APTES molecules attached to the inner wall. Unfortunately, the modified material was not tested in composites, so no conclusions can be drawn concerning their influence on material properties. [53]

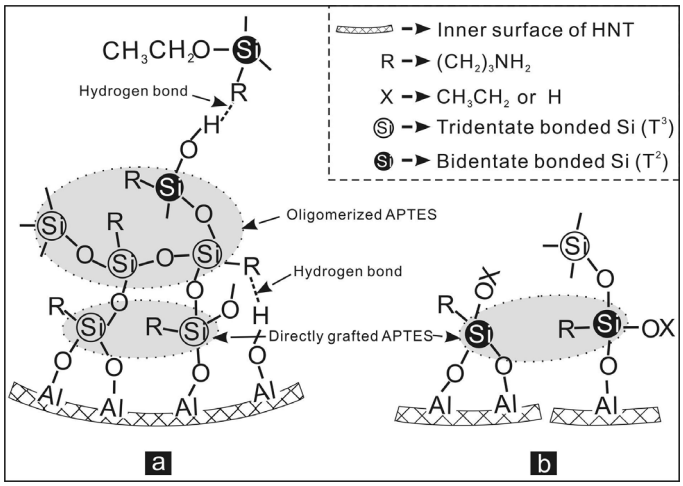

Figure 2.2.4.2–1 *Modification of HNTs with silane* [53].

Another method was modification of HNTs with methacrylic acid (MMA) and sorbic acid (SA). These acids act as interfacial modifiers and are adsorbed to the surface of HNTs, probably via strong hydrogen bonds. For SBR rubber, a 4 to 5 fold increase in tensile and tear strength is achieved when the ratio of HNT/SA is 40/12 phr. Improvements of the same magnitude are reported with MMA. [54]

2.2.4.3 Nanoclays

As discussed, aluminosilicates, which are used as nanoclays, have two layered silicate structures with gap in–between. The attraction between these sheets is weaker than in some other clay materials, because the cationic structure between the layers balances the charge distribution. Within the layers, isomorphic substitution of Al^{3+} with Mg^{2+} or Fe^{2+} generates excessive negative charge. This charge is balanced by ions, like Na^{+} and Li^{+}, which makes clay a hydrophilic material, and makes the clay expandable by water. [7, 55]

The modification of clay nanomaterials is focused on making the clay more hydrophobic, by exchanging the hydrophilic cations within the structure by more hydrophobic ones. This is done mainly by organic cations, such as alkylammonium ions; the modified clays are then called organoclays. Nearly all commercially available nanoclays are modificated this way. [7, 55]

The modification mechanism for making clay more hydrophobic using cation exchange method is shown in Fig. 2.2.4.3–1. The widened gallery makes it easier for a polymer chain to intercalate into the gallery. The mostly used alkylammonium ions are based on primary alkyl amines, but secondary and tertiary amines have also been tested. Ammonium ions with an alkyl group having more than 8 carbon atoms have proven to promote exfoliation, while shorter ions result in an intercalated structure. [7]

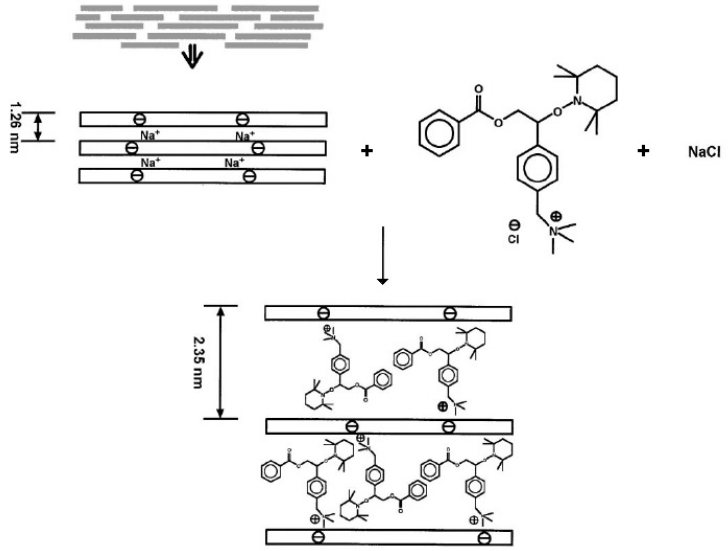

Figure 2.2.4.3–1 *Basic mechanism of the cation exchange method for modification of layered silicates [39].*

Ion–dipole interactions also provide a way of intercalating small molecules into the gallery, thus making it easier for the polymer chains to enter the structure. The edges of the clay sheet can be made more hydrophobic by silane modification. This method can also be used together with ammonium modification in order to provide even better interactions between the filler and the matrix. Additionally, compatibilizer systems are used, in which one end of the compatibilizing polymer is favourable for the filler and the other end for the matrix polymer. [7, 39]

2.2.4.4 Calcium carbonate

With calcium carbonates, three surface modification techniques have been utilized

- Non–reactive treatment
- Reactive coupling and
- Grafting

A non–reactive treatment lowers the surface tension of the filler and decreases the filler–filler interactions. This leads to lower aggregation of the $CaCO_3$, and improvements in homogeneity, surface equality and processability are achieved. However, tensile and yield stress are decreased. Calcium and magnesium stearates, silicone oils, waxes and ionomers are used as non–reactive modifiers with nano $CaCO_3$. [56]

In reactive modification, reactive groups on the $CaCO_3$ surface are used to make it more compatible with polymer matrix. Many different kinds of modification have been used, including alkylalkoxysilanes, alkylsilyl chlorides, dialkyltitanates and stearic acid. Although $CaCO_3$ does not have–OH groups on its surface, some reactivity with silanes is reported. [56]

The third method is grafting of polymer chains onto the nano $CaCO_3$, or grafting the matrix polymer with groups more compatible with $CaCO_3$. Small polymers can penetrate into and the agglomerated $CaCO_3$ and react with the activated sites. Polymers attached to the $CaCO_3$ reduce the surface tension, making the filler more readily dispersible. Irradiation grafting is one process used for this modification. [56]

2.3. Mixing

2.3.1. Principles of mixing

Mixing a rubber compound is a complex process and is affected by many variables. The goal of the mixing process is to achieve an even distribution and dispersion of the additives in the compound, which processes well in the next steps, cures efficiently and shows the required properties. This needs to be achieved with a minimum mixing time and energy consumption during mixing. In addition to the actual processing parameters, the feeding order and timing of the feeding are the most important variables regarding successful mixing. [4, 57]

To achieve a good mixing result, the number of additions should be kept as small as possible, because during feeding ineffective mixing occurs. Fillers should be added as early as possible to make use of the high shear stresses, which improves dispersion. Shear stresses are higher in the beginning of the mixing process due to the higher viscosity of the polymer. Plasticizers lower the viscosity and they should be fed later in the mixing scheme. The metal surfaces in the mixing chamber may be overlubricated by plasticizers and thus cause decreased mixing efficiency. This can be avoided, if fillers are fed at the same time to absorb excess plasticizers or the plasticizers are added in multiple stages. After addition of the curing agents, the temperature should not reach levels, at which vulcanization occurs, unless it is part of the mixing scheme. Scorching of rubber must be avoided during the mixing. [4, 57, 58]

Rubber compounds are mixed in one or two stages. In one stage mixing, all ingredients, except sulphur and other curing agents, are mixed in one cycle. The curing system is then added on a mill afterwards. In a two stage system, the elastomer, fillers and plasticizers are added during the first stage of the mixing. The material is then removed from the mixing chamber and allowed to cool down. In the second stage, the cold material is fed again into the mixer, where curing agents are added. As a good dispersion of ingredients is achieved during the first mixing stage, high shear forces are not needed and temperature generation can easier be kept under control in this stage. [4, 57, 58]

Two stage processes reduce the throughput of the mixer as well as increase mixing time compared to the one stage method. However, a second step is necessary, if dispersion

requires intensive mixing, downstream processes require fast cure activity, or if compounds need subsequent treatment or transportation. It is also used when the masterbatch of the first stage is the basis for different formulations or it is used in blends. [4, 57, 58]

2.3.2. Feeding order

The following mixing principles are applied:

- Conventional
- Late oil addition
- Upside–down
- Sandwich

In conventional mixing, the elastomer is fed first into the mixer and plasticized. In the next feeding phase, fillers and liquid ingredients are added, as shown in Figure 2.3.2–1. Fillers and liquids that are difficult to incorporate and disperse are added first. This may lead to long cycle times, if multiple additions are needed. Benefits of long mixing cycles are slow heat generation during mixing, which makes one pass mixing feasible. This conventional mixing method results in good distribution and dispersion of all ingredients. Several variations of this method exist: One of the variations is a method, in which a part of the liquid plasticizers is added together with the fillers to prevent cakeing of the filler or to increase bulk density of the filler. [4, 57, 58]

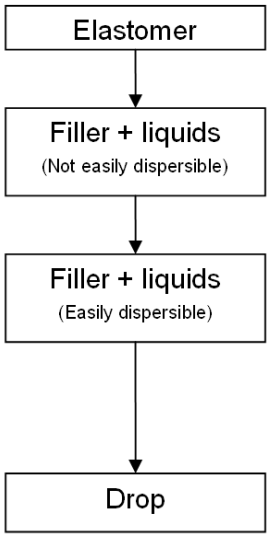

Figure 2.3.2–1 *Conventional mixing method.*

In the late oil addition method, elastomers and fillers are fed into the mixer first as seen in Figure 2.3.2–2. These components are mixed with high rotor speed, so that good incorporation, distribution and dispersion are achieved in less than two minutes. Mixing is continued with a lower rotor speed, until the liquid plasticizers are incorporated.

Good dispersion is achieved with this mixing technique due to the high shear stresses in the beginning of the mixing. However, mixing of highly viscous materials at high rotor speeds consumes more power and makes the mixing expensive. This technique usually requires two–stage mixing. [4, 57, 58]

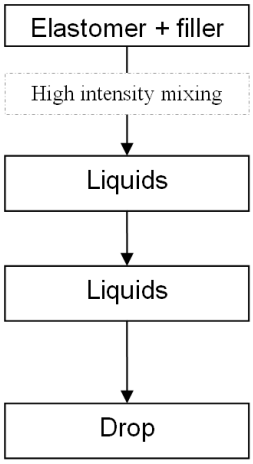

Figure 2.3.2–2 *Late oil addition method.*

Liquid plasticizers are added in the second feeding phase in one or multiple stages, depending on its quantity. Addition of large quantities of liquid plasticizers may cause slippage between rubber and the rotor, or rubber and chamber wall. Machines capable of injecting oil straight into the mixing chamber, are usually used with this mixing technique. [4, 57, 58]

An upside–down mixing scheme is shown in Figure 2.3.2–3. In the upside–down mixing method, all the dry ingredients, except for the elastomer, are mixed first. Then all the liquids are added and mixing is continued so that a paste is formed and temperature starts to rise again. At this point, the elastomer is finally added. It is often the fastest and simplest way of mixing, and is preferably used for compounds with less than 25 % of elastomer: in these cases, the elastomer does not fill the chamber adequately. This method is also used for elastomers that have low self–adhesion, like EPDM. It is a very effective mixing method, when the compound has high amounts of liquid plasticizers and the fillers with a large particle–size are used. Fillers with low structure, small particle–size or low surface energy can not efficiently be mixed with this technique. [4, 57, 58]

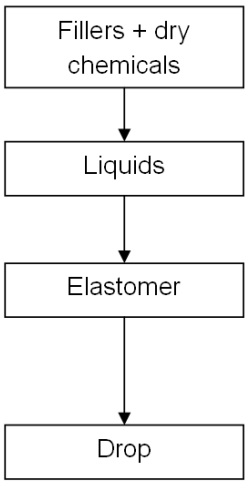

Figure 2.3.2–3 *Upside–down method.*

The sandwich method is used when two polymers with different solubilities and/or polarity are mixed. In the first phase, one of the polymers is mixed with fillers and plasticizers. The solubility towards the other polymer might be enhanced, when the polymer is mixed with the ingredients. In the second phase, the remaining polymer is added to the mixer and mixing is proceeded to completion. When fillers have different solubilities or polarities towards the polymers, this method enhances the homogenous distribution and dispersion and results in enhanced properties of the compound. [4, 57, 58]

2.3.3. Mixing equipment

The rubber mixing equipment can be divided into three groups: mills, internal mixers and continuous mixers. Continuous mixers are usually single or twin screw extruders.

The mill is a mixing machine, on which the rubber is fed through two cylindrical rolls. Mixing happens when the material is forced to travel through the small space between the rolls. The gap between the rolls can be controlled. Different ingredients are fed on the rolls and mixing is ensured by passing the rubber sufficient times. As the rubber material needs to be handled and folded manually on the mill, to gain sufficient dispersion and distribution of the additives, the mixing times for a batch can be as long as one hour. Because of the easy cleaning of the equipment, mills are often used with coloured or white products. [4]

Internal mixers are the mostly used mixers in the rubber industry. The basic structure of internal mixers is illustrated in Fig. 2.3.3–1. Rubber is fed into the machine through a feeding hatch. A piston pushes the rubber into the mixing zone and seals the mixing chamber. The mixing is done by rotors; usually a two rotor setup is used. The ready rubber compound is ejected though a hatch at the bottom of the mixing chamber. [4]

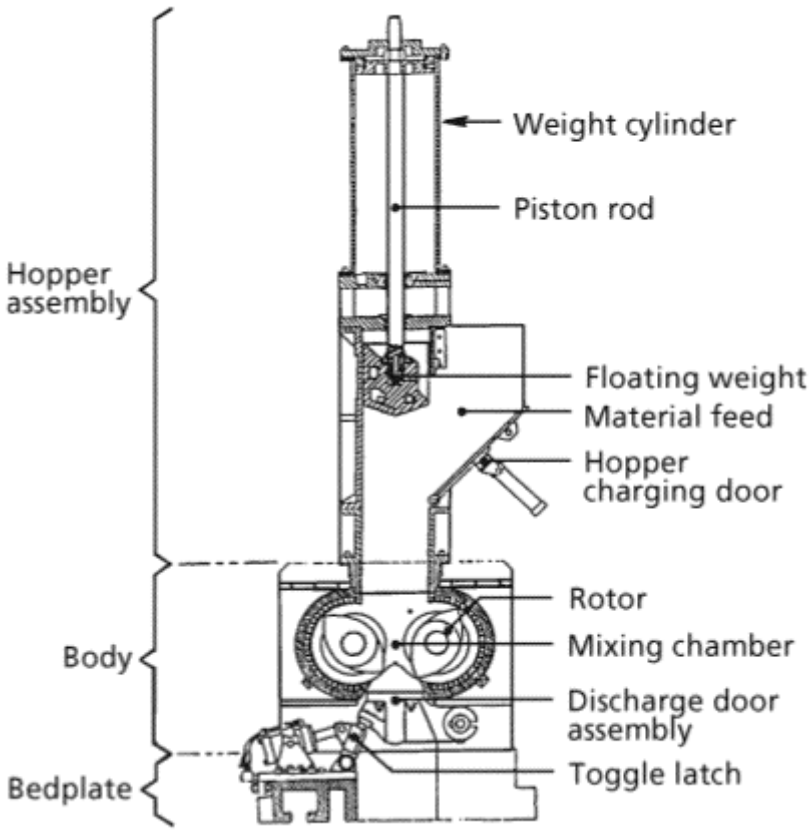

Figure 2.3.3–1 *Structure of an internal mixer. [3]*

Internal mixers are divided into two categories depending on their rotor design, intermeshing and tangential (Banbury) mixers. In tangential mixers, the screw flights are tangential to each other and there's a small gap between them. A tangential rotor can be seen in Fig 2.3.3–2 A. The rotating movement of the rotor can be altered and different rotating directions and speeds can be used. Dispersion takes place between the rotor flight and the chamber wall. [4, 12, 58]

In intermeshing mixers, the screw flights are intermeshing and there's a small gap between the flights and the rotors hulls. An intermeshing rotor is illustrated in Fig. 2.3.3–2 B. Intermeshing rotors need to rotate with same speed and in opposite directions, because of the intermeshing geometry. In these mixers, dispersion happens between the chamber wall and rotor flight and also between the rotors. In the beginning of the mixing process, dispersion occurs in the gap between the rotors. Later the dispersion takes place in the gap between the rotor flight and the chamber wall. This is where the most effective dispersion happens. [57, 58]

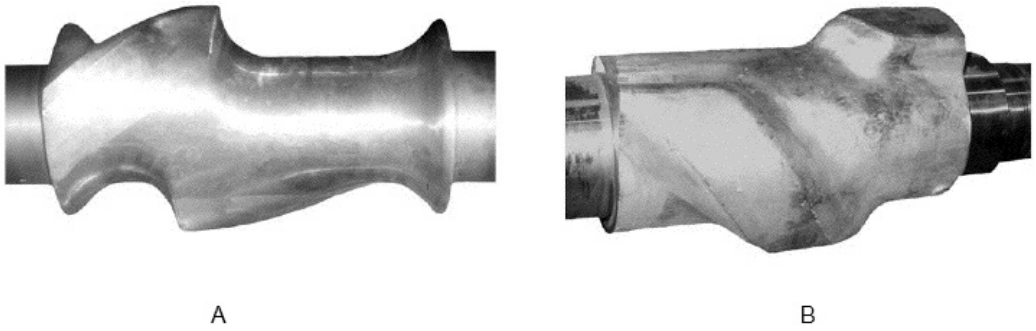

Figure 2.3.3–2 *Different rotor types A Tangential rotor. B Intermeshing rotor [58].*

As the tangential mixer has larger ingestion zone than the intermeshing one, the feeding and incorporation fillers is faster. [3] Tangential mixers also discharge material faster and thus the total cycle time is shorter than in an intermeshing mixer. Tangential mixers are used when high production rate is desired. Intermeshing rotors tend to be little larger than tangential ones and take more space in the chamber. This leads to reduced batch size. [57] The material flow in the intermeshing mixer is characterized by a large contact surface between rubber and metal, enhancing the heat transfer and improving the temperature control. This makes one stage mixing easier to execute. A tangential machine produces weaker flow interactions between the rotors and the distributive mixing is not as effective as with intermeshing rotors. [3] More differences are shown in Table 2.3.3–1. [4, 57, 58]

Table 2.3.3–1 *Differences in intermeshing and tangential mixing machines [58].*

Observation	**Tangential rotor**	**Intermeshing rotor**
Average fill factor	Up to 78%	Up to 75%
Speed of ram descent after feed	Relatively fast	Depends on rotor shape, but generally slow(er)
Time for ram to bottom	30-50% into cycle	50-100% into cycle, depending on rotor shape
Power peak occurs	Earlier in cycle	Later in cycle
Mix development	Disperse/Distribute	Distribute/Disperse
Material motion around chamber	Towards centre, with greater distributional flow with more recent rotor designs	Each rotor carries material towards opposite chamber end, resulting in excellent distributional flow
Oil incorporation	Slower	Faster
Mix temperature control	Poorer - lower surface/volume ratio in mixing chamber	Better - higher surface/volume ratio in mixing chamber
Form of dump	Large lump	Rough sheet

2.3.4. Mechanism of mixing

Three overlapping mixing mechanisms can be distinguished:

- Incorporation,
- Dispersion, and
- Distribution.

In the incorporation step, different components are mixed to one homogenous mass, and the filler is incorporated into the rubber matrix. During the dispersion and distribution stages, fillers and other additives are broken down to smaller particles and dispersed homogenously throughout the matrix. A homogenous compound is the result of both, dispersion and distribution, acting simultaneously. The formation of homogenous compound is shown in Fig 2.3.4–1. [3]

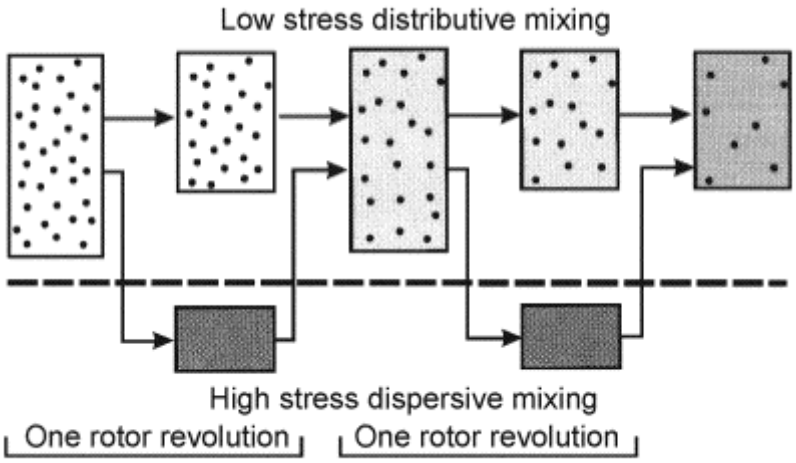

Figure 2.3.4–1 *Co–operative action of dispersion and distribution in a mixing procedure* [3].

2.3.4.1 Incorporation

During incorporation, rubber and the different additives are transformed into a cohesive and substantially incompressible mass [3]. Incorporation is schematically illustrated in Fig. 2.3.4.1–1. At this stage, rubber is substantially deformed, which gives rise to a large surface area. This facilitates incorporation of the filler into the rubber phase. The large filler particles are broken into smaller units, the agglomerates. This causes the surface area of the fillers to increase and makes incorporation more effective. Rubber is able to migrate inside agglomerates and causes the density to rise, until the solid density is reached. Aggregate formation is very small during incorporation, [3. 4]

Figure 2.3.4.1–1 *Incorporation of fillers in a matrix [59].*

Incorporation can be divided in three overlapping stages:

1. Encapsulation,
2. Subdivision,
3. Immobilisation.

During encapsulation, filler particles are surrounded by the elastomer forming a coarse heterogeneous mass. Encapsulation is achieved with free–surface folding flows that usually occur between the rotors in an internal mixer. After encapsulation, the mass is capable of undergoing viscous flow. [3]

At the subdivision stage, the rubber starts to achieve a uniform composition at microscopic level as a consequence of the elongational flow and shear forces.[3] At the same deformation rate, elongational flow is much more effective in incorporating and breaking fillers. Subdivision is illustrated Fig. 2.3.4.1–2. Mixing machines have been designed to produce high shearing action, which makes shearing flows the main method of incorporation and breaking up fillers [57]. Rubber mediates the stresses to the filler particles causing them to break into aggregates. Broken filler particles are then again covered by rubber. Subdivision produces a finer structure, where the distance between filler particles and the particle size is decreased. [3]

Figure 2.3.4.1–2 *Subdivision of rubber matrix [59].*

During immobilisation, elastomer molecules migrate to internal voids of filler particles. This process happens during the whole incorporation process, parallel with the encapsulation and subdivision step. Rubber chains trapped in the voids are shielded from further stresses. [3]

2.3.4.2 Dispersion

In dispersive mixing, filler agglomerates are broken down and particle size decreases, as is seen from the Fig. 2.3.4.2–1. This requires high shear and more energy than the incorporation process. High shear is needed to break the filer–filler interactions. [57] As a result, the viscosity of a compound is decreased. At the beginning of the dispersion stage, high stresses are generated by shear and elongational flow due to the high viscosity and incompressibility of the rubber. The large size of the filler agglomerates makes them very susceptible to fracture, making the dispersion process very fast. When agglomerates are broken down, some of the immobilised rubber inside the void is freed. The mobilized rubber lowers the viscosity of the compound, thus making the dispersion

more difficult by lowering the attainable stress level. At the same time, the critical stress needed to break the smaller filler agglomerates, increases. These conditions make it very difficult to obtain an optimal dispersion. [3]

Figure 2.3.4.2–1 *Dispersion of fillers in matrix [59].*

2.3.4.3 Distribution

This stage distributes agglomerates evenly in the matrix without breaking them. Distribution of fillers is shown in Fig. 2.3.4.3–1. It is achieved by both elongational and shear flows. Elongational flow is more efficient but it is not easily achieved in an internal mixer. In addition, the elongation rates produced are usually low and periods of elongational flow are usually very short. [60] Distribution is a result of these two flows combined with material movement and folding in the internal mixer. [3]

Figure 2.3.4.3–1 *Distribution of fillers in a matrix [59].*

2.3.5. Fillers and mixing

Mixing of a compound is affected by the affinity between the filler and polymer. The level of interaction between filler and polymer can be measured by wetting: When filler and matrix have a high affinity towards each other, wetting is good and no phase separation occurs. This makes incorporation and dispersion easier and better mixing is achieved. Good wetting usually results in good adhesion between the filler and polymer [60]

Wetting is affected by

- Surface and interfacial tension,
- Polarity,
- Surface contamination,
- Irregularities and flows at the interface, and

- Arrangement of resin and other additives at the boundaries.

Usually, good wetting requires a high surface tension of the filler, a low interfacial tension and a low surface tension of the polymer, leading to low contact angles. Polarity also affects the wetting behaviour: If the polarity of the filler and the polymer are more alike, the affinity between them is higher. This is not the case with most of the rubber filler combinations. Contaminants at the surface usually decreases the wetting. Effects of the interface irregularities and flows, as the effect of resin and additives at the boundaries is complex and can not be simplified. [60]

Filler–filler interactions also play an important role in mixing. The main types of interactions are electrostatic forces, van der Waals forces and forces caused by moisture. Electrostatic forces are determined by filler conductivity: the higher the conductivity, the lower the inter–particle forces. These forces are usually quite small. Moisture causes attractive forces through liquid bridges. The forces can be high, if a critical moisture content is reached. Rough surfaces decrease the force significantly. Van der Waals forces depend on the distance between the particles, their density, shape and size. With decreasing size, the attractive forces increase. This leads to agglomerates that are tightly bound together, and makes very small particles hard to disperse, because the hydrodynamic forces that mediate the stress to the agglomerate also decrease with particle size. This leads to the conclusion that high shearing forces are needed to break nanofiller particles in order to compensate the loss of hydrodynamic forces. The hydrodynamic forces can also be increased with increasing interactions between the filler and polymer. These forces are also affected by the viscosity of the matrix polymer; this is why the most effective dispersion occurs at the early stages of mixing when temperature is still low. [60]

After the filler particles are dispersed, it is possible that the dispersed particles form new agglomerates. This is called flocculation and is not well understood in the case of filled polymers. At least three forces are involved: van der Waals, electrostatic forces and repulsive forces caused by the polymer layers absorbed to the surface of filler. [60] With nanofillers this is a serious problem due to the high filler–filler interactions, and the agglomeration enhanced by the high surface area.

The structure of the agglomerate also affects the mixing behaviour. If the filler has a complex open structure, the agglomerates can absorb more rubber inside. This increases the duration of the incorporation phase and the bound / occluded rubber content. When the large structured agglomerates are broken fresher surface is formed. These new surfaces can bind / occlude more rubber. The larger the agglomerate size, the easier they are to break and to disperse. The final size of the agglomerates is still controlled by the particle size and the filler–filler interactions. [3]

When the surface area of the agglomerate increases, the interactions between the filler and polymer are enhanced. The surface area is affected by the particle size of the filler: The smaller the particle size is, the larger the surface area becomes. Smaller primary particles have smaller cavities between them, which makes incorporation of rubber inside the agglomerate more difficult. A high surface area also increases the viscosity because of the stronger interactions. [3]

3. EXPERIMENTAL

In the experimental part EPDM compounds with different nanofillers were manufactured and tested. Six different nanofillers were tested in the screening phase, to determine what fillers would be most interesting for closer inspection. For materials that were chosen for closer inspection, the influence of the filler loading was inspected using filler loadings 0,5; 1; 2,5; 5 and 7,5 phr. One of the materials in the follow-up test, was modified to improve the properties of the nanocomposite.

3.1. Materials

The polymer used in this study was EPDM Keltan 512x50, an oil extended type delivered by DSM, the Netherlands. Keltan 512 is an amorphous broad molecular weight elastomer. It is used for extrusion, low hardness profiles, hoses and roll coverings. Filler materials are introduced in Table 3.1–1. The silane used to modify the halloysite nanotubes was (triethoxysilylpropyl)tetrasulfide (Si 69 from Evonik Industries, Germany). It contains 22,5 % sulphur and has a density of 1,1 g/cm^3. Other materials are stearic acid, ZnO, CaO, polyethylene glycol, carbon black (N550), calcium carbonate, paraffinic oil (Nypar 40), sulphur, CBS, TMTD, ZDBC, ZMDC and MBT. These materials were delivered to me with no specifications and were used as is.

Table 3.1–1 *Some properties of the nanofillers.*

Trade name	Baytubes C 150 P	Halloysite nanotubes	Multifex-MM	Nanofil 5	Nanofil 116	Nanomer I. 30P
Manufacturer	Bayer	Sigma-Aldrich	Specialty Minerals	Rockwood Clay Additives	Rockwood Clay Additives	Nanocor
Abreviation	MWCNT	HNT	MF	N5	N116	NR
Material	Agglomerated multi-walled carbon nanotube	Halloysite clay	CaCO3	Montmorillonite clay	Montmorillonite clay	Montmorillonite clay
Shape	Tube	Tube	Globular	Platelet	Platelet	Platelet
Dimensions **- Diameter** **- Length**	 13-16 nm 1-10 µm	 ~30 nm 0,5-4 µm	 0,07 µm	 < 10 µm	 < 20 µm	 15-20 µm
Surface area	-	64 m^2/g	19 m^2/g	-	-	-
Bulk density	1,4-1,6 g/cm^3		0,17 g/cm^3	0,21 g/cm^3	0,5 - 0,8 g/cm^3	-
Specific gravity	-	2,53	2,71	1,4-1,8	2,6	2,85
Modification	-	-	-	Unpolar surface treatment	Na+ activated	Amine treatment

3.2. Compounding

3.2.1. Equipment

Compounding of the rubber compound was done in a Krupp Elastomertechnik GK 1,5 laboratory mixer. Specifications of mixer can be seen in Table 3.2.1–1 and the mixer in Figure 3.2.1–1. Milling was done on a standard two roll mill.

Table 3.2.1–1 *Specifications of the mixing machine.*

Ram pressure	8 bar
Rotor type	Intermeshing
Chamber volume	1,5 l
Adjustable cooling system	
Automatic mixing	

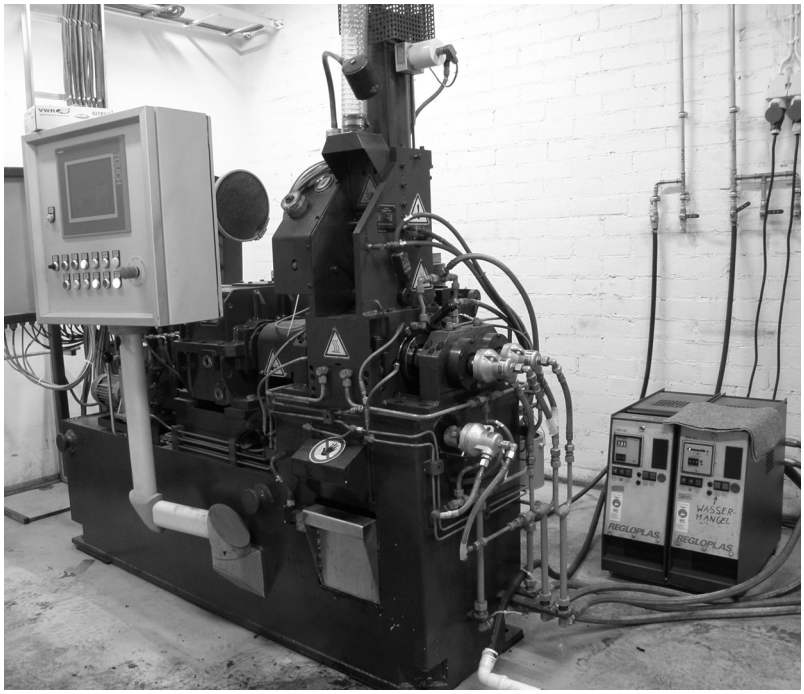

Figure 3.2.1–1 *Internal mixer used for the compounding of the nanocomposites.*

3.2.2. Recipes

Chemicals in powder form were weighed in cups and fillers and oils in LD–PE plastic bags. Raw materials in cups were poured into the mixing chamber, and bags were fed as such, after cutting off the excess part of the bag. This was possible, as the amount of LD–PE was small compared to the weight of the compound, and the bag material melted during mixing. The recipe was based on an existing recipe of an extrusion quality EPDM compound. The mixer size allowed imitating the mixing scheme used for the material on industrial scale. The fill factor was 70 %. In the first recipe, 10 phr carbon black was replaced by six different nanomaterials; the recipe is shown in Table

3.2.2–1. Nanomaterials for this study were carbon nanotubes, halloysite nanotubes, nano–size calcium carbonate, nanoclay with unpolar surface treatment, activated nanoclay and amine modified nanoclay.

Table 3.2.2–1 *EPDM recipe for testing different types of nanofillers.*

Material	Phr
Keltan 512 x 50 oil	150
Stearic acid	1
ZnO	5
CaO	6
Polyethylene glycol	1,5
Carbon black N550	105
Calcium carbonate	40
Paraffinic oil	30
Nanofiller	10
Sulphur	1
CBS	0,4
TMTD	0,9
ZDBC	0,4
ZMDC	0,4
MBT	1,2
wt-% of filler	2,83

In Table 3.2.2–2, the recipes for testing the effect of filler loading are shown. In this series, a part of the carbon black was replaced by MWCNT, halloysite nanotubes and activated nanoclay with different loadings: 0,5; 1; 2,5; 5; 7,5 phr.

Table 3.2.2–2 *Recipes used in studying effects of filler loading.*

Material	Phr			
Keltan 512 x 50 oil	150			
Carbon black N550	115,0	114,5	112,5	110,0
Paraffinic oil	30,0			
Calcium carbonate	40,0			
Halloysite nanotubes	0,0	0,5	2,5	5,0
Si-69	0,0	0,05	0,25	0,5
Stearic acid	1,0			
ZnO	5,0			
CaO	6,0			
Polyethylene glycol	1,5			
Sulphur	1	0,99	0,94	0,89
CBS	0,4			
TMTD	0,9			
ZDBC	0,4			
ZMDC	0,4			
MBT	1,2			
wt-% of filler	0,00	0,14	0,70	1,39

The third recipe shown in Table 3.2.2–3 gives the compound composition for the silane–modified halloysite nanotubes. 0,6; 2,5 and 5 phr of carbon black were replaced by halloysite nanotubes. The silane / halloysite ratio was chosen as 1:10, close to the

ratio in silica–silane compounds. As the silane contains 22,5 % of sulphur, the amount of sulphur in the curing system needed to be adjusted accordingly.

Table 3.2.2–3 *Recipe used with modification of HNTs.*

Material	Phr			
Keltan 512 x 50 oil	150			
Carbon black N550	115,0	114,5	112,0	107,0
Paraffinic oil	30,0			
Calcium carbonate	40,0			
Halloysite nanotubes	0,0	0,5	2,5	5,0
Si-69	0,0	0,05	0,25	0,5
Stearic acid	1,0			
ZnO	5,0			
CaO	6,0			
Polyethylene glycol	1,5			
Sulphur	1	0,99	0,94	0,89
CBS	0,4			
TMTD	0,9			
ZDBC	0,4			
ZMDC	0,4			
MBT	1,2			
wt-% of filler	0,00	0,14	0,70	1,39

3.2.3. Mixing scheme

In all mixing procedures, the cooling system was set to 40 °C. The mixing scheme used with unmodified nanomaterials is shown in Table 3.2.3–1. In this scheme, the addition of the ingredients was done in three stages: First, rubber and chemicals were added and they were mixed for 30 s at 45 rpm. Afterwards, all fillers and oil were added and mixing was continued until the temperature rose to 90 °C. At this stage, the vulcanization system was added and the rotor speed was raised to 50 rpm to reach the drop temperature of 110 °C. The periods for feeding the additives were set to a maximum of 30 seconds. After dropping the compound, sulphur was added and it was milled for approximately 15 minutes. The compound was finally sheeted to a thickness of 2 mm.

Table 3.2.3–1 *Mixing scheme used in testing different nanofillers.*

Material	Time	Rotor speed
Keltan 512 Stearic acid ZnO CaO Polyethylene glycol	0 min	45 rpm
Carbon black N550 Calcium carbonate Paraffinic oil Nanofiller	0,5 min	45 rpm
CBS TMTD ZDBC ZMDC MBT	When 90 °C is reached	50 rpm
Drop	When 110 °C is reached	

For modified halloysites, the mixing scheme was different, because halloysites and the silane needed to react with each other for 5 minutes at 145 °C. The mixing scheme is given in Table 3.2.3–2. The materials were again fed in three stages: First the rubber was masticated at a rotor speed of 45 rpm for 1 minute. Then carbon black, calcium carbonate and oil were added and mixed for 1 minute. The oil was added in order to saturate the surface and structural voids of CB and $CaCO_3$ and thus prevent the reaction of the coupling agent with the conventional fillers in the next phase. Then the halloysite filler and the silane were added. After mixing for 1 min, chemicals were added and the rotor speed was set to 100 rpm to reach 145 °C. The rotor speed was manually adjusted to keep the temperature at approximately 145 °C for 5 minutes for the silanization. After 5 minutes, the rubber was discharged and milled together with sulphur and accelerators for approximately 15 min. Again, the compound was sheeted out to 2 mm thickness. In both mixing processes, the chamber temperature was set at 40 °C and the ram pressure was 8 bars.

Table 3.2.3–2 *Mixing scheme used for modification of HNTs.*

Material	Time	Rotor speed	Operation
Keltan 512	0	45 rpm	
Carbon black N550 Calcium carbonate Paraffinic oil	1 min	45 rpm	
Halloysite nanotubes Si-69	2 min	45 rpm	
Stearic acid ZnO CaO Polyethylene glycol	3 min	Varying rpm	Rise temperature to 145 °C
	~9 min	Varying rpm	Drop after 5 mins at 145 °C

3.3. Test methods

3.3.1. Tensile test

Tensile testing was done according to SFS ISO 37. The testing machine used was a Messphysik tensile testing machine, equipped with grips suitable for rubber testing. The equipment is shown in Figure 3.3.1–1. The rate of traverse was 500 mm/min and the length was 25 mm. The test specimen was a 1A type. The test was done under normal laboratory conditions. Pressures of 200 kN and 300 kN were used in forming specimens. Higher pressure was used from filler loading testing onward to achieve more accurate thickness of the specimens.

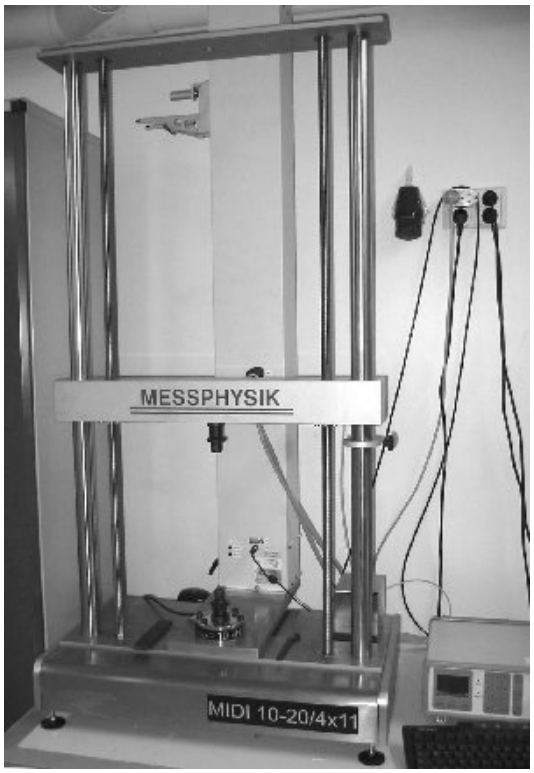

Figure 3.3.1–1 *Messphysik tensile testing machine.*

3.3.2. Hardness

Testing was done with AFFRI Hardness Tester (Figure 3.3.2–1) according to ASTM D2240 – 00, Shore A method. To ensure a thickness of at least 4 mm, two sheets of rubber were used. The hardness after 15 seconds was recorded. The test was done under normal laboratory conditions.

Figure 3.3.2–1 *Affri hardness tester.*

3.3.3. Tear strength

The tear strength was tested with the same equipment as the tensile properties: the Messphysik tensile testing machine. The test was done according to SFS ISO 34–1 and the specimen was a Trouser type 1 (method A). The tear strength was measured in the milling direction. Testing rate was 100 mm/min and the tear strength was calculated from the maximum force value gained during testing using the formula

$$T_s = \frac{F}{d} \qquad (1)$$

where F is the maximum force and d is the average thickness of the specimen in the region of the tip of the crack. The test was conducted under normal laboratory conditions. Pressures of 200 kN and 300 kN were used in forming specimens. Higher pressure was used from filler loading testing onward to achieve more accurate thickness of the specimens.

3.3.4. Compression set

Compression set tests were done at the Teknikum laboratory. They were carried out according to SFS ISO 815–1. Testing equipment is shown in Figure 3.3.4–1. Type A test specimens were used. A compression of 25 % was used, because the hardness of the compound was below 80 IRHD. The testing temperature and time were chosen to be 70 °C and 24 h, respectively. To ensure that specimens would not stick to the plates, silicone coated paper was used between the specimen and the plate. The compression set was calculated using formula

$$C\% = \frac{h_0 - h_1}{h_0 - h_s} \times 100 \quad (2)$$

where h_0 is the initial thickness of the test specimen, h_1 thickness of the specimen after recovery and h_s is the height of the spacer. After heating specimens were allowed to recover for 30 minutes, before the final height was measured. A pressure of 200 kPa was used and the vulcanization time was T90 + 8 minutes, if T90 was 5 minutes or shorter and T90 + 10 minutes for higher T90 values to ensure sufficient vulcanisation.

Figure 3.3.4–1 *Compression set testing equipment.*

3.3.5. Rheological measurements

The vulcanization behaviour of different compounds was studied in an Alpha Technologies Advanced Polymer Analyzer 2000, shown in Figure 3.3.5–1. The test was carried out three times for each compound. Vulcanization was studied using a testing time of 25 minutes and a temperature of 160 °C. The applied strain was 0,2 degrees and the frequency was 50 Hz. Cure behaviour, viscosity and torque were reported. Cure rate index was calculated using formula

$$CRI = \frac{100}{T90 - T1} \quad (3)$$

Figure 3.3.5–1 *Advanced Polymer Analyzer.*

The Mooney viscosity was determined using an Alpha Technologies Mooney viscometer MV 2000 shown in Figure 3.3.5–2. The Mooney viscosity was measured soon after mixing and sulphur addition. It was measured using 1 minute preheating time and 4 minute testing period, while the temperature was 100 °C.

Figure 3.3.5–2 *Mooney viscometer.*

3.3.6. Bound rubber

For the determination of bound rubber content, three 0,2 g samples were taken from each vulcanized sample. Every sample was cut into 3 pieces and placed in an empty bag after weighing. The specimens were the placed in toluene for 96 hours; the solvent was changed every 24 hours. After 96 hours of swelling, the specimens were allowed to dry for 72 hours in an air–conditioned cabinet at ambient temperature. The dried samples were weighed and bound rubber content was calculated using the following formula:

$$BDR\% = \frac{m_0 - \left((m_2 - m_3) - \frac{m_{cpd\_other}}{cpd} \times m_s \right)}{m_0} \times 100 \quad (4)$$

where $m_0 = m_s \times \frac{m_{cpd}}{cpd}$ (5)

where m_0 is the rubber content in the sample, m_2 is combined weight of bag and sample, m_3 is the weight of the dried bag and sample, m_{cpd_other} is the amount of other solvable constituents in the structure, m_s is the weight of the dry sample before swelling, m_{cpd} is the weight of the rubber in the whole compound in phr and cpd is the total weight of the compound in phr. The calculations are based on the assumption that all but the bound rubber and the filler are dissolved. [61]

4. RESULTS AND DISCUSSION

4.1. Influence of different nanofillers on compound properties

4.1.1. Cure characteristics

Cure characteristics of all tested materials are shown in Figure 4.1.1–1, 4.1.1–2 and 4.1.1–3. It is obvious from the graphs that the nanomaterials affect the curing behaviour differently. With the exception of multiwalled carbon nanotubes (Baytubes), all other nanofillers increase cure time, at least to a small extent. For halloysite nanotubes and activated clay (Nanofil 116), the cure time is doubled compared to the pure CB compound. Unpolar treated nanoclay (Nanofil 5) also shows a notable increase in cure time. These increases can be explained by the appearance of a marching modulus, which is seen in the rheograms. For materials with a marching modulus, crosslinking does not reach a final plateau value, and the cure time determined with APA is automatically taken from the maximum testing time used. The rheograms of different nanocomposites are shown in Figure 4.1.1–2. The appearance of the marching modulus might be explained with an interaction between the curing agents and the nanofillers: the rather polar curing agents interact more effectively with the polar nanofillers than with the non–polar EPDM. For the other materials, unpolarly treated nanoclay, nano–sized calcium carbonate (Multifex) and amine treated nanoclay (Nanomer), a small increase in cure time is observed. A marching modulus can also be seen with these materials, but the effect is much smaller and they almost reach a plateau. For the MWCNT compound, a reduction in cure time compared to the CB compound can be seen: the presence of the MWCNTs seem to speed curing up.

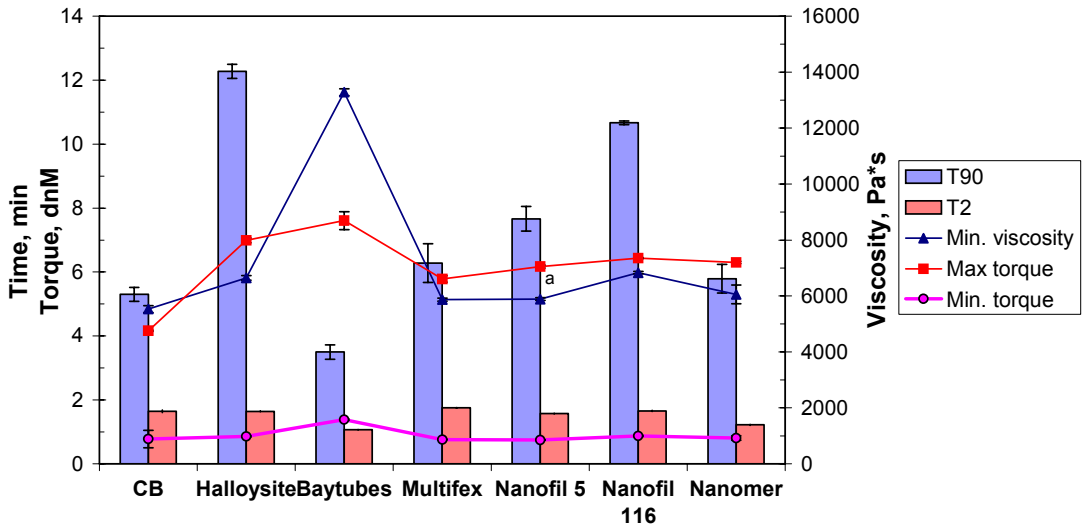

Figure 4.1.1–1 *APA results for different nanofillers with 10 phr filler loading.*

Scorch time was only affected by the MWCNT and the amine treated nanoclay. In both cases there was a small decrease in scorch time compared to the CB compound. For MWCNTs, the decrease is probably again caused by the activating effect of the nanotubes. For amine treated nanoclay, the decrease can be attributed to the amine modification used: amines are known to accelerate vulcanization.

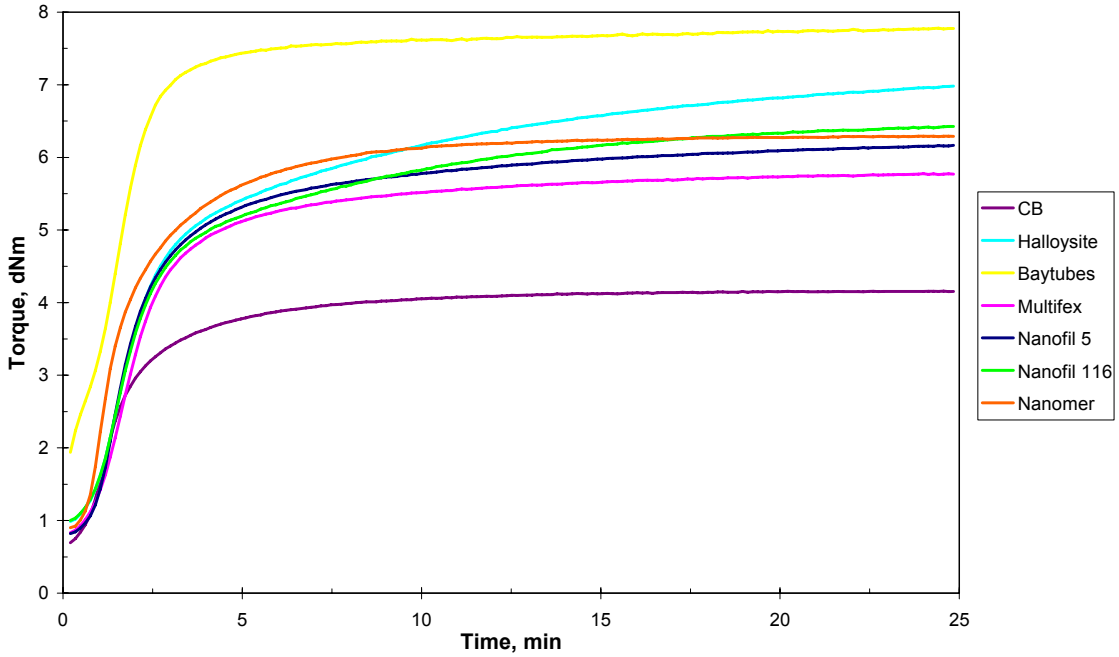

Figure 4.1.1–2 *Rheograms for different nanocomposites with 10 phr filler loading.*

For all nanofillers, the maximum torque and the delta torque (Figure 4.1.1–3) increased compared to the CB compound. This can be attributed to the increased surface area of the filler and thus the enhanced interaction between the filler and the polymer. The strongest effect is seen for the tube–like fillers, MWCNTs and HNTs, with an increase of 83 % and 68 % respectively: They might have an additional physical interaction with the polymer resulting in an extra contribution to crosslinking of the material. The increase can also be attributed to the high aspect ratio of the fillers, which is lower for the HNTs compared to the MWCNTs resulting in a lower torque with the HNT filled compound. This effect might also be caused by the adsorption of the curatives on the filler surface, which was stated to be stronger for HNTs than for MWCNTs based on the curing kinetics. Additionally, MWCNT has more bound rubber than HNTs, which also contributes to the torque values. It must be noticed though, that the initial torque for the MWCNT filled material is also higher, so the delta torque value is closer to the values of the other materials, as seen in Figure 4.1.1–3. Basically, three groups of fillers can be distinguished in terms of influence on delta torque: the high aspect ratio nanotubes, the clay materials and the only particulate filler $CaCO_3$, which has the biggest dimensions, a low amount of chemically active groups and no modification. So the most prominent characteristic for the delta torque is the physical appearance, the shape of the filler: nanotubes contribute to the crosslinking, the platelet–structured silicates have an

intermediate position in terms of aspect ratio and surface area, and the $CaCO_3$ is the least effective due to its large particle size and low surface area. However, the filler–polymer interaction will also play a role.

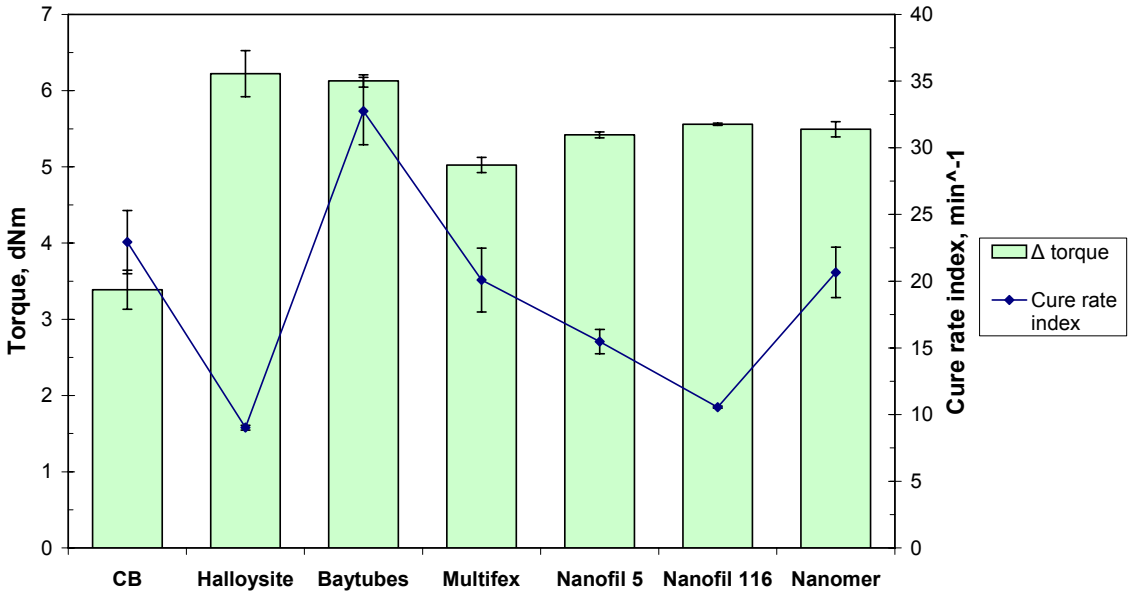

Figure 4.1.1–3 *APA results for different nanofillers with 10 phr filler loading.*

For the other fillers, the limited increase in maximum torque is a consequence of the low degree of interaction between polymer and filler; therefore the increase in relative surface area only slightly increases the torque values.

The MWCNT filled compound has evidently the highest viscosity. This can be explained by the higher surface area, aspect ratio and especially by the higher bound rubber content. Surprisingly, the viscosity of the HNT compound is in the same range as the viscosity of the other compounds and is significantly lower than the viscosity of the MWCNT compound. Halloysites were expected to show similarities with CNTs, but in terms of viscosity, they are more comparable with the other silicate fillers used in this study. This becomes also very clear from the bound rubber values (Figure 4.1.2–1), showing that the polymer filler interaction is significantly lower for HNTs compared to CNTs.

The cure rate index (CRI) is also affected by the marching modulus, as is the curing time. From the cure rate index can be seen, that MWCNT significantly increase the cure rate. One factor might be the increase in effective filler volume by bound rubber for the MWCNTs, which reduces the volume available for chemicals and thus increases the concentration of the curing agents in the free polymer. The slowest cure rate index is found for the HNTs and activated clay filled material; these materials also have highest marching modulus. Marching modulus decreases the cure rate by increasing the cure

time. For the material with a minor marching modulus, the polar treated nanoclay, a small decrease in the cure rate index can be seen

4.1.2. Bound rubber

In Figure 4.1.2–1, the bound rubber contents of the materials with 10 phr of the different nanofillers are presented. The formula used to calculate the bound rubber content makes some simplifications, but the results should nonetheless give a good overview of the amount of bound rubber. The shape of the specimens was not exactly the same, which affected the accuracy of the test that caused variation in the results.

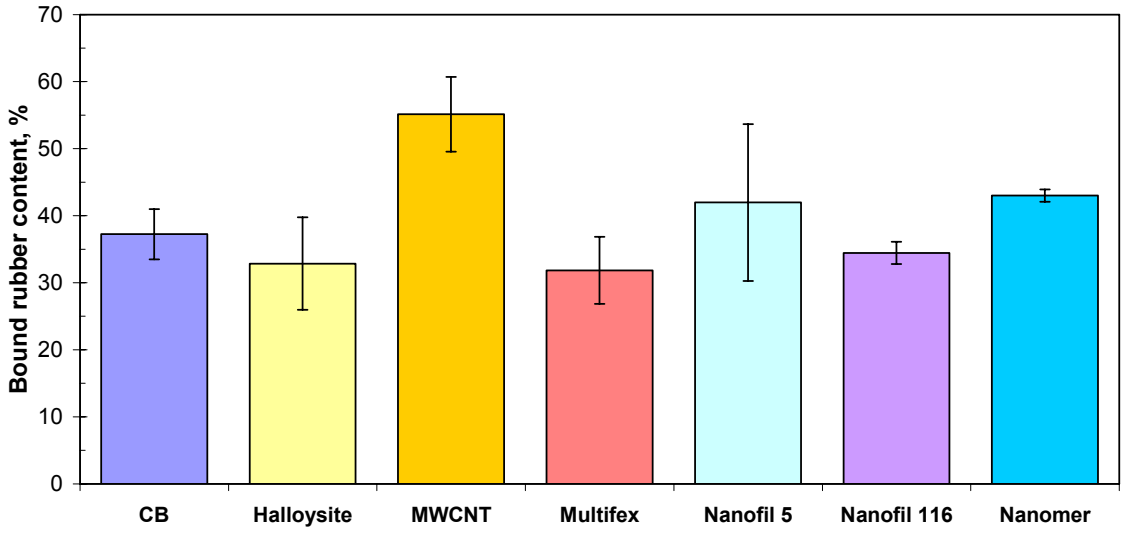

Figure 4.1.2–1 *Bound rubber content of nanocomposites with 10 phr of different nanofillers.*

MWCNT as a filler lead to a much higher bound rubber content than the other materials, which show the carbon nanotube's ability to bound rubber mechanically and chemically. A difference in bound rubber content of the CB compound with and without MWCNT was expected, due to the larger surface area and different structure of the MWCNTs. CB reference had also little longer final mixing phase than the other materials and this could cause increase in bound rubber content.

4.1.3. Tensile test

Tensile strength increases slightly with addition of nanofillers according to Figure 4.1.3–1. The difference between the nanofiller–materials is small; the unpolar treated nanoclay and the amine treated nanoclay give the lowest values in this series, which is about 1,5 MPa lower than the highest value found for the activated clay filled material. These two materials differ in surface modification, of which the details are not revealed, but it seems as if their efficiency for elastomer reinforcing is fundamentally different. Another factor might be the degree of exfoliation and intercalation. The amine treatment

of the nanoclay filler has only a small effect on tensile strength. However, this ranking in terms of mechanical properties has to be done with caution, as the mixing and curing of the samples was not always the same, as explained above.

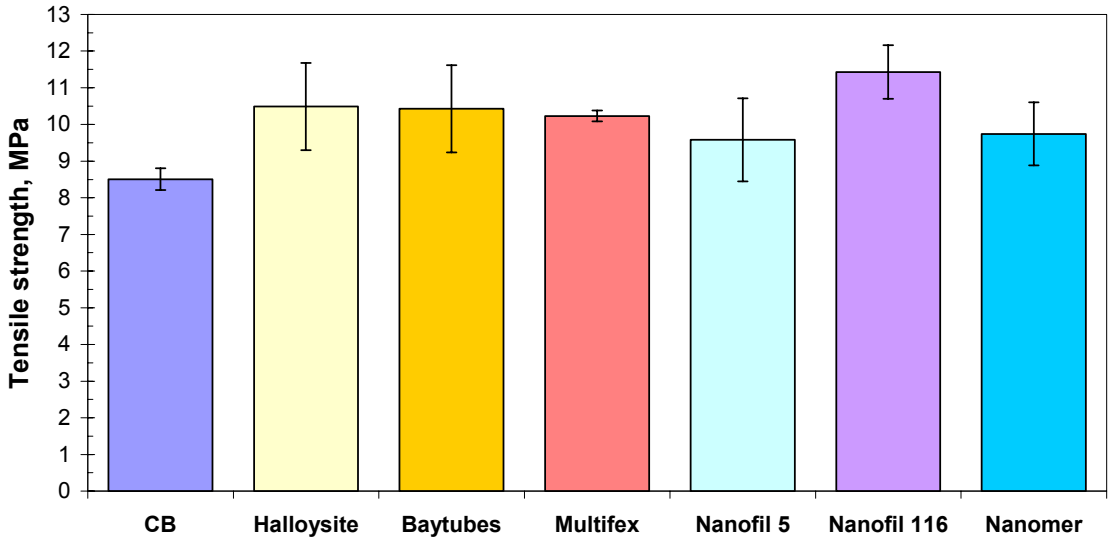

Figure 4.1.3–1 *Tensile strength of nanocomposites with 10 phr of different nanofillers.*

In the case of MWCNT and HNT, an even higher tensile strength was expected due to their high aspect ratios. However, different factors play together: besides the aspect ratio, the polymer–filler interaction, the filler–filler interaction and physical network formation have to be considered. The addition of nano calcium carbonate results in a comparable tensile strength as the addition of nanotubes. This is surprising, as the $CaCO_3$ has a much larger particle size and should have much weaker interactions. A possible reason is that the structure of the $CaCO_3$ might be effective for a good physical filler–polymer interaction.

4.1.4. Tear strength

The tear strength of different nanocomposites is shown in Fig. 4.1.4–1. Tear strength was expected to rise with addition of the nanofillers with high surface area, as the filler particles in the matrix hinder the crack propagation. The higher the relative surface area of the filler, the more pronounced the effect should be.

However, the results do not show an improvement when the nanofiller is added. With the addition of HNTs, $CaCO_3$ and unpolar treated nanoclay, tear strength decreases, while for the other materials, tear strength is comparable to the tear strength of the CB filled compound. An explanation might be a low degree of dispersion of these fillers, leading to large agglomerates instead of a homogenous dispersion of smaller aggregates.

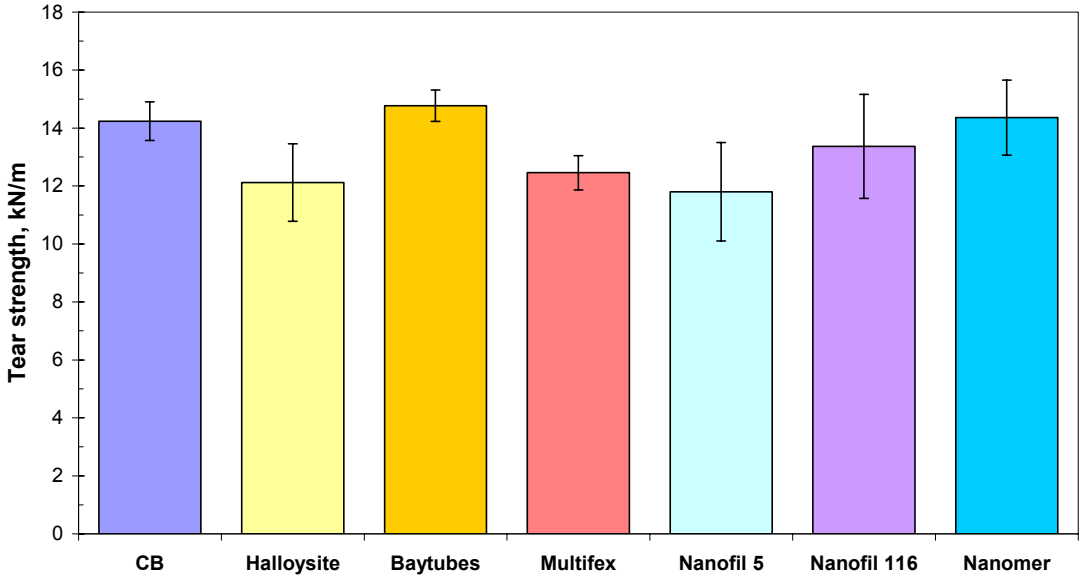

Figure 4.1.4–1 *Tear strength of nanocomposites with 10 phr of different nanofillers.*

4.1.5. Hardness

The hardness of different nanomaterials can be seen in the Figure 4.1.5–1. It is increased with addition of nanofillers compared to the CB compound, what was expected. With the nanotube materials, MWCNT and HNT, the hardness increases the most, followed by platelet materials Nanofil 5 and 116, which have equal hardness. Addition of the nano–sized calcium carbonate filler results in the smallest hardness increase compared to CB, probably due to the low filler–polymer interaction, as can be seen from the low bound rubber values. The ratio of elastic to glassy polymer is low in this case. The layered clays result in an intermediate hardness increase, lower than the nanotube filled material, which is probably due to their specific structure and surface area.

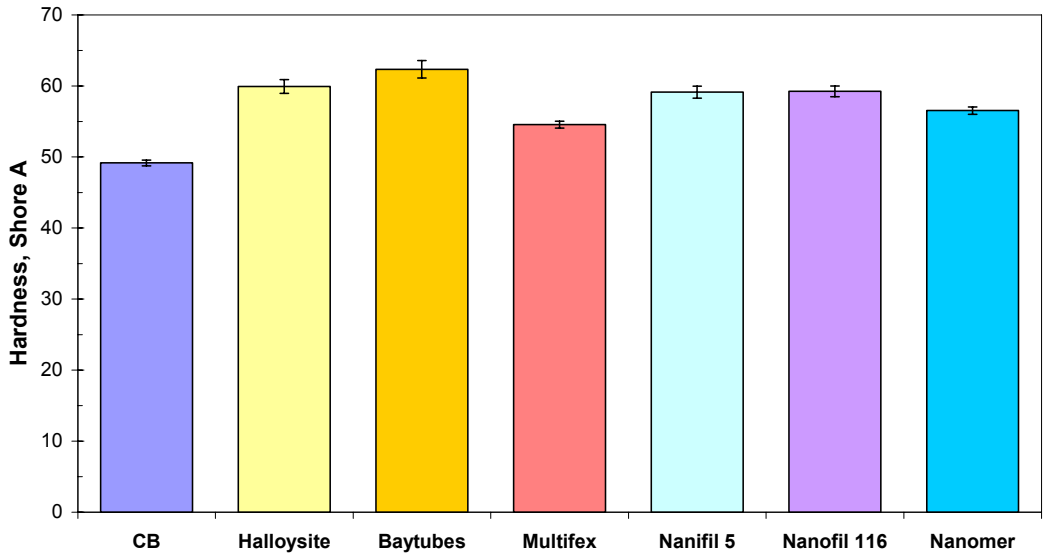

Figure 4.1.5–1 *Hardness of nanocomposites with 10 phr of different nanofillers.*

4.1.6. Compression set

The compression test results are shown in Figure 4.1.6–1. Surprisingly, the HNT filled material shows the lowest compression set. The marching modulus was expected to influence the compression set of the HNTs, layered clays and calcium carbonate so that their compression set would be higher than with MWCNT: Crosslinking was expected to continue leading to higher compression set values. However, in this series a high marching modulus of HNTs and activated clay is combined with a low compression set. Apparently, the temperatures used for the compression set measurements are not high enough to initiate further crosslinking. The MWCNT filled material shows the highest compression set and was found to be slightly higher than the CB compound. In this case, the presence of the carboneous material seems to activate further crosslinking during the test. The anorganic fillers in general show low compression set values. The weaker polymer–filler interactions seen in the bound rubber measurements decreases the compression set in this case.

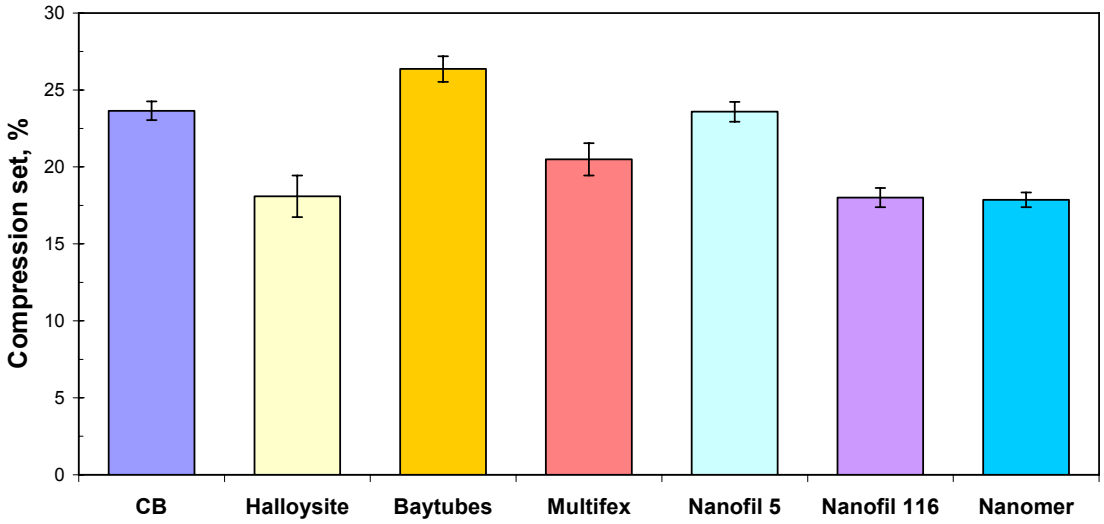

Figure 4.1.6–1 *Compression set results for materials filled with 10 phr of different nanofillers.*

4.1.7. General conclusions

From the bound rubber measurements can be concluded, that the MWCNT composites have a much better polymer–filler interaction than to the other materials, caused by the more suitable surface morphology and chemistry as well as the higher surface area of the carbon nanotubes. The unmodified mineral materials had the lowest polymer–filler interactions. However, a higher bound rubber content did not necessarily result in better properties; other factors also influence the strength of the materials.

For other properties, the MWCNT's also result in a special position. The addition of MWCNT caused a much higher viscosity and a slightly higher torque than the addition

of the other materials, again due to the better polymer–filler interactions. These interactions are also enhanced by the high surface area and aspect ratio of this filler. HNT composites also had an increased torque, which suggests that the shape of the materials affects the torque more than the viscosity. HNT composites and the other silicate–containing composites had comparable viscosities.

The delta torque values increased with all nanofillers due to the higher surface area. Especially the fillers with a high aspect ratio enhance crosslinking, and the particulate filler $CaCO_3$ has the smallest influence on it.

In spite of the significant influence on the curing behaviour, a comparable increase in mechanical properties was not found. Nanofil 116 lead to the highest tensile strength, followed by the nanotubes HNTs and MWCNTs. The tear strength of the CB–filled material was maintained when MWCNT, activated clay and amine treated clay composites were added. With addition of the other fillers, a slight decrease was observed. Hardness increased slightly with the addition of all nanofillers. The highest hardness was achieved for the MWCNT composites, but the difference to the HNT and Nanofil 116 nanocomposites was small. The compression set values showed significant differences: carbon nanotubes and Nanofil 5 resulted in an increase, while other fillers caused a decrease in compression set. The lowest compression set value was found for HNT, Nanofil 116 and Nanomer, which was surprising as they showed a marching modulus.

4.2. Effect of filler loading on properties

4.2.1. Mooney viscosity

Mooney viscosities before and after addition of the curing additives for the compounds with MWCNTs, HNTs and layered clays with different filler loadings are shown in Figure 4.2.1–1. The viscosity decreases in all cases when the curing additives are added: This is caused by the extra milling that results in polymer chain scission. The addition of HNT and N116 results in a slightly higher viscosity than the addition of MWCNT.

The behaviour of the activated clay nanocomposite is quite different from the behaviour of the compounds containing the tube materials. In the case of nanotube materials, radical changes for the lowest concentration are observed. With MWCNTs, viscosity reaches a maximum at 0,5 phr loading; with 1 phr of MWCNTs viscosity shows a minimum, causing a drop of approximately 30 Mooney units. This behaviour was confirmed by repeated mixing and testing of the compound. The same trend is found for the bound rubber tests (Figure 4.2.2–1): a maximum amount of bound rubber is found for a 0,5 phr filler loading, followed by a sharp decrease when 1 phr filler is added. At higher filler loadings, the dispersion might get reduced and agglomerates might start to

form, which decreases the amount of bound rubber by decreasing the surface area. There is a balance between increasing surface area by higher nanofiller loadings and reduced surface area by a decreasing degree of dispersion, which in the sum, results in increasing viscosity values. By the addition of HNTs, the viscosity decreases first with 0,5 phr loading and increases then rapidly to a maximum at 1 phr loading. After this, viscosity levels off at a value in–between. This trend again is paralleled by the trend found for the bound rubber values: Low viscosity goes together with low BDR values, and vice versa. Again, the shape is not the only determining factor for the bound rubber formation.

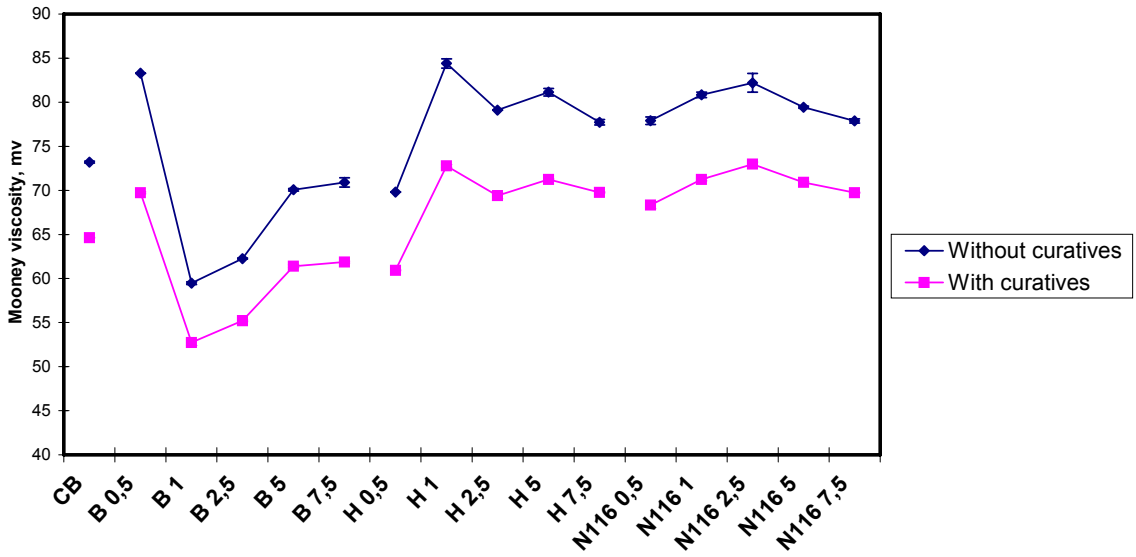

Figure 4.2.1–1 *Mooney viscosity of MWCNT, HNTs and activated clay filled compounds. B=Multiwalled carbon nanotubes, H=Halloysite nanotubes and N116=Activated nanoclay. The numbers designate the filler loading in phrs.*

There is no radical change in viscosity with the addition of activated clay: a slight increase in viscosity for the lowest concentration, and a smooth peak at 2,5 phr loading. The BDR content confirms this trend.

4.2.2. Bound rubber

Bound rubber test results for the rubber nanocomposites with varying filler loading can be seen in Figure 4.2.2–1. The bound rubber content (BDR%) of MWCNTs drops radically between 0,5 and 1 phr loading. This can be result of lower surface area due agglomeration or poor dispersion. MWCNT have the highest BDR% at 0,5 phr and the lowest at 1 phr. When the filler loading is increased, MWCNTs reach the same level of BDR% as activated clay. This up–and down–trend is probably the balance between higher surface area and lower dispersion with increasing nanofiller loading.

For HNTs, the amount of bound rubber does not show a clear trend for activated clay, the BDR content is more constant and a little lower than that of CB. The structure of the agglomerates is smaller than for carbon black, and the surface is incompatible with the polymer.

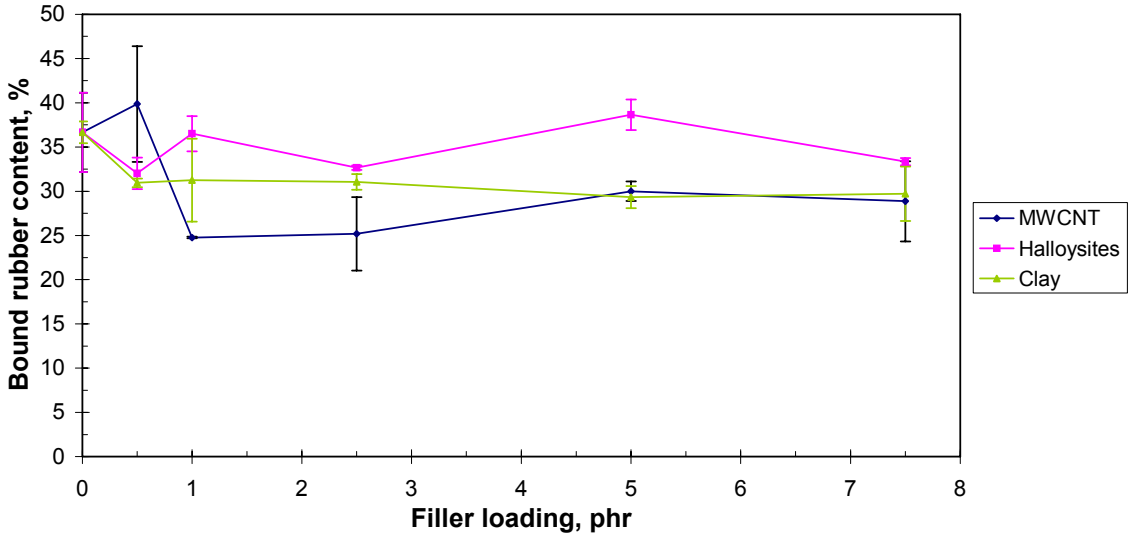

Figure 4.2.2–1 *Bound rubber of compounds containing MWCNT, HNTs and activated clay vs. filler loading.*

4.2.3. Cure characteristics

The cure behaviour of MWCNT is shown in Fig 4.2.3–1 and 4.2.3–2. With MWCNT, the scorch time is not affected by the filler loading, except for a small decrease for 0,5 phr loading, and the cure time shows a slight increase for the lowest loading. With higher loadings, the cure time decreases slightly and reaches the same level as the CB compounds. Viscosity and the maximum torque show the same trends: For a 0,5 phr loading they are higher than the values of the CB compounds, and at 1 phr the values are below the CB equivalents. After 1 phr loading, they start to increase linearly with increasing filler loading. An explanation for the different behaviour for the lowest concentration might be that agglomeration does not occur and a drastic change in properties can be seen due to the increased surface area. Agglomeration is expected to happen between loadings of 0,5 and 1 phr, resulting in increasing viscosity and torque values.

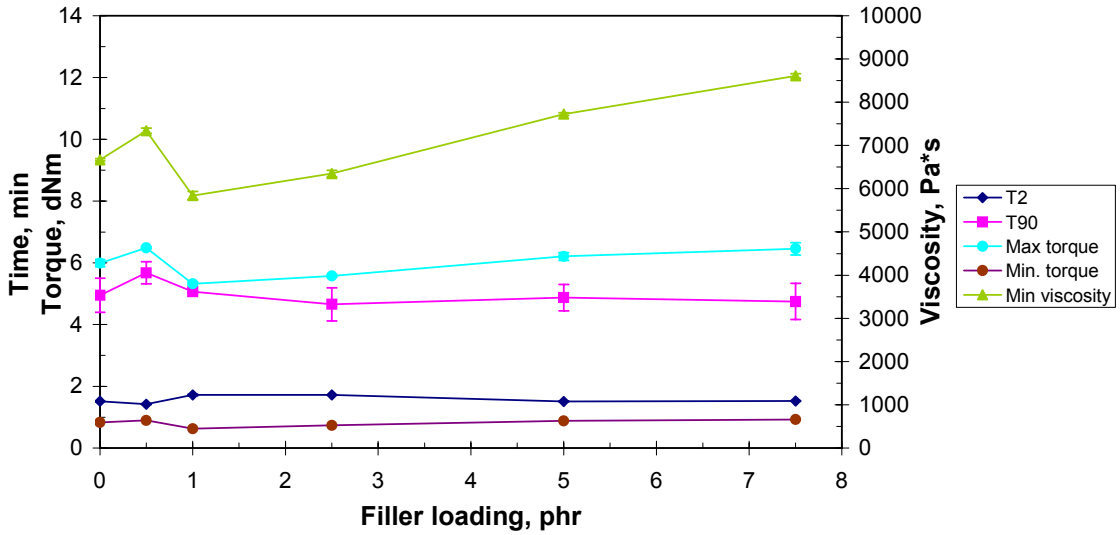

Figure 4.2.3–1 *Cure characteristics of compounds with MWCNTs.*

In Figure 4.2.3–2, the cure rate index and delta torque values are shown. The delta torque is not affected by the filler loading, but the cure rate drops below the value of the CB compound at 0,5 phr loading, and rises back to the same level as the CB compound at 1 phr, where it levels off. The decreased cure rate indicates a deactivation of the curing additives on the large surface of the filler. This effect is more pronounced when the dispersion is high.

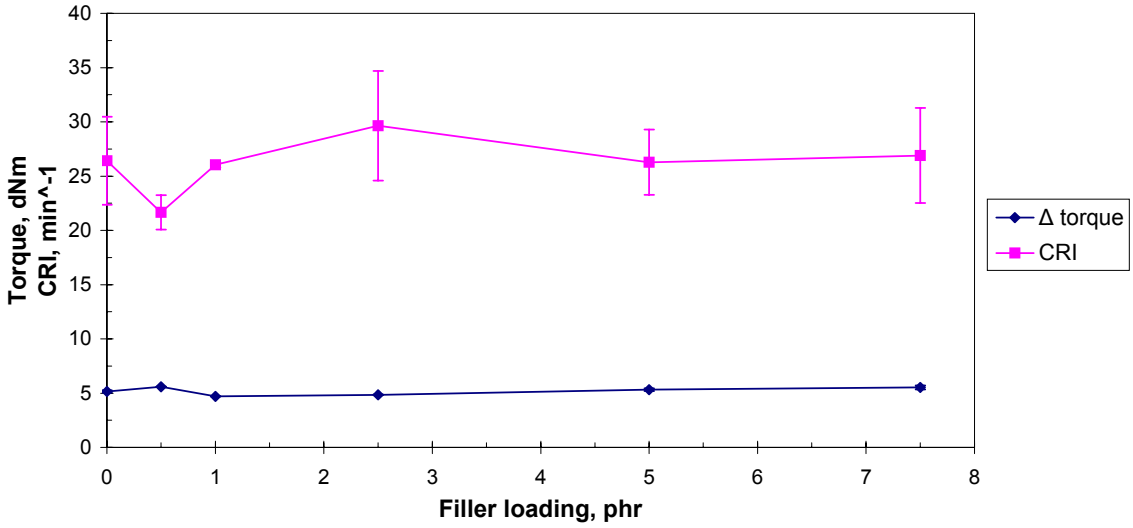

Figure 4.2.3–2 *Cure characteristics of compounds containing MWCNTs.*

The rheograms for MWCNTs composites is shown in Figure 4.2.3–3. The vulcanisation behaviour with 0,5 is much faster and reaches higher torque than with higher filler loadings.

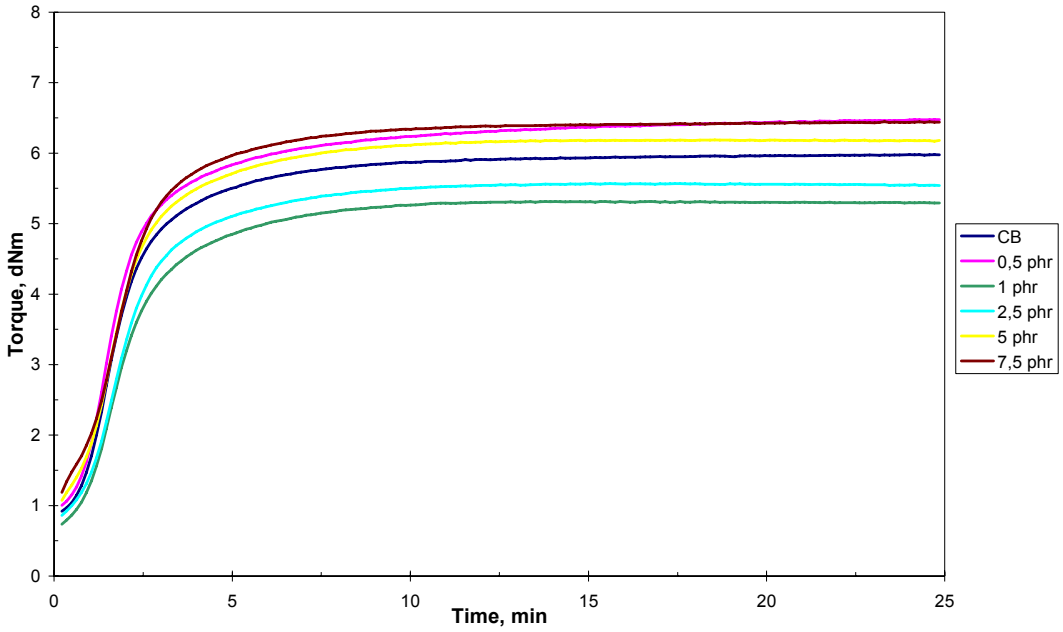

Figure 4.2.3–3 *Rheograms for MWCNT composites with different filler loadings.*

In Figure 4.2.3–4, the results for the addition of HNTs are shown. Scorch time is not affected by the increased HNT loading. An obvious difference to the MWCNT compound is the massive increase in cure time, when the amount of HNT is increased over 1 phr. This is caused by the marching modulus between the 2,5 and 5 phr loadings as can be seen in the Figure 4.2.3–5. As the torque does not reach a plateau, the cure rate keeps growing. Torque and viscosity reach their high point at 2,5 phr loading. After 2,5 phr no change is detected with further increase of the filler loading. Higher filler content should result in a higher viscosity and torque value; however here it seems that with the addition of HNTs a certain level of interaction is reached that does not change any more with increasing filler loading.

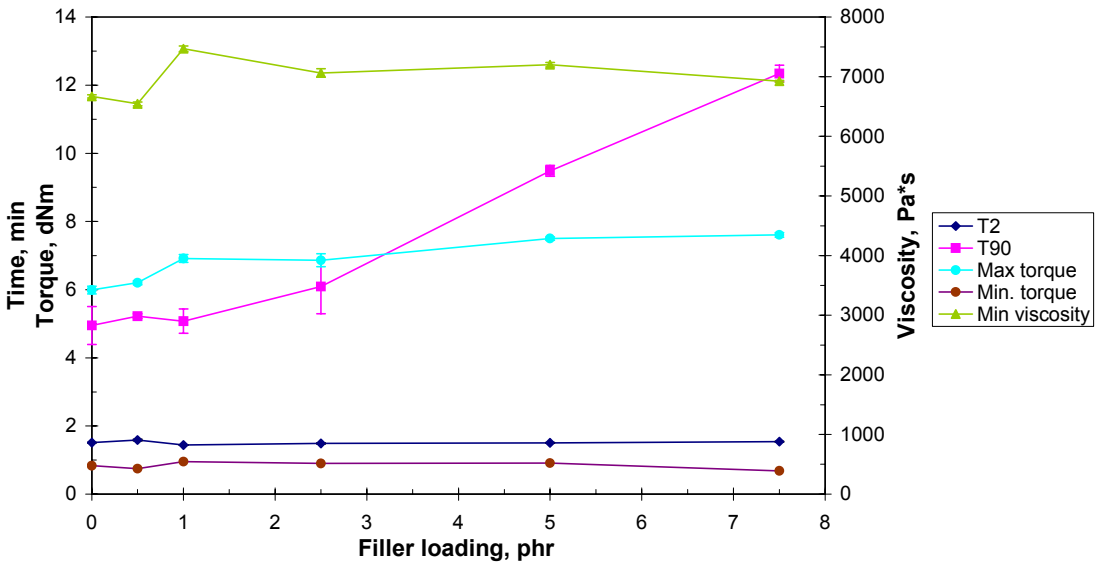

Figure 4.2.3–4 *Cure characteristics of compounds containing HNTs.*

In figure 4.2.3–5, the torque change and curing rate for HNT compounds are shown. Here, the CRI decreases due to the marching modulus when HNTs are added to the compound. The marching modulus also causes an increase in delta torque with increasing filler loading. The marching modulus behaviour gets more pronounced with higher filler loadings. This is expected because the increased surface area adsorbs more curatives. The development of the marching modulus can be seen in the rheograms of the compounds in Figure 4.2.3–6.

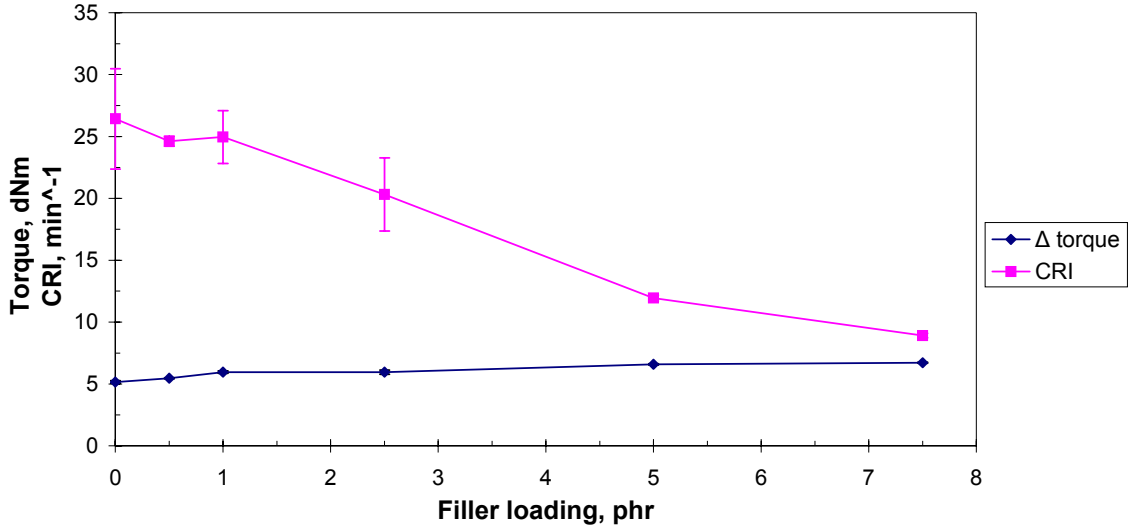

Figure 4.2.3–5 *Cure characteristics of compounds containing HNTs.*

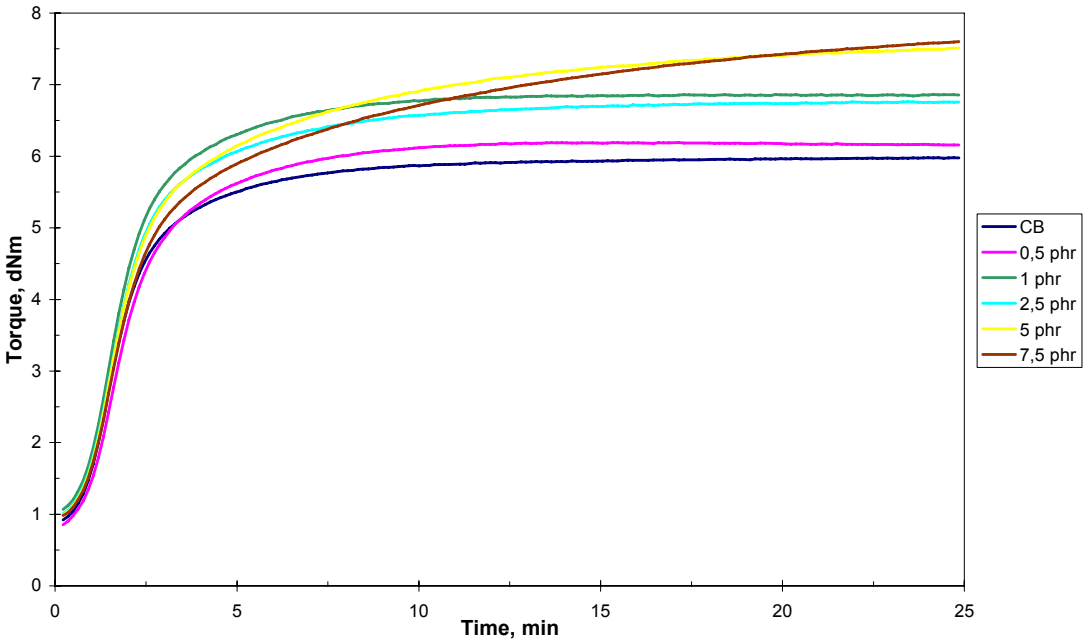

Figure 4.2.3–6 *Rheograms of HNT composites with different filler loadings.*

The cure characteristics of N116 filled compounds can be seen in Figure 4.2.3–7. Scorch time is independent from filler loading and does not change with filler addition.

Cure time increases rapidly after 1 phr, caused by the marching modulus. Viscosity and torque keep rising up to a concentration of 1 phr, after which the marching modulus interferes with the results. This raises the question, if the properties would still increase when the marching modulus could be prevented. It is possible that at a loading of 1 phr agglomerates start to form and this would also affect the torque and viscosity.

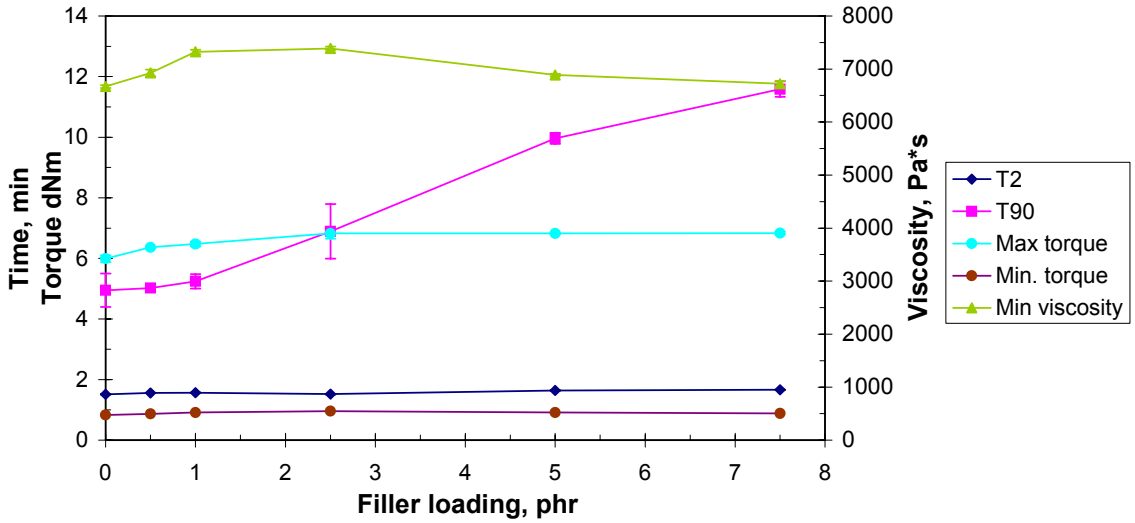

Figure 4.2.3–7 *Cure characteristics of compounds containing activated clay.*

Figure 4.2.3–8 represents the delta torque and cure rate index for the N116 compounds. As was expected, the cure rate starts to decrease rapidly after 1 phr, when the marching modulus appears. The same effect comes to the fore in the CRI values, which start to rise very slowly. The rheograms are shown in the Figure 4.2.3–9. As in the case of HNT's, a marching modulus appears at concentrations higher than 1 phr.

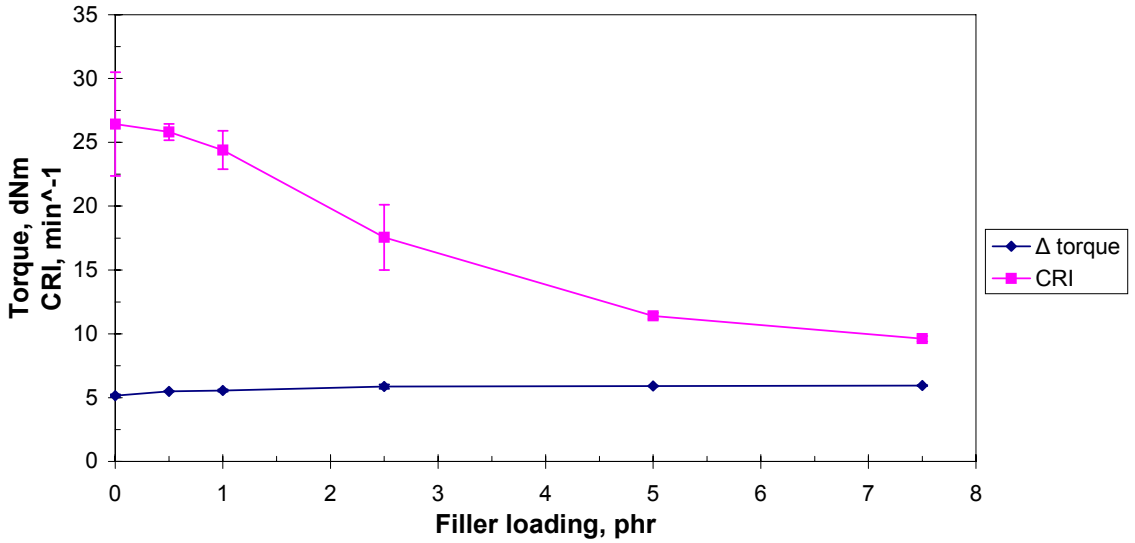

Figure 4.2.3–8 *Cure characteristics of compounds containing activated clay.*

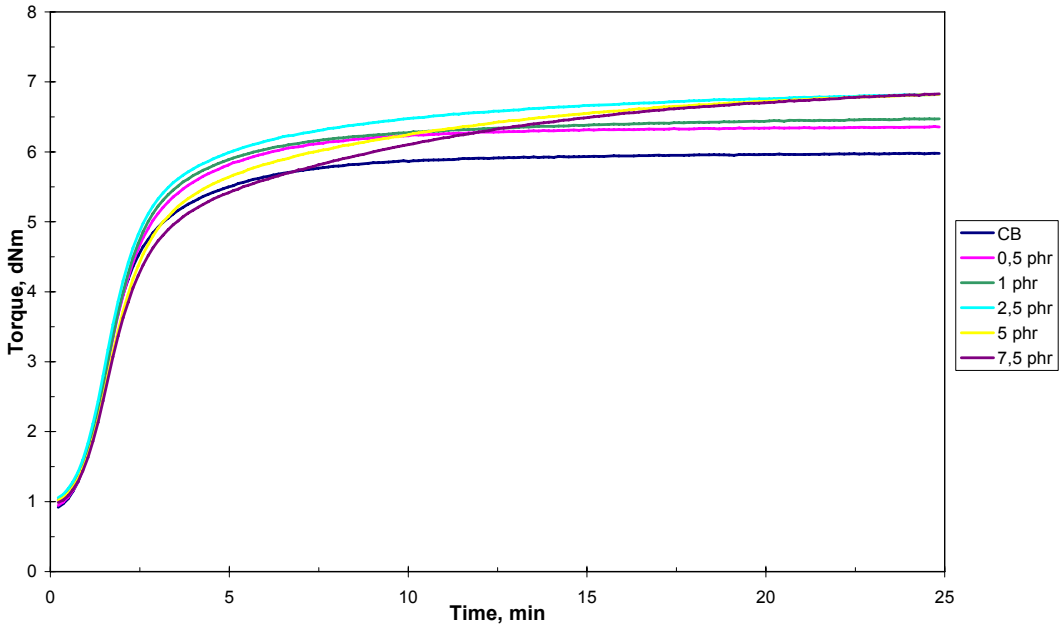

Figure 4.2.3–9 *Rheograms for activated nanoclay composites with different filler loadings.*

4.2.4. Tensile test

The tensile strength of compounds containing MWCNT, HNTs and activated clay are shown in Figure 4.2.4–1. No significant enhancement in tensile strength is observed for any of the nanofillers. HNTs and activated clay seem to retain tensile strength of the CB–filled material, or slightly enhance it. For the activated clay and HNTs material, the change in the curing behaviour (marching modulus) might affect the tensile strength. However, the tensile strength does not change after the marching modulus appears at 1 phr, so this has no influence on the strength of the material. The average tensile strength of the clay filled material is comparable to the strength of the CB filled material, even at low concentrations. A reason for this might be the poor interactions between filler and matrix or a poor dispersion of the nanofiller. The average tensile strength for the HNT filled material is slightly higher, and the strength of the MWCNT filled material is slightly lower than the CB filled material.

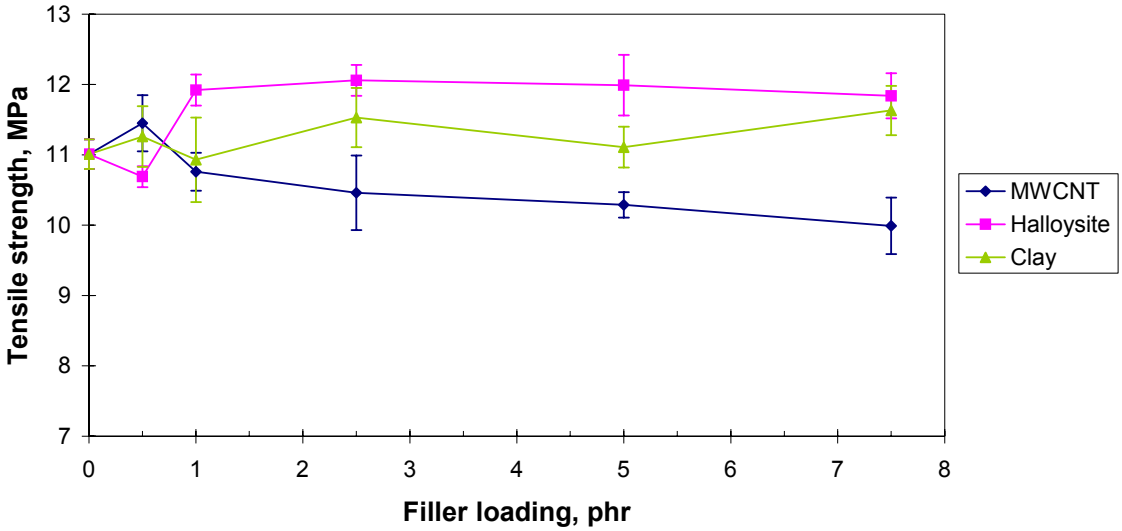

Figure 4.2.4–1 *Tensile strength of MWCNT, HNTs and activated clay filled material vs. filler loading.*

With MWCNTs, the tensile strength decreases when filler loading is increased. There are a small increase in the tensile strength with 0,5 phr loading, a discontinuity as seen before. With higher loadings, tensile strength decreases slightly, ending up 2 MPa lower than the strength of the CB filled compound at 7,5 phr loading. The bound rubber content is higher at 0,5 phr, this enhances the tensile strength by increasing the effective filler volume and showing a good filler–polymer interaction. After 0,5 phr loading, the bound rubber content decreases rapidly and this effect is lost.

4.2.5. Tear strength

The tear strength in correlation with the filler loadings for MWCNT, HNTs and activated clay are shown in the Figure 4.2.5–1. With the addition of MWCNT, the tear strength increases until 1 phr loading; at this concentration the tear strength is slightly higher than the strength of the CB filled material, although the deviation is rather large. After 1 phr, the tear strength shows a downward trend for all fillers: This might be the result of an increasing degree of agglomeration of the fillers with increasing loading. The slightly improved tear strength of the MWCNT material is attributed to better interactions between the filler and the polymer for the MWCNT filled compounds compared to the other two fillers.

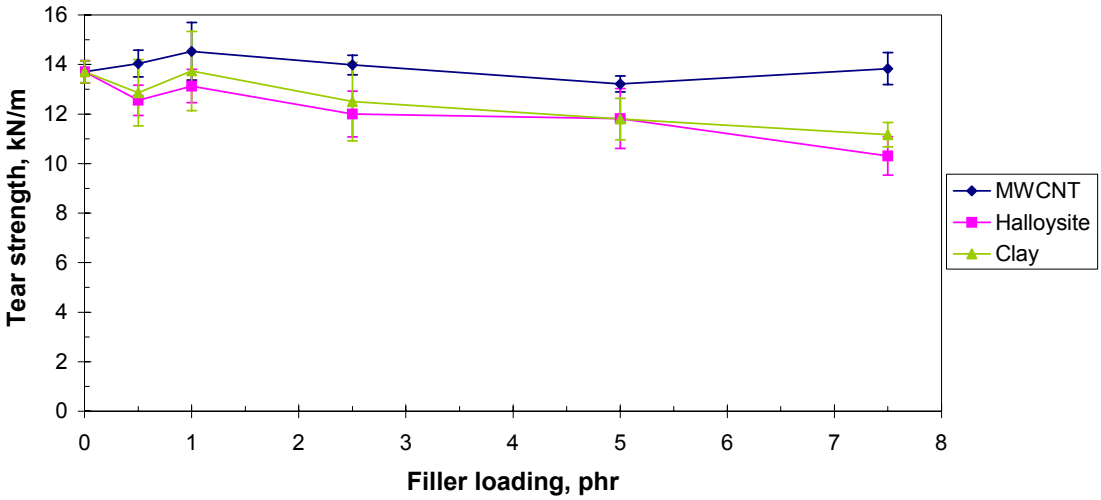

Figure 4.2.5–1 *Tear strength of compounds containing MWCNT, HNTs and activated clay vs. filler loading.*

4.2.6. Hardness

The hardness of compounds containing MWCNT, HNTs and activated clay are shown in Figure 4.2.6–1. Hardness does not increase with addition of these nanofillers. This was unexpected, because the addition of filler should increase hardness. The hardness increases slightly for low concentrations of HNTs and N116, after which it levels off at a slightly higher value compared to the hardness of the CB compound. The MWCNT compound again shows a different behaviour: it increases for the addition of 0,5 phr of filler, decreases for 1 phr and then increases slightly again. The low hardness can be attributed to agglomeration with higher concentrations and to the poor filler–polymer interactions.

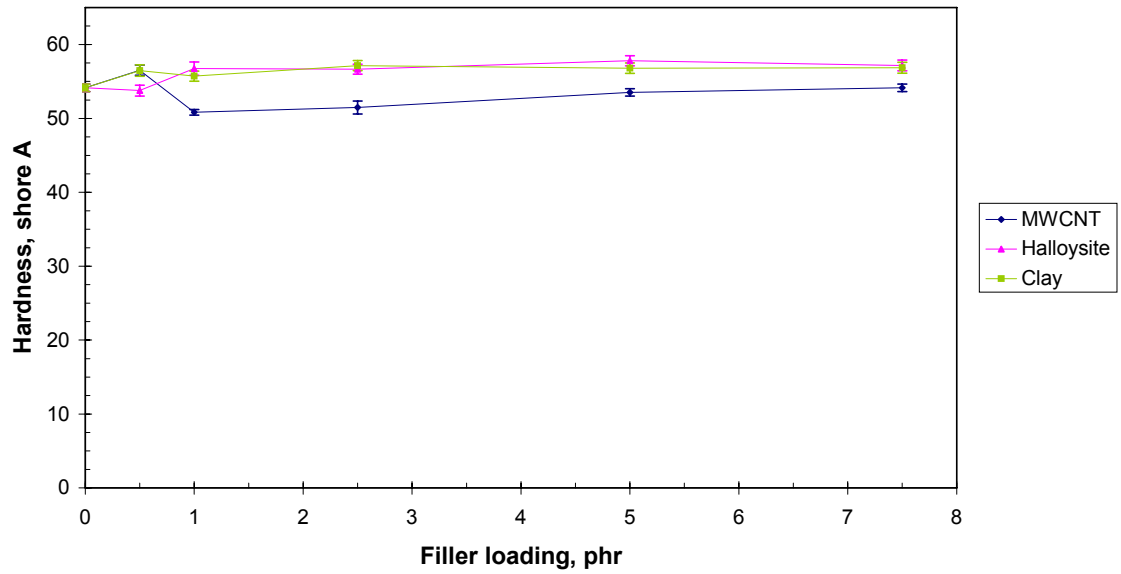

Figure 4.2.6–1 *Hardness of MWCNT, HNTs and activated clay vs. filler loading.*

4.2.7. Compression set

The compression set of compounds with MWCNTs, HNTs and activated clays are shown in Fig. 4.2.7–1. Compression set should be increasing with increasing filler content, but this is not the case with HNTs and activated nanoclay fillers. The poor interactions between the polymer and filler decrease the compression set. Activated clay and HNTs result in lower compression set values than the MWCNTs, despite the fact that they show a marching modulus, as seen earlier in the screening series (Figure 4.1.5–1.) This would indicate an inactivation of the curing process, probably by adsorption of curing agents on the filler.

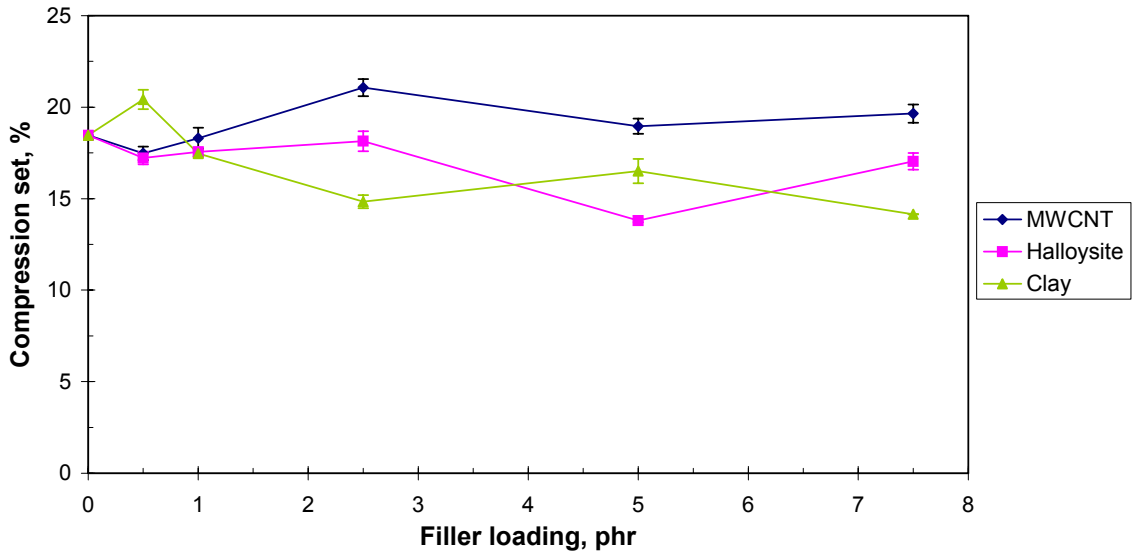

Figure 4.2.7–1 *Compression set of compounds with MWCNT, HNTs and activated clay vs. filler loading.*

For MWCNT there is a drop in compression set for 0,5 phr loading; compression set then increases with increasing filler fraction and thus higher surface area. Agglomeration again might contribute to the higher compression set for higher filler loadings.

4.2.8. Conclusions

For the carbon nanotubes, a better polymer–filler interaction is observed for a 0,5 phr filler loading compared to higher loadings. This is expressed as a higher bound rubber content and an increased viscosity. At concentrations higher than 0,5 phr, agglomeration might occur, thus decreasing the viscosity. For this higher concentrations range, activated nanoclay and HNT result in a higher bound rubber content and Mooney viscosities compared to MWCNT as a filler. For the compounds containing HNT, a discontinuity is also found for the lowest concentration; however, in this case the

viscosity is lowered. This goes together with a low bound rubber content; both indicating a low polymer–filler interaction.
The cure characteristics of the HNT and activated clay filled materials are controlled by the marching modulus; the marching modulus is observed for concentrations from 1 phr on. The torque increases until the marching modulus appears. The marching modulus is probably connected to the polar characteristics of the fillers. The MWCNT composites experience a small increase in cure time at 0,5 phr loading, as does the torque value compared to CB compound.

The influence on mechanical properties was less than expected. Tensile strength and hardness parallel the trends found for bound rubber and Mooney viscosity. For higher concentrations, the order of decreasing strength is HNT, activated clay which is similar with CB, followed by MWCNT. At a concentration of 0,5 phr nanofiller, the order is reversed. For tear strength, only the MWCNT composites reach the level of the CB compound, while the other nanofillers result in a decrease with increasing filler loading. This might indicate better dispersion and lower agglomeration of MWCNT compared to the other two materials. In terms of compression set, HNT and activated clay cause a decrease with higher filler loadings, despite the marching modulus, due to the curing retarding influence of curative adsorption.

General conclusions of these investigations are, that

- low nanofiller concentrations have a larger effect, which differs from the effect at higher concentrations'
- no significant advantage is gained with higher nanofiller loadings.

Therefore, the investigation should be concentrated on lower filler loadings and surface modification of the nanofillers, so that agglomeration- and dispersion-problems can be solved.

4.3. Properties of silane modified halloysite nanotubes

4.3.1. Mooney viscosity

The Mooney viscosities of compounds with modified and unmodified HNTs are shown in Figure 4.3.1–1. The viscosity of the compound with the modified HNTs decreases less after sulphur addition; in this case, milling is less effective as the viscosity of the compound is lower due to better dispersion or the longer mixing time. The modification has no effect on the Mooney viscosity for 0,5 phr loading. With higher loadings, the compound with the modified filler has a lower viscosity. The surface modification results in a decreased viscosity when there is enough silanol present. The modification is done in order to make the filler and the polymer more compatible, the filler gets an unpolar coating, which matches better with the unpolar EPDM. This results in an easier

dispersion, thus in a lower viscosity of the filled compound. Also the longer mixing time of the modified HTN composites affects the viscosity in the same manner.

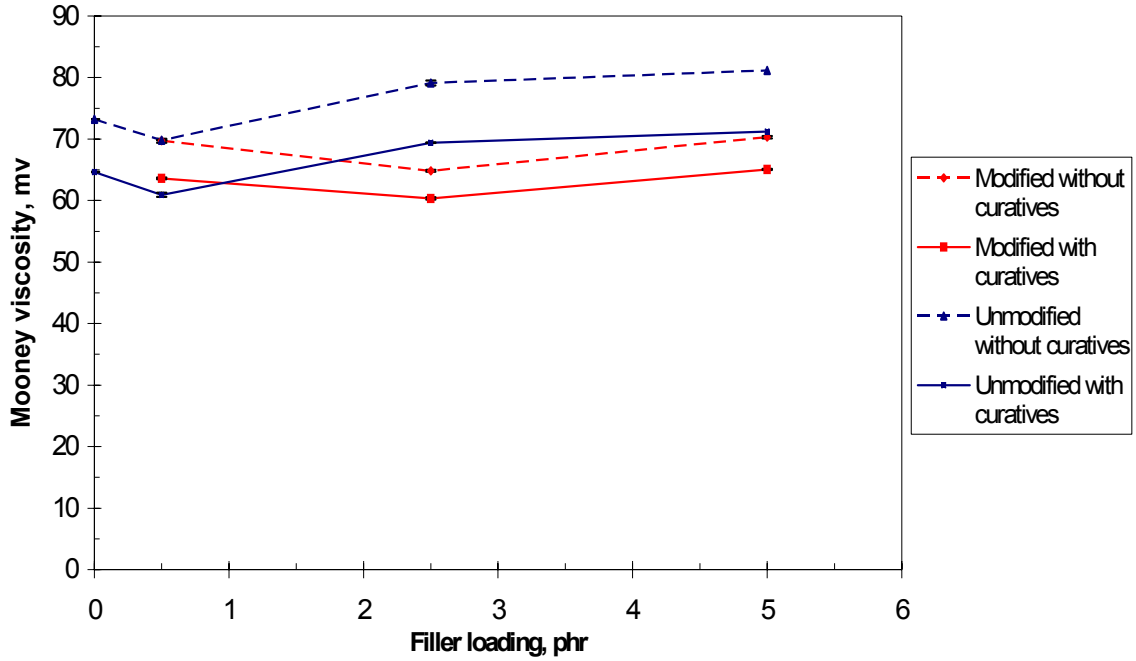

Figure 4.3.1–1 *Viscosity of compounds containing modified and unmodified HNTs.*

4.3.2. Cure characteristics

The cure and scorch times for modified HNTs are shown in Figure 4.3.2–1. The modification prolongs scorch and cure time, because the silane interacts with the curing process. The silane seems to trigger the marching modulus for the compound with 0,5 phr HNT's, which causes the large T90 compared to the unmodified filler. The marching modulus is observed for the compounds containing 5 phr nanofillers, independent of the filler modification. The rheograms are given in Figure 4.3.2–2.

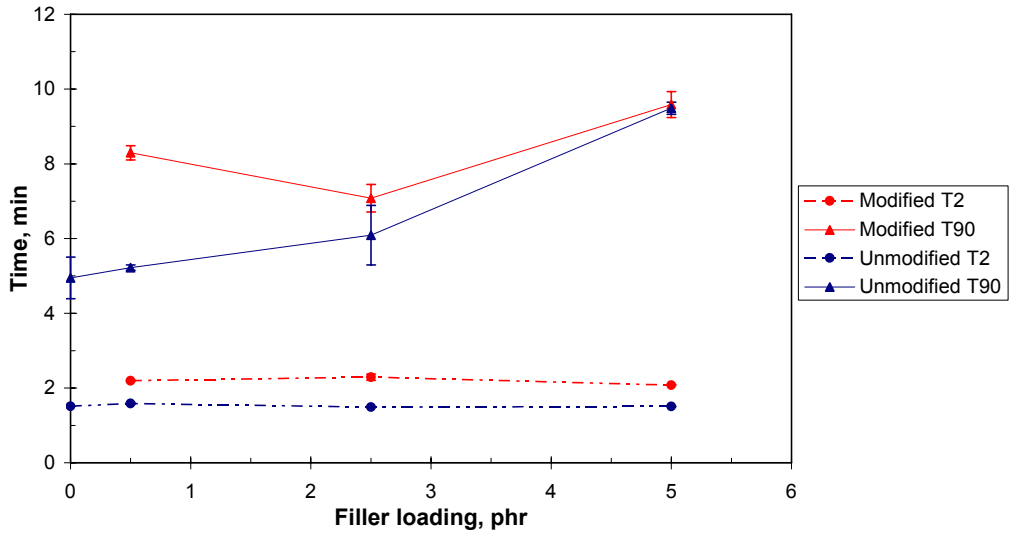

Figure 4.3.2–1 *Cure characteristics of modified and unmodified HNTs.*

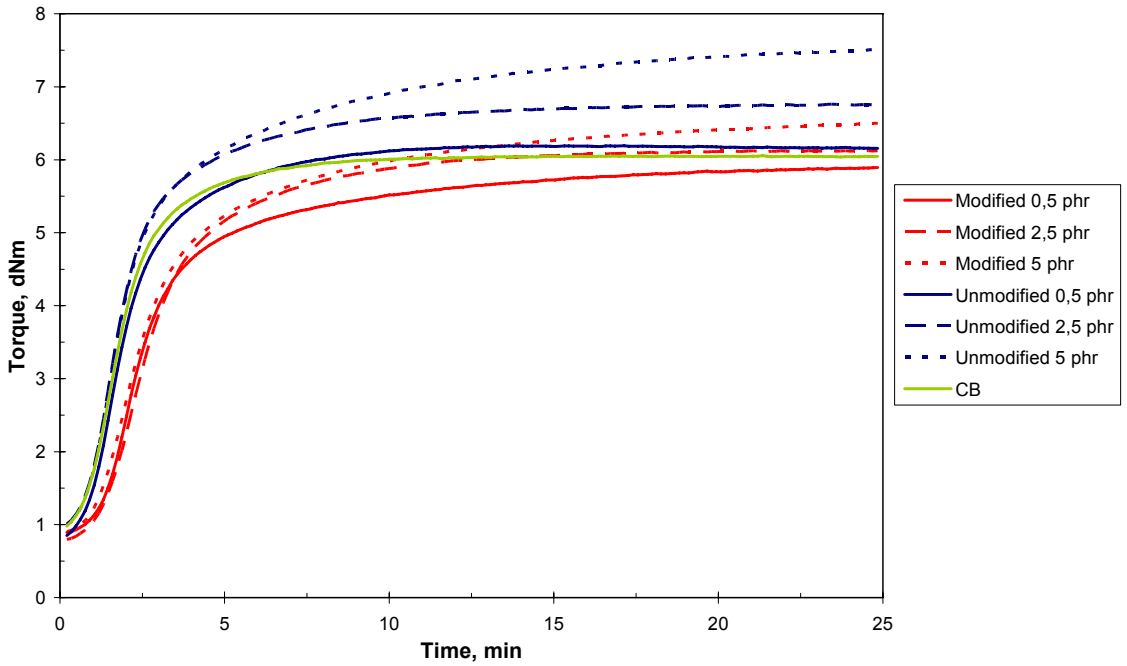

Figure 4.3.2–2 *Rheograms of modified and unmodified HNT composites.*

The maximum torque and minimum viscosity for modified and unmodified HNT containing compounds can be seen in Figure 4.3.2–3. Modification lowers the torque, but it is still slightly higher than for the CB compound. Viscosity is also lower for the compound with the modified filler for all loading levels, and it does not change after 0.5 phr. Modified HNTs giving a lower viscosity than CB. The torque and viscosity decreases can be attributed to the surface modification.

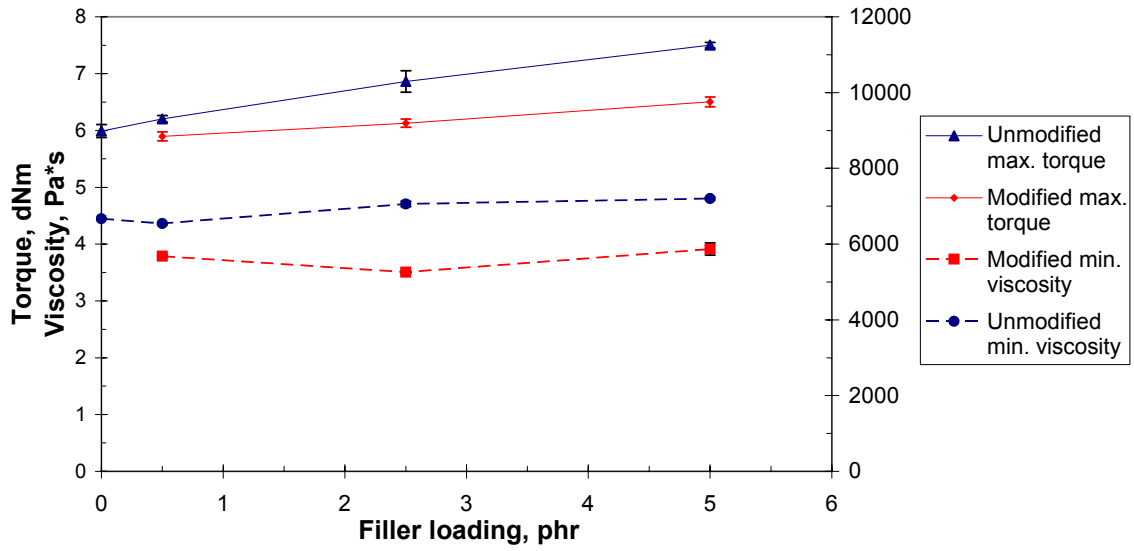

Figure 4.3.2–3 *Cure characteristics of compounds containing modified and unmodified HNTs.*

The curing rate and delta torque for modified and unmodified HNTs are given in Figure 4.3.2–4. The delta torque does not change much with modification or filler loading

level. This indicates that no improvement in crosslinking is achieved by the modification.

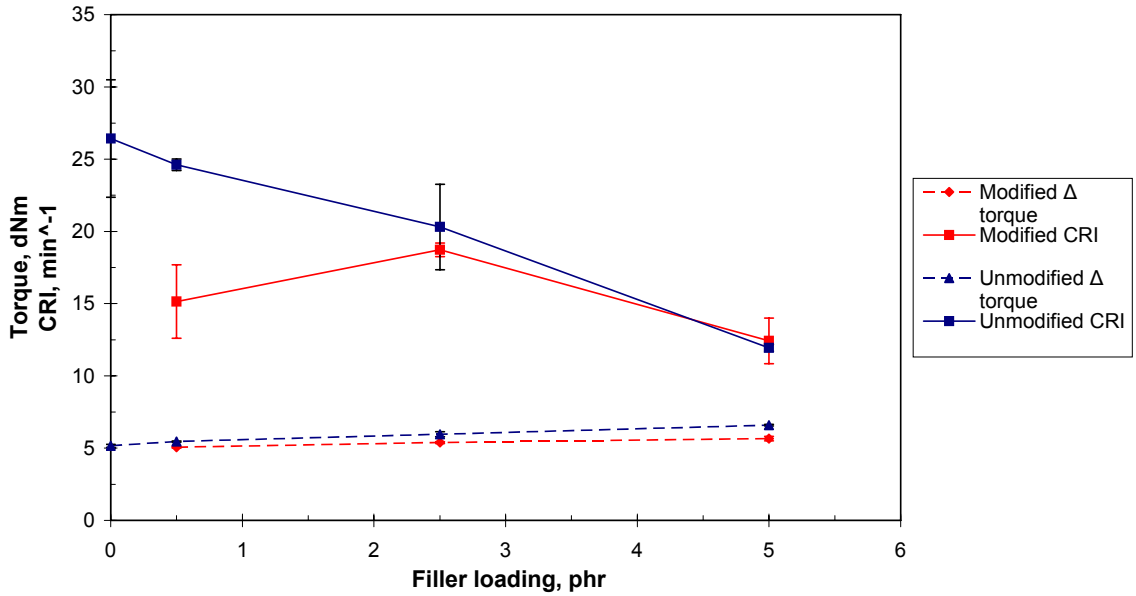

Figure 4.3.2–4 *Cure characteristics of compounds containing modified and unmodified HNTs.*

4.3.3. Bound rubber

Bound rubber results for unmodified and modified HNTs can be seen in Figure 4.3.3–1: The modification increases the bound rubber content. This indicates a better dispersion as well as a more intensive polymer–filler interaction. The difference between modified and unmodified filler diminishes with increasing filler loading. Difference can also be consequence of the longer mixing time that needs to be used with silane modification.

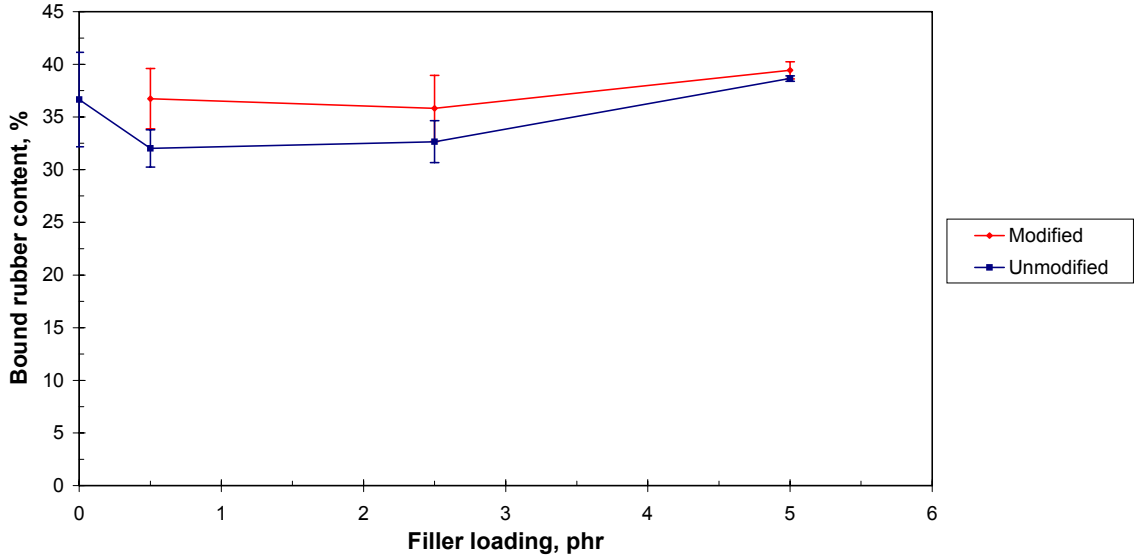

Figure 4.3.3–1 *Bound rubber measurements of compounds containing modified and unmodified HNTs.*

4.3.4. Tensile test

The modification does not have a significant impact on the tensile strength of HNT composites as can be seen in Figure 4.3.4–1. For the lower concentration, 0,5 phr, the discontinuity, which was observed in the concentration study, is again observed for the untreated filler, but disappears for the modified material. When modified HNTs are added, the tensile strength does not change at all. The silane coating, which should result in an additional crosslinking due to the sulphur moiety, does not have the expected effect on strength. One reason for the missing effect might be the low amount of silane that has to be added to the compound, which is difficult to disperse.

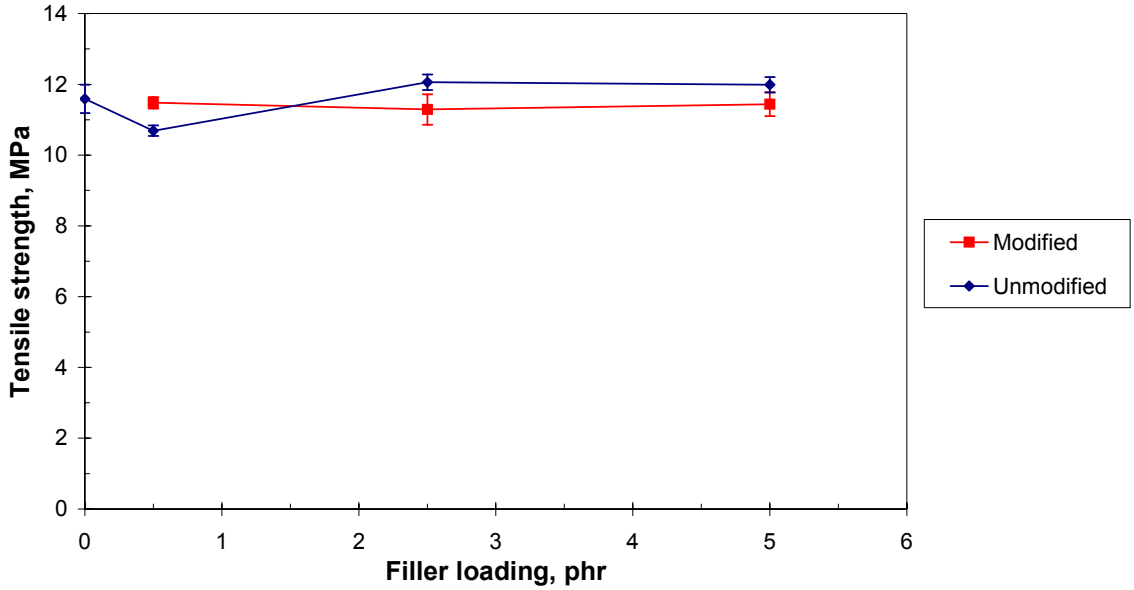

Figure 4.3.4–1 *Tensile strength of material containing modified and unmodified HNTs.*

4.3.5. Tear strength

From Figure 4.3.5–1 it is obvious that the modification increases tear strength of the HNT filled material slightly. Tear strength is still lower than for the CB compound, and decreases further with increasing filler loading. The enhancement gained with the modification of the filler might be due to better interactions between the filler and the polymer, as well as an enhancement of dispersion or reduction of agglomeration.

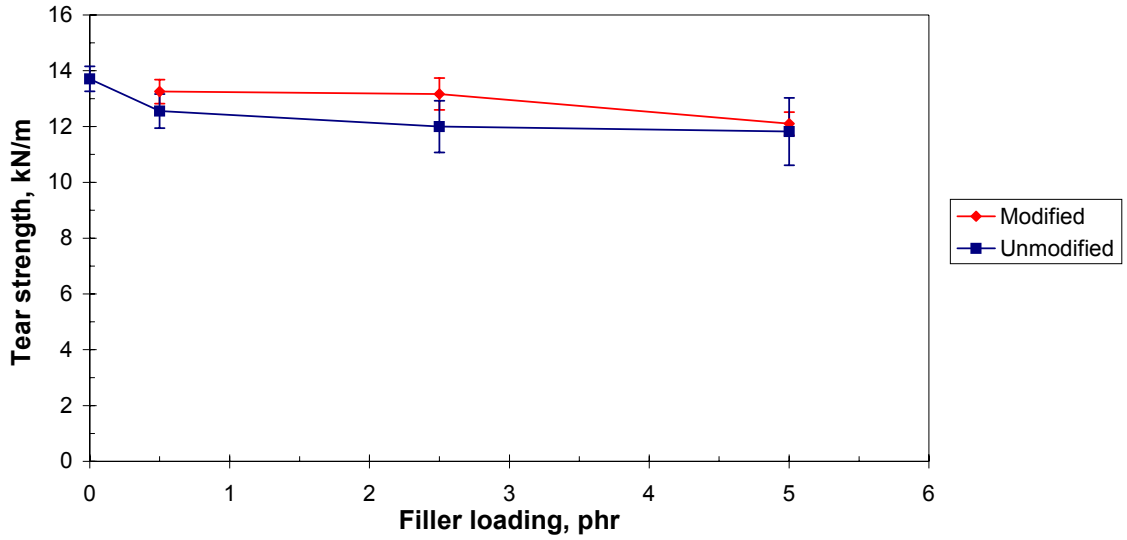

Figure 4.3.5–1 *Tear strength of compounds containing modified and unmodified HNTs.*

4.3.6. Hardness

In Figure 4.3.6–1, the hardness of modified and unmodified HNTs composites is shown. The hardness does not change significantly with modification. No difference is detected for a low filler loading, for higher loadings the material with unmodified filler has a slightly higher hardness. The lacking influence on hardness is again an indication that the surface modification is not very efficient.

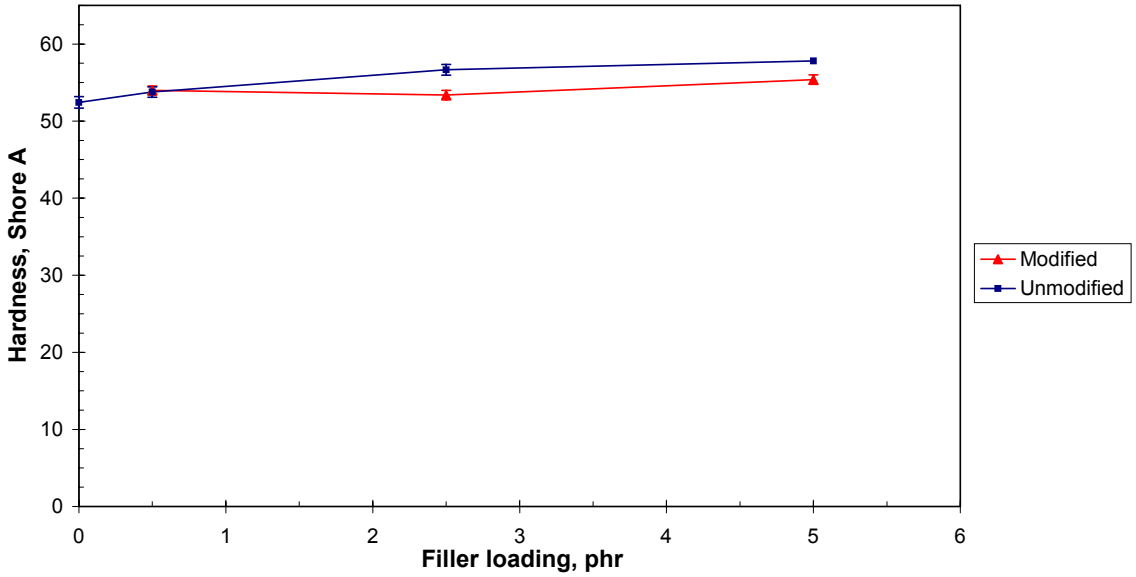

Figure 4.3.6–1 *Hardness compounds containing modified and unmodified HNTs.*

4.3.7. Compression set

The effect of modification on compression set can be seen in Figure 4.3.7–1. Modification does not result in any significant change in compression set at all.

Compared to the material with unmodified HNTs, the compression set is higher, probably due to the presence of the sulphur donor functionality of the silane.

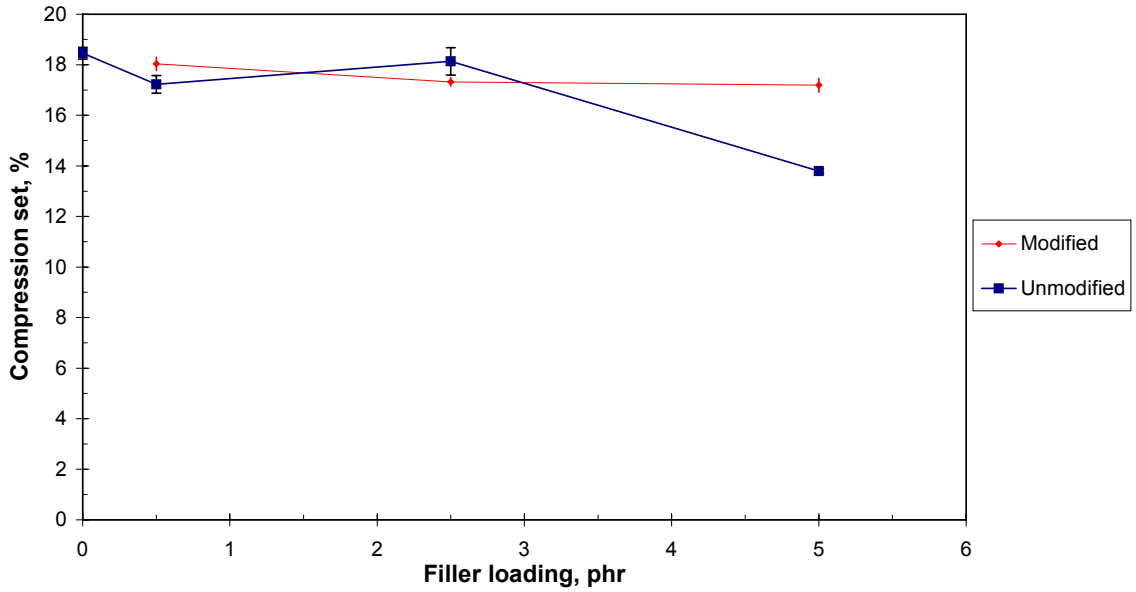

Figure 4.3.7–1 *Compression set of modified and unmodified halloysite nanotubes.*

4.3.8. Conclusions

The surface modification of the nanofillers with silanes leads to a reduction of the viscosity and decrease in bound rubber content. Both trends can be attributed to the longer mixing period, leading to a higher degree of polymer scission. Additionally, the compatibilization of the filler with the silane will result in a lower viscosity.

The Addition of the silane has no significant effect on the appearance of the marching modulus: For higher concentrations of the filler, a marching modulus is observed in both cases.

In terms of mechanical properties, no significant difference is seen between the modified and unmodified HNT composites. Only compression set at higher nanofiller loadings is higher for the material containing the modified filler. None of the other properties does not change significantly.

4.4. Microscopic investigation

In Figure 4.4–1, 3 different SEM pictures of nanocomposites and as a reference one picture of a CB compound are given. In the carbon black compound, larger micrometer–sized particles are visible, which very probably are the conventional calcium carbonate. CB agglomerates or aggregates are also visible as small white spots on the background. These fillers can also be seen in the nanocomposites. However, the nanofillers are not visible in these pictures, as the dimensions of the fillers are so small that they can not be

seen with the 2000x magnification. However, this means that no large scale agglomeration is present with any of the nanofillers or loadings. Only one large agglomerate of MWCNTs was found during the SEM study, indicating that the concentration of large agglomerates is rather low.

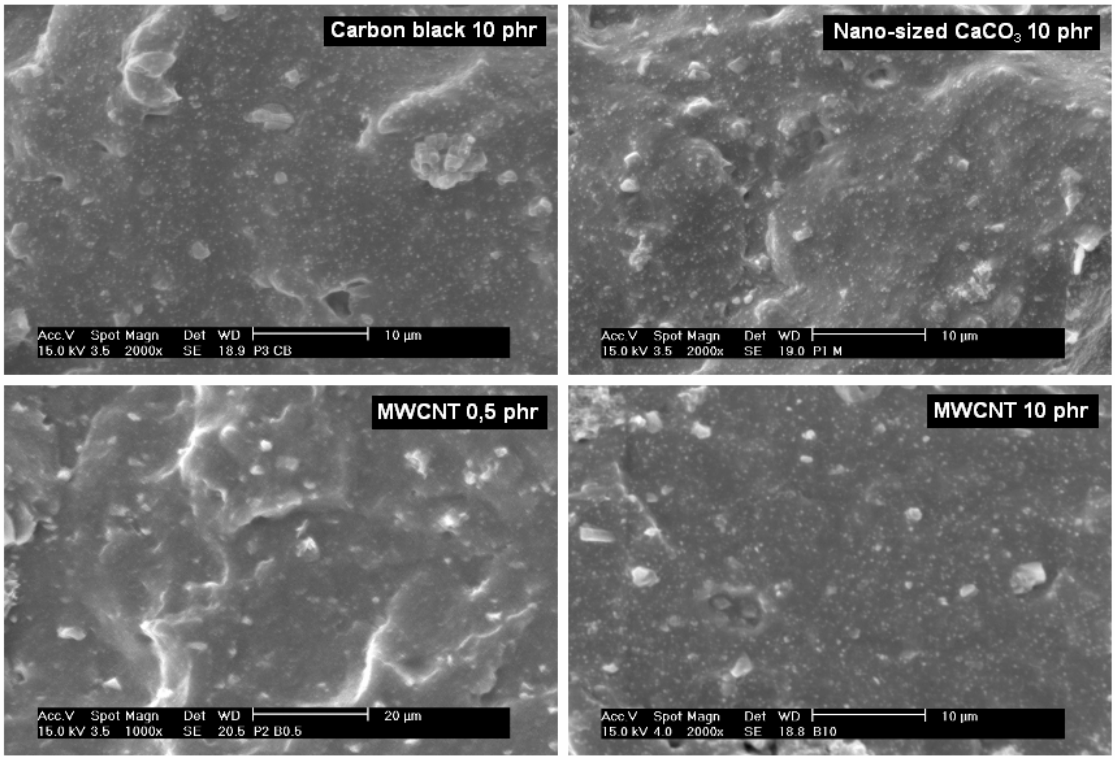

Figure 4.4–1 *SEM microscope of different nanocomposites. CB, $CaCO_3$ and MWCNT with 10 phr loading are with 2000x magnification and MWCNT with 0,5 phr filler loading is with 1000x magnification.*

5. OVERALL CONCLUSIONS

The goal of this study was to prepare nanofiller reinforced EPDM rubber with enhanced properties. During the mixing no differences were observed between the materials. This was quite surprising, because the MWCNT containing compound had a much higher viscosity and torque compared to other materials. To get a closer view on the influence of the nanofillers on the mixing process, an extensive analysis of the fingerprints should be made. Another point of interest is the effect of different mixing setups on the properties of the materials.

The viscosity of compounds containing MWCNTs differ from the other materials: It shows the highest viscosity. This needs to be taken account in processing of MWCNT composites. During mixing, the high initial viscosity might be an advantage, because higher shear forces can be applied, leading to better dispersion.

Nanofillers had a significant impact on the vulcanization behaviour of the compound. With clay–based materials, the vulcanization time was increased, especially with halloysite nanotubes and activated clay. This was caused by the marching modulus of these materials. The behaviour of the nanoclays is determined by the modification agent and by the chemical nature of the filler. The polar accelerators can be adsorbed onto the polar filler surface, which leads to retardation of the vulcanization process. When MWCNTs are added, curing is faster compared to the CB filled compound; this is partly caused by the high bound rubber content. Bound rubber decreases the free rubber volume and the probability of crosslinking reactions increases.

The marching modulus, that appears whenever clay is added, affects the properties of the filled vulcanizates, because the cure time cannot be determined precisely and the crosslinking increases with time. This may lead to different mechanical properties with industrially viable curing times.

In the comparative investigation of different nanomaterials, none of the nanofillers was distinctly better than the others. The nanofillers had only a minor effect on the mechanical properties of the compound. A different behaviour of tube–like nanofillers compared to globular or layered fillers was observed, due to the high aspect ratio of the former.

MWCNT and HNT composites were selected for closer inspection due their great potential for reinforcement based on the high aspect ratio. They also behave differently than the other materials in the tests. Activated clay was chosen for the next stage investigation as it had the best properties from the clay materials.

The properties of the compounds with nanofillers are dependent on filler loading to some extent, as could be seen with the HNT, MWCNT and activated clay nanocomposites. The behaviour of the material with low filler loadings (0.5 phr) was generally different from the behaviour of higher loadings. The addition of clay nanofillers resulted in different trends than the addition of MWCNTs. For tensile strength and hardness, there is no significant change in the properties for higher loadings than 1 phr, while tear and compression set decrease with increasing filler loading for the clay–containing materials. MWCNT filled rubbe have better properties for low filler loadings, which might be attributed to better dispersion. It can also be due to a synergistic behaviour of MWCNTs and CB that has been observed in several studies. The research should therefore be directed towards lower concentrations, because higher concentrations do not result in accordingly improved properties, with current technology.

The curing behaviour of the clay–filled rubber is also significantly affected by the filler loading. There seems to be a limit, below which the marching modulus does not appear with HNT and activated clay composites. It can also been seen that the torque development stops, when the marching modulus appears. It might be possible to achieve better properties, if the marching modulus can be prevented or controlled. If the reaction between clay and curatives could be controlled by the addition of certain chemicals, marching modulus might be prevented. Altering the amount of PEG in the recipe might be a good start.

HNT composites were modified with silane to enhance polymer–filler interactions. Silanol has been used successfully as modificator with silica. The structure of the HNTs resembles the one of silica, and thus silane might be suitable for it as well. The silane modification increases scorch and curing time. The silanol acted as a combatibilizator between the EPDM and HNTs causing the Mooney viscosity to drop. With silane modification, no significant improvement in mechanical properties was detected. A slight increase in tear strength was obtained for all filler loadings.

In literature, significant enhancement of properties is described with small nanofiller loadings; the results of this study are not as good as expected. In the references, the best properties are gained with the solvent manufacturing method, but good properties are also reported with the normal mixing method. However, the compound in this study was much more complex than those reported in literature. It is possible that the high amount of conventional fillers or the complex accelerator system prevented the nanofiller from working properly. This leads to the conclusion that simpler compounds should be used for screening in the first phases of a study. In literature, the appearance of a marching modulus was not reported, which would indicate that his behaviour is characteristic for this curing system or compound.

With nanofillers, significant improvements of elastomer properties are not easily achieved, when the current nanofillers and traditional mixing methods are used. In the future, methods to improve the dispersion and filler–polymer interaction are needed. The main research should be focused on different surface modifications of the fillers and structural compatibilization by grafting. It might be necessary to use modifications specifically tailored for certain compound–filler combinations to achieve an adequate reinforcing effect.

6. REFERENCES

[1] Seppälä, J., Polymeeriteknologian perusteet, 5. painos, Helsinki 2003, Otatieto, s. 206–220.

[2] Ciesielski, A., An Introduction to Rubber Technology, Shawbury 1999, Smithers Rapra Technology, p. 19–20 31–44 50–55 106–108.

[3] White, J. R., De, S. K., Rubber Technologist's Handbook , Shawbury 2001, Smithers Rapra Technology, p.36–38 61–64 131–167 167–190 209–251.

[4] Laurila, T., Kumitekniikka: Lyhyt johdatus kumitekniikan perusteisiin, 1 painos ed., Vilppula 2007, Opetushallitus, p. 42–44 84–98 107–129.

[5] Datta, R. N., Rubber Curing Systems, 1st ed., Shawbury 2002, Smithers Rapra Press, p. 5–19 26–29.

[6] Dick, J. S., Annicellim, R. A., Rubber Technology: Compounding and Testing for Performance, 1st ed., Munchen GER 2001, Hanser Gardner Publications, p. 395–397.

[7] Bhowmick, A. K., Current Topics in Elastomers Research , Boca Raton 2008, CRC Press, p. 1104–23–57 463–484.

[8] Baba, M., Gardette, J.–L., Lacoste, J., Crosslinking on ageing of elastomers: I. Photoageing of EPDM monitored by gel, swelling and DSC measurements, Polym Degradation Stab, 63(1999)1, pp. 121–126.

[9] Rothon, R. N., Particulate–Filled Polymer Composites, 2nd ed., Shawnbury 2003, Smithers Rapra Press, p. 303–350.

[10] Mushack, R., Bachmann, W., Neuburger silica – a natural, functional filler, GAK Gummi Fasern Kunststoffe, 49(1996)8, pp. 620–624.

[11] Dierkes, W., Economic Mixing of Silica–Rubber Compounds, Ph.D Thesis, Enschede 2005, University of Twente, p. 9–30

[12] Indian Rubber Institute., Rubber Engineering, 1st ed., New York 2000, McGraw–Hill Professional, p. 242–262 557–645.

[13] Wypych, G., Handbook of Fillers, 3rd ed., Toronto 2009, ChemTec Publishing, p. 223–276 325–368 373–427 435–450.

[14] Gent, A. N., Engineering With Rubber: How to Design Rubber Components, 2nd ed., Munchen 2001, Hanser Gardner Publications, p. 365, 23–27.

[15] Advani, S. G., Processing and Properties of Nanocomposites, Singapore 2006, World Scientific Publishing Company, p. 450.

[16] Fakhru'l–Razi, A., et al., Effect of multi–wall carbon nanotubes on the mechanical properties of natural rubber, Compos.Struct., 75(2006)1–4, pp. 496–500.

[17] Yan, N., et al., Carbon nanotubes/carbon black synergistic reinforced natural rubber composites, Plast.Rubber Compos., 38(2009)7, pp. 290–296.

[18] Bokobza, L., Multiwall carbon nanotube elastomeric composites: A review, Polymer, 48(2007)17, pp. 4907–4920.

[19] Korea University: Nanotube and Nanodevice Laboratory [WWW], [viitattu: 17.05.2010], Saatavissa: http://nanotube.korea.ac.kr/study_eng_2.html.

[20] Das, A., et al., Coupling activity of ionic liquids between diene elastomers and multi–walled carbon nanotubes, Carbon, 47(2009)14, pp. 3313–3321.

[21] Perez, L. D., et al., Preparation, characterization, and physical properties of multiwall carbon nanotube/elastomer composites, Polym.Eng.Sci., 49(2009)5, pp. 866–874.

[22] Bokobza, L., Kolodziej, M., On the use of carbon nanotubes as reinforcing fillers for elastomeric materials, Polym.Int., 55(2006)9, pp. 1090–1098.

[23] Bokobza, L., et al., Blends of carbon blacks and multiwall carbon nanotubes as reinforcing fillers for hydrocarbon rubbers, J.Polym.Sci.Part B, 46(2008)18, pp. 1939–1951.

[24] Bokobza, L., Bilin, C., Effect of strain on the properties of a styrene–butadiene rubber filled with multiwall carbon nanotubes, J. Appl. Polym. Sci., 105(2007)4, pp. 2054–2061.

[25] De Falco, A., Goyones, S., Carbon nanotubes as reinforcement of styrene–butadiene rubber, Appl.Surf.Sci., 254(2007), pp. 262–265.

[26] Bokobza, L., Mechanical, electrical and spectroscopic investigations of carbon nanotube–reinforced elastomers, Vib.Spectrosc., 51(2009)1, pp. 52–59.

[27] Bhattacharyya, S., et al., Improving reinforcement of natural rubber by networking of activated carbon nanotubes, Carbon, 46(2008)7, pp.1037–1045.

[28] Pasbakhsh, P., et al., Influence of maleic anhydride grafted ethylene propylene diene monomer (MAH–g–EPDM) on the properties of EPDM nanocomposites reinforced by halloysite nanotubes, Polym.Test., 28(2009)5, pp. 548–559.

[29] Rooj, S., et al., Preparation and properties of natural nanocomposites based on natural rubber and naturally occurring halloysite nanotubes, Mater Des, 31(2010)4, pp. 2151–2156.

[30] Ismail, H., et al., Morphological, thermal and tensile properties of halloysite nanotubes filled ethylene propylene diene monomer (EPDM) nanocomposites, Polym.Test., 27(2008)7, pp. 841–850.

[31] Pasbakhsh, P., et al., The partial replacement of silica or calcium carbonate by halloysite nanotubes as fillers in ethylene propylene diene monomer composites, J. Appl. Polym. Sci., 113(2009)6, pp. 3910–3919.

[32] Wan, C., et al., Cure characteristics and mechanical properties of NR/SBR blends filled with nano–sized $CaCO_3$, Prog.Rubber Plast.Recycling Technol., 21(2005)2, pp. 101–115.

[33] Mishra, S., Shimpi, N. G., Patil, U. D., Effect of Nano $CaCO_3$ on thermal properties of Styrene Butadiene Rubber (SBR), Journal of Polymer Research, 14(2007)6, pp. 449–459.

[34] Mishra, S., Shimpi, N. G., Mechanical and Flame–Retarding Properties of Styrene–Butadiene Rubber Filled with Nano–$CaCO_3$ as a Filler and Linseed Oil as an Extender, J. Appl. Polym. Sci., 98(2005)6, pp. 2563–2571.

[35] Mishra, S., Shimpi, N. G., Studies on mechanical, thermal, and flame retarding properties of polybutadiene rubber (PBR) nanocomposites, Polym.–Plast.Technol.Eng., 47(2008)1, pp. 72–81.

[36] Jin, F., Park, S., Thermo–mechanical behaviors of butadiene rubber reinforced with nano–sized calcium carbonate, Mater.Sci.Eng.A, 478(2008)1–2, pp. 406–408.

[37] Mishra, S., et al., Comparative Study of the Mechanical and Flame–Retarding Properties of Polybutadiene Rubber Filled with Nanoparticles and Fly Ash, J. Appl. Polym. Sci., 96(2005)1, pp. 6–9.

[38] Dennis, H. R., et al., Effect of melt processing conditions on the extent of exfoliation in organoclay–based nanocomposites, Polymer, 42(2001)23, pp. 9513–9522.

[39] Alexandre, M., Dubois, P., Polymer–layered silicate nanocomposites: Preparation, properties and uses of a new class of materials, Mater. Sci. Eng. R. Rep., 28(2000)1, pp. 1–63.

[40] Tan, H., Isayev, A. I., Comparative study of silica–, nanoclay–and carbon black–filled ethylene propylene diene monomer (EPDM) rubbers treated by ultrasound, Rubber Chem. Technol., 81(2008)1, pp. 138–155.

[41] Mousa, A., Cure characteristics and thermal properties of sulfur–cured EPDM–based composites by compounding with layered nano–organoclays, Polym.–Plast.Technol.Eng., 45(2006)8, pp. 911–915.

[42] Chang, Y.–W., et al., Preparation and properties of EPDM/organomontmorillonite hybrid nanocomposites, Polym.Int., 51(2002)4, pp. 319–324.

[43] Liu, B., et al., Novel preparation and properties of EPDM/montmorillonite nanocomposites, J. Appl. Polym. Sci., 99(2006)5, pp. 2578–2585.41

[44] Gatos, K. G., Karger–Kocsis, J., Effects of primary and quaternary amine intercalants on the organoclay dispersion in a sulfur–cured EPDM rubber, Polymer, 46(2005)9, pp. 3069–3076.

[45] Ahmadi, S. J., Huang, Y., Li, W., Fabrication and physical properties of EPDM–organoclay nanocomposites, Compos.Sci.Technol., 65(2005)7–8, pp. 1069–1076.

[46] Li, P., et al., High–performance EPDM/organoclay nanocomposites by melt extrusion, Appl.Clay.Sci., 40(2008)1–4, pp. 38–44.

[47] Sui, G., et al., Processing and material characteristics of a carbon–nanotube–reinforced natural rubber, Macromol.Mater.Eng., 292(2007)9, pp. 1020–1026.

[48] Kónya, Z., et al., Large scale production of short functionalized carbon nanotubes, Chem.Phys.Lett., 360(2002)5–6, pp. 429–435.

[49] Eitan, A., et al., Surface modification of multiwalled carbon nanotubes: Toward the tailoring of the interface in polymer composites, Chem.Mater., 15(2003)16, pp. 3198–3201.

[50] Liu, P., Modifications of carbon nanotubes with polymers, Eur. Polym. J., 41(2005)11, pp. 2693–2703.

[51] Lin, Y., et al., Functionalizing multiple–walled carbon nanotubes with aminopolymers, J. Phys. Chem. B, 106(2002)6, pp. 1294–1298.

[52] Sham, M. L., et al., Cleaning and functionalization of polymer surfaces and nanoscale carbon fillers by uv/ozone treatment: A review, J. Compos. Mater., 43(2009)14, pp. 1537–1564.

[53] Yuan, P., et al., Functionalization of halloysite clay nanotubes by grafting with γ–aminopropyltriethoxysilane, J.Phys.Chem.C, 112(2008)40, pp. 15742–15751.

[54] Guo, B., et al., Styrene–butadiene rubber/halloysite nanotubes nanocomposites modified by sorbic acid, Appl. Surf. Sci., 155(2009)16, pp. 7329–7336.

[55] Koo, J. H., Polymer Nanocomposite: Processing, Characterization and Applications, 1st ed., New York 2006, McGraw–Hill Professional Publishing, p. 10–19.

[56] Yu, Z.–Z., Mai, Y.–L., Polymer nanocomposites , 1st ed., Boca Raton 2006, Woodhead Publishing Ltd, p. 414–435.

[57] Johnson, P. S., Rubber Processing: An Introduction, Munchen 2001, Hanser Gardner Publications, p. 9–50.

[58] Wood, P. R., Mixing of Vulcanisable Rubbers and Thermoplastic Elastomers, Shawbury 2004, Rapra Technology Limitd, Rapra Review Reports, 15, 10, p. 4–27.

[59] Palmgren, H., Processing conditions in the batch–operated internal mixer, Rubber Chem. Technol., 48(1975)2, pp. 463–494.

[60] Rauwendaal, C., Polymer mixing: A Self–Study Guide, Munchen 1998, Hanser Publishers, p. 25–87.

[61] Leblanc, J. L., hardy, P., Evolution of Bound Rubber During the Storage of Uncured Compounds, Kautschuk Gummi Kunstoffe, 44(1991)12, pp. 1119–1124.